STRUCTURAL CHARACTERISTICS OF BORAX-METAKAOLIN AND BORAX-FLY ASH BASED GEOPOLYMER SYSTEMS

by

Öznur Cansu Seçkin

B.S., Chemical Engineering, Middle East Technical University, 2013

Submitted to the Institute for Graduate Studies in
Science and Engineering in partial fulfillment of
the requirements for the degree of
Master of Science

Graduate Program in Chemical Engineering

Boğaziçi University

2017

To Deniz…

ACKNOWLEDGEMENTS

Firstly, I would like to acknowledge the guidance, interest and patience of my supervising advisor Assoc. Prof. Sezen Soyer Uzun.

I also thank to T. Özturan and N. Özyurt-Zihnioğlu at Boğaziçi University for compressive strength measurements and A. Uzun at Koç University for FTIR spectroscopy measurements.

Furthermore, I would like to voice my gratitude to Dr. Burcu Selen Çağlayan and Samira Kurtoğlu for their help and patience during spectroscopy measurements.

I am thankful to my colleagues, especially Dilara Kahraman, Ezgi Nergis Akıncı, İnci Arslan, Aycan Aydın, Devran Soyman, Ceren Sengül and Sinem Nalbant for their friendship, moral support and suggestions throughout this study.

I would like to thank to my family, for their continuous support, not only for this thesis but also for my life.

Lastly, but certainly not least, I would like to thank to my love, Deniz Üzel, for his continuous support, patience and endless help. This thesis would not be done without him.

This work was also supported by Bogazici University Research Fund through Project BAP13A05P5.

ABSTRACT

STRUCTURAL CHARACTERISTICS OF BORAX-METAKAOLIN AND BORAX-FLY ASH BASED GEOPOLYMER SYSTEMS

The main focus of this study is to investigate the effect of inclusion of borax on structural properties of metakaolin and C type fly ash based geopolymers. Various structural characterization techniques including Fourier Transform Infrared Spectroscopy (FTIR), X-Ray Diffraction (XRD), Scanning Electron Microscopy (SEM) and Thermogravimetric Analysis (TGA) are performed to analyze a set of borax containing metakaolin and fly ash-based geopolymers with molar B/Si ratios between 0 and 1. Compressive strength tests are also carried out to understand the effect of boron inclusion mechanical strength values. In the first part of thesis, borax-metakaolin based geopolymer samples are investigated. Geopolymers have amorphous character together with quartz and boron-including crystalline components in borax- metakaolin based geopolymer systems. The intensity of the FTIR bands in this system increases systematically with B/Si ratio. This situation is also consistent with observation of needle and star like crystalline structures in the SEM measurements. The geopolymer with B/Si ratio of 1 has a peak at 620 cm^{-1} which is assigned to polyborosiloxane bridges, showing incorporation of boron atoms into the silica network. The second part of this thesis includes comparison of structural characteristics borax- metakaolin and borax-fly ash based geopolymers with different B/Si ratios. The FTIR results of geopolymers exhibit borosiloxane bridge as a small peak at 685 cm^{-1} and shoulder at 875 cm^{-1}. Borosilicate structural units are also seen at 630 cm^{-1} in the Raman spectrum of borax-fly ash based geopolymers supporting the FTIR results. The presence of new structural units related to boron addition are observed same as the SEM images as the star and needle like structures. Boron content seems to have positive effect in compressive strength.

ÖZET

BORAKS-METAKAOLIN VE BORAKS- UÇUCU KÜL BAZLI JEOPOLİMER SİSTEMLERİNİN YAPISAL ÖZELLİKLERİ

Bu araştırmanın ana odağı, boraksın metakaolin ve C tipi uçucu kül esaslı jeopolimerlerin yapısal özelliklerine olan etkisinin araştırılmasıdır. Bu amaçla molar B/Si oranı 0 ile 1 arasında değişen boraks-metakolin ve boraks-uçucu kül bazlı jeopolimerler Fourier Dönüşümü Kızıl Ötesi Spektroskopi (FT-IR), X-Işını Kırınımı (XRD), Taramalı Elektron Mikroskopisi (SEM) ve Termogravimetrik Analiz (TGA) gibi çeşitli yapısal karakterizasyon teknikleri ile incelenmiştir. Boraksın eklenmesinin jeopolimerler üzerindeki mekanik etkisini ölçmek için basınç dayanımı testleri de yapılmıştır. Tezin ilk bölümünde boraks-metakaolin bazlı jeopolimerler incelenmiştir. Boraks-metakaolin bazlı jeopolimer sisteminlerinin kuartz ve bor içeren kristal bileşenleri ile birlikte amorf bir yapıya sahip olduğu gözlenmiştir. Boraks-metakaolin- bazlı jeopolimer numunelerinin FTIR bandlarının yoğunluğunu B /Si oranına bağlı olarak sistematik olarak artmaktadır. Bu durum, SEM ölçümlerinde kristal yapıların varlığını gösteren iğne ve yıldız benzeri yapıların gözlenmesi ile de uyumludur. B/Si oranı 1 olan boraks-metakaolin bazlı jeopolimerin 620 cm^{-1}'de sahip olduğu bant poliborosilikat köprüsünün parmak izi olarak kabul edilmektedir. Bu bantın varlığı bor atomlarının silika ağı içine katıldığının kanıtıdır. Tezin ikinci bölümünde farklı B/Si oranlarına sahip boraks-metakaolin ve boraks-uçucu kül esaslı jeopolimerlerin yapısal özelliklerinin ile karşılaştırılması üzerine çalışılmıştır. Boraks-metakolin ve boraks-uçucu kül bazlı jeopolimerlerin FTIR sonuçlarında 685 cm^{-1}'de ve 875 cm^{-1}'de görülen bantlar Borosilikat köprüsünün varlığını göstermektedir. Boraks-uçucu kül bazlı jeopolimerlerin Raman spektrumunda yer alan 630 cm^{-1}'deki borosilikat yapısına ait bant FTIR sonuçlarını desteklemektedir. Bor ilavesi ile jeopolimerlerde yıldız ve iğne benzeri yeni yapısal birimler SEM görüntülerinde ortaya çıkmıştır. Bor eklenmesinin jeopolimerlerde basınç dayanımına pozitif yönde etki ettiği görülmüştür.

TABLE OF CONTENTS

LIST OF FIGURES

LIST OF TABLES

1. INTRODUCTION

The population of the world increases at a great rate, for that reason, the construction of new houses becomes inevitable. Therefore, demand for cement as being raw material of construction industry increases day by day. However, cement manufacturing gives rise to huge amount of CO_2 emissions. To illustrate, a ton of cement production results in 0.74 to 1.24 tons of CO_2 emission [2]. The greenhouse gases such as CO_2 play a vital role in global warming. Global warming is considered as one of the significant treats to environment due to being the major cause of climate change. Therefore, emission of CO_2 from human activities should be reduced since it is responsible of 65 % of global warming [3]. Since the production of Portland cement results in large amounts of CO_2 emissions; the studies focusing on the replacement of the Portland cement with innovative and environmentally friendly materials such as geopolymers gain importance among researchers in the last years [4].

Geopolymers are classified as inorganic polymers. They come into prominence due to their unique properties such as durability and mechanical resistance. They can also be used for encapsulating hazardous wastes. Geopolymers take attraction due to having favorable properties such as heat, acid and fire resistance; high compressive strength and also low shrinkage [5]. Davidovits reports that geopolymers can be obtained from polymerization reaction of alkaline based materials with geological or waste products which include silica and alumina [6]. These inorganic materials, namely geopolymers, display amorphous structures even they have the same chemical composition with zeolites.

Geopolymer synthesis includes following steps as;

- Dissolution of aluminosilicate sources with metal hydroxide solution such as NaOH or KOH,
- Formation of a gel phase due to polymerization reaction of particles,
- Hardening of gel phase by the elimination of water [7].

Kaolinite, metakaolin, granulated blast furnace slag, geologic minerals rich in silica and alumina are widely used in geopolymer synthesis route as aluminosilicate source [1]. In addition to these materials, industrial wastes such as red mud [8, 9] and Pozzolanic wastes [12] are used as raw materials for geopolymerization.

Turkey has the largest boron deposits in the world with a worldwide share of 72% in terms of B_2O_3 content [13]. Tincalconite ($Na_2B_4O_7$-$10H_2O$), colemanite ($Ca_2B_6O_{11}$-$5H_2O$) and ulexite ($NaCaB_5O_9$-$8H_2O$) are the most important commercial ores and they can be used in order to produce different compounds such as boric acid, anhydrous boric acid and anhydrous borax [10, 14]. 1.3 million tons of average boron ores are produced in Turkey annually [11].

Boron is utilized in wide application areas such as in the structure of space, military and air vehicles; nuclear applications; electronics and communication sector; agriculture; glass industry; production of chemicals, detergent, ceramics and polymeric materials; development of nano-technological products; metallurgy and construction [15]. The studies are performed by researchers to find different application areas for boron compounds such as utilization of them as binders in order to improve mechanical and compressive strength of cement [20].

The focus of this study is the utilization of borax in metakaolin and fly ash based geopolymers and characterization of these materials by diffraction, spectroscopic and microscopic techniques. The geopolymerization procedure includes addition of alkali activator which is sodium silicate; metakaolin and fly ash as aluminosilicate source. Anhydrous borax is added to geopolymer matrix as the main boron source. The geopolymers are produced with varying B/Si molar ratios.

1.1. Properties Of Geopolymers

Geopolymers are stated as a new group of aluminosilicate materials obtained by alkali activation of materials that are rich in alumina and silica [6]. Aluminosilicate raw materials are chemically dissolved in alkaline environments such as KOH or NaOH and this procedure is referred as alkali activation. The geopolymers are classified as inorganic materials. However, there exist significant differences between geopolymers and inorganic polymers since the kind of silicon and aluminum precursors used are different in the synthesis route. Inorganic polymers are produced by utilization of alkoxides in alcohol-water solution as precursor, on the other hand, geopolymers are synthesized by employing a solid aluminosilicate raw material activated by a strong alkaline solution [16]. In the formation phase of geopolymers, heterogeneous reaction occurs between aluminosilicate solid materials and strong alkaline silicate environment.

The sources used in geopolymer synthesis are aluminosilicate sources which are inactive fillers supporting Al^{3+} ions such as metakaolin or kaolinite and also geopolymer liquor including a sodium silicate solution as binder or alkali hydroxide solution [17]. The synthesis mechanism of geopolymer depends on dissolution of aluminosilicate sources in alkaline environment to obtain aluminosilicate gel and polycondensation to develop networked polymeric oxide structure.

Geopolymers are becoming more popular due to their superior properties such as fire and heat resistance, high mechanical strength and low shrinkage [19]. In addition to the fact that geopolymers need less energy consumption with less CO_2 emission, these innovative products have acid and freeze –thaw cycle resistance, low permeability and availability for immobilization of toxic metal ions [17, 18]. Moreover, geopolymers can be synthesized with the utilization of different low cost aluminosilicate raw materials, for example minerals such as perlite, bentonite, kaolinite or by products such as fly ash, alumina red mud and slag [9, 17].

1.2. Raw Materials Used In Geopolymerization

1.2.1. Properties of Metakaolin

Metakaolin is an aluminosilicate based material and widely preferred in geopolymer synthesis due to including high amount of SiO_2 and Al_2O_3 [8, 17, 25]. Metakaolin is classified as a reactive aluminosilicate mineral and obtained by calcination of kaolinite at a specific temperature range (600–900 ^oC) [91]. Kaolinite is transformed to metakolin by thermal treatment at 700 ^oC in this thesis. After heat treatment of kaolinite, crystalline nature of kaolinite transforms into an amorphous structure as a result of losing internal water and dehydroxylation. Metakaolin exhibits a disordered structure compared to kaolinite. Turkey is considered as a significant kaolinite producer with approximately 850000 metric tons annually production capacity [90]. In addition to main components of metakaolin such as SiO_2 and Al_2O_3; the formations such as Fe_2O_3, CaO, MgO, SO_3, Na_2O and K_2O can be included in lower amounts. Metakolin is a more active raw material for geopolymerization reactions compared to silica fume and fly ash [91].

Metakaolin is selected as aluminosilicate source in this study since it is known to be active for geopolymerization [25] and it is a relatively pure compound compared to industrial wastes such as fly ash and red mud. Purity is an advantage in the evaluation of characterization results.Both metakolin and metakaolin based geopolymers are investigated by different diffraction, spectroscopic and microscopic characterization techniques to obtain structural information.

X-Ray Diffraction (XRD) is used to identify the crystalline phases present in raw materials and synthesized geopolymers. A previous study related with the synthesis and characterization of metakaolin based geopolymers indicates that XRD results of metakaolin and kaolinite are quite different. Kaolinite displays a crystalline structure whereas metakaolin is mainly amorphous.

As a result of dehydroxylation process by heating, kaolinite loses its characteristic crystalline structure and a broad peak forms in XRD pattern of metakaolin at 20-28^{o} [25]. Although, most of the crystal phases of kaolinite disappear with calcination, quartz preserves its presence. Metakaolin based geopolymers display a broad hump in their XRD pattern which is an evidence of successful geopolymerization reaction [27].

Fourier Infra-Red (FTIR) spectroscopy provides vibrational spectra of the raw materials and geopolymeric specimens. This technique proves the existence of Si-O, Si-O-Si and Si-O-Al bonds related with geopolymer structure. FTIR spectrum of kaolinite consists of Si-O stretching vibrations at 116 cm^{-1}, Si-O-Si vibrations at 1029 cm^{-1}, and Si-O-Al lattice vibrations at 1014 cm^{-1} . The bands present in the low frequency region (759, 694 and 536 cm^{-1}) are related with Si-O and Al-O vibrations. Band centered at 536 cm^{-1} belongs to $Al(O, OH)_6$ octahedra in kaolinite whereas 464 cm^{-1} corresponds to bending or stretching of T–O–T (T: Si or Al) bridge of aluminosilicates. After heat treatment of kaolinite, the band at 1029 cm^{-1} disappears. New bonds are seen in FTIR spectrum of metakaolin such as 1080 and 465 cm^{-1} which are related to stretching modes of Si–O and T-O-T(T=Si or Al) bonds [25]. The characteristic bands and corresponding vibrational modes in metakolin based geopolymers can be seen in Table 1.1 [31].

Table 1.1. Several characteristic bands for metakaolin based geopolymers [31]

Vibration	**cm^{-1}**	**Mode**
Si-O	1100-1080	Symmetrical Vibration
Si-O-Al	1008	Asymmetrical Vibration
Al-O-H	914	Stretching Vibration,
Si-O-H	840	Bending Vibration
Al-O	798	Stretching Vibration, IV coordinated
Si-O	694	Symmetrically Stretching Vibration
Si-O-Al	540	Bending Vibration
Si-O	469	In-plane Bending Vibration

Scanning Electron Microscopy (SEM) can be used to study the morphologhy of metakaolin and metakaolin based geopolymers. This fast and nondestructive technique gives information about surface properties, particle size and also particle distribution [17]. SEM images belonging to metakaolin displays rounded packed aggregates and clumps of lamellar particles with different size and orientation [92]. The SEM images of metakaolin based geopolymers are expected to be consistent with XRD patterns as giving details of crystalline or amorphous structures of geopolymers.

Thermogravimetric analysis (TGA) is performed to measure the thermal stability of materials. Thermal behavior of geopolymers can be categorized into four sequential stages according to study associated with alkali-activated waste catalyst-metakaolin based geopolymers [86]. The steps are;

(i) Dissipation of free water
(ii) Decomposition of geopolymer components
(iii) Dehydroxylation of zeolitics
(iv) Stabilization of weight loss

Since metakaolin is obtained after thermal treatment, weight loss at the first stage which is removal of free water is expected to remain at low amounts. During calcination of kaolinite, most of the free water is lost.

1.2.2. Properties of Fly Ash

A large variety of aluminosilicates are used in the geopolymer synthesis. The aluminosilicate raw materials used in geopolymer production are classified as naturally occurring such as kaolinite or industrial by products and waste materials such as fly ash. The studies concerning utilization of fly ash in geopolymers gain importance in recent years among researchers due to its availability and improved properties such as durability in final product [81].

Fly ash is a by-product formed after coal combustion process which occurs at high temperatures in the range of 1400 °C and 1700 °C. Fly ash comprises 75-80 % of the total ash production from combustion of coal in thermal plants and the total amount of coal ash is approximately 349 million tons in worldwide in 2000 [84]. The fly ash production in Turkey is 15 million tons annually; however, only 1% of the total amount is used in cement and brick production process [93]. Fly ash is classified as a ferro aluminosilicate material and includes generally Si, Al, Fe, Ca, Mg, K and Na elements. According to ASTM 618, fly ash types are divided into two groups; namely C class and F class. The amount of the oxides of silicon, aluminium, and iron by mass is greater than 70 % and calcium oxide is less than 10 % in F class fly ash [84].

Fly ash and fly ash based geopolymers are investigated by different diffraction, spectroscopic and microscopic characterization techniques. Fly ash has more impurities compared to metakaolin. Thereofore, XRD might be a helpful characterization technique to identify the different crystal formations in fly ash. According to XRD results, the impurities in fly ash are mainly quartz (SiO_2), clay minerals, calcite (CaO) and aragonite ($CaCO_3$), hematite (Fe_2O_3), pyrite (FeS_2), anhydrite ($CaSO_4$) and gypsum ($CaSO_4.2H_2O$) [81, 82, 84, 93]. It should be noted that XRD pattern of fly ash displays a broad feature between 20-38^o indicating the presence of disordered phases. During geopolymerization reactions, the new crystal formations can generate and also disappear. To illustrate, in one of the previous researches which focused on synthesis and characterization of coal fly ash based geopolymers; sodalite, halite and tobermorite phases appear in geopolymers which are not present in raw material. However, quartz and mullite phases of fly ash preserve their existence after geopolymerization.

FTIR measurements play critical role due to exhibiting geopolymerization band. The level of geopolymerization can be understood as comparing to FTIR spectrum raw material with geopolymers. The fly ash samples taken from different thermal power plants which are Soma Unit IV, Çatalağzı, Çayırhan and Tunçbilek in Turkey show three characteristic bands at 1100, 1000 and 660 cm^{-1} due to Si-O-Si asymmetric stretching, Si-O and Al-O vibrations; respectively; according to FTIR results [93].

A broad peak is also positioned between 800 and 1400 cm^{-1}. SiO_4 groups show their presence at 900 and 1160 cm^{-1}. The peak around 1410 cm^{-1} is attributed to C–O stretching. The fly ash based geopolymers have the bands at 460 cm^{-1} is related to Al–O and Si–O in plane and bending modes. The other characteristics bands at 730 cm^{-1} and 820 cm^{-1} belong to octahedral Al and tetrahedral Al–O stretching; respectively. Asymmetric Al–O and Si–O stretching bands associated with geopolymerization are positioned in the region between 900 and 1030 cm^{-1} [81].

Raman spectroscopy can be utilized in order to determine the degree of conversion of the raw materials to the final geopolymer product. The Raman band near 460 cm^{-1} is the characteristics of aluminosilicate materials according to a study on geopolymerization index of fly ash geopolymers [77].

SEM images of fly ash samples shows the presence of spherical particles with smooth outer surfaces called as cenospheres. After geopolymerization reaction, partially reacted cenospheres and gel formation are observed according to SEM results. The gel formation is related with dissolution of aluminate and silicate phases in geopolymer structure [81, 84].

1.2.3. Properties of Borax

Turkey has the largest boron reserves of the world with 803 million tons of boron deposits [20]. Boron production is implemented by five operation zones; 4 of them integrated to mine and plant facilities and one of them has only plant facility. 120000 tons of clay and fine wastes are manufactured in production cycles of these facilities.

The possible utilization of boron wastes as a fluxing agent in production of red mud brick is investigated by carrying out characterization and mechanical strength tests by adding different amounts of boron wastes (5, 10 and 15 wt %) to red mud.

The results of the tests reveal that the utilization of - boron wastes which include Fe_2O_3, Al_2O_3 and SiO_2 leads to an improvement in the mechanical performance of bricks and decrease firing temperature. Due to leading improvements in mechanical properties, usage of boron wastes is possible in ceramic industry [11].

The effect of fly ash and borax waste in wall tiles with addition of the wastes in a range of 2–10% are also studied recently in literature. The result of this study reveals that addition of borax waste increases firing strength up to 6% compared to standard wall tile [21]. The firing strength is directly related with amount of borax waste. Therefore, it is possible to say that utilization of boron in different type of materials such as industrial wastes or ceramics improve the mechanical and thermal properties of products.

There is only few research related with the utilization of borax in geopolymer production in literature as far as we know. The first study belongs to Williams and Riesen who synthesized borosilicate geopolymers using silica fume and borax [22]. In order to characterize the geopolymers and observe the effects of boron on structural properties, XRD and SEM measurements are performed. The geopolymer specimens have amorphous microstructure with minor amounts of boron crystals according to XRD results. The microstructure of geopolmers show glassy matrix with pores similar to traditional geopolymers. The compressive strength of this borosilicate geopolymer is found as 56 MPa which is a promising value. The other studies covering the utilization of borax with fly ash for boroaluminosilicate geopolymer synthesis are performed by Nazari. The effect of NaOH concentration and curing temperature are also investigated, during the design of geopolymer synthesis [23, 24]. FTIR and SEM techniques are used to characterize the samples. FTIR results of the boroaluminosilicate geopolymers show B-O formation according to the studies of Nazari. Star like crystalline structural units are observed in SEM images which might be related to the presence boron phases. The compressive strength of geopolymers improved up to 64 MPa from 20-25 MPa with addition of borax to geopolymer mixture.

In this thesis, borax is utilized in the synthesis of metakaolin and fly-ash based geopolymers. This study can lead to employment of borax compounds in different sectors where geopolymers are used such as construction. Metakaolin and borax based geopolymers are synthesized for the first time in literature according to our knowledge. The participation of boron content to geopolymer structure can be understood by characterization techniques. In the study performed by Huang and Li [34], synthesis of hybrid polyborosiloxane material resulted in Si-O-B vibrations in FTIR spectra at 870 cm $^{-1}$ and 698 cm-$^{1.}$ The presence of this band proves the incorporation of boron content into the silica network. As Huang and Li, the role of boron in geopolymer structure can be revealed by application of characterization techniques on geopolymer samples.

According to a study which produces borax and polymer based composites, XRD pattern of borax exhibit peaks at 2Θ values of 10º, 20.5º, 30.5º, 41.2º and 51º. The B-O peak is present at around 10 º, 20 º and 30.5 º [44]. According to XRD diagram of borax, it is possible to say that borax has a crystalline nature. In previous studies related to the synthesis of magnesium borax or copper borax, XRD is applied to investigate the differences between different boron ores [87, 88, 89]. Three main peaks of tincalconite mineral are reported to be positioned at 2θ values of 30.639°, 20.365° and 20.289° [88]. In a study conducted by Yüksel [26] on anhydrous borax, XRD diagram confirms the crystalline structure of the borax. The miller indices of the anhydrous borax are given at Table 1.2.

Table 1.2. Miller indices of natural anhydrous borax [26].

2Θ (º)	**(h k l)**
22	(1 0 2)
23	(1 1 2)
29	(1 2 2)
33.2	(1 3 0)
42	(0 4 1)
48	(0 1 6)

Table 1.2. Miller indices of natural anhydrous borax [26] (Cont.).

50	(2 4 1)
55	(4 2 5)
58	(4 3 1)
65	(0 5 10)
67	(1 2 14)
70	(5 1 10)
76	(3 5 7)
79	(6 3 0)

According to, Infra-Red spectrum of borax [39], a strong absorption band is seen as a result of the presence of B-O band in the region between 1380 and 1310 cm^{-1}. In addition; the peaks at 1420, 1150, 1079, 1000, 949 and 832 cm^{-1} show the presence of B-O bonds [39]. B-O bonds are classified as triangular and tetrahedral geometry present at 1341 and 1131 cm^{-1}, respectively [44]. There is a strong band present in the hydroxyl region 3340 cm^{-1} due to O-H stretching since the presence of water in the borax structure. Borax can lose its water content in dry and a slight change in spectrum can be observed [40]. The absorption bands between the regions 1300-1700 cm^{-1} show the bending and stretching vibration of B-O-B in BO_3 triangles. Moreover, the stretching vibration of BO_4 bonds exists between 900- 950 cm^{-1} [41]. It is also said that as a result of the existence of the BO_3 triangle, a broad strong absorption band is exhibited in 800-1100 cm^{-1} [42]. The bands seen around 1000 cm^{-1} belong to borates [43]. B-O-H bond gives rise to peaks at 819 cm^{-1} [44].

The properties of sodium–calcium borates and sodium borates including ulexite, probertite, tincalconite and boric acid retrieved from different regions in Turkey are studied in one of the previous studies [87]. Tincalconite ($Na_2B_4O_7.5H_2O$) and boric acid are also utilized for magnesium borate and copper borate synthesis [88, 89]. The FTIR results related to previous work related to boron including compounds are given at Table 1.3.

Table 1.3. Positions of FTIR bands related to boron including bonds

	[23, 24]	[33]	[34, 42]	[35]	[36	[39]	[41]	[44]	[87]	[88]	[89]
Bond Type	Geopolymer	Elemental Boron	Polymer	Boron doped nanowire	Composite	Borax	Borate Glass	Composite	Sodium Borate (Tincalconite)	Sodium Borate (Tincalconite)	Sodium Borate (Tincalconite)
B-O	1380-1310 cm^{-1}	1410 cm^{-1}				1380-1310, 1420, 1150, 1079, 1000, 949, 832 cm^{-1}		1341 cm^{-1} (triangular), 1131 cm^{-1} (tetrahedral)	1411 and 1252 cm^{-1} (asymmetric stretching of 3-coordinated boron / 1076 and 974 cm^{-1} (Asymmetric stretching of 4-coordinated boron) 856 and 756 cm^{-1} (symmetric stretching of 4-coordinated boron)	1120–980 cm^{-1} (asymmetric stretching of tri-coordinate boron)/ 780 cm^{-1} (Symmetric stretching of tri-coordinate boron)	1419 and 1343 cm^{-1} (asymmetric stretching of tri-coordinate boron between 1232 and 912 cm^{-1}, (asymmetric stretching of tri-coordinate boron)
B-O-B in BO_3 triangles			1500-1300, 1100-800 cm^{-1}				1700-1300 cm^{-1}	703 cm^{-1}			
BO_4							950-900 cm^{-1}		1076 and 974 cm^{-1} (symmetric stretching of 4-coordinated boron) and of 856 and 756 cm^{-1}		

Table 1.3. Positions of FTIR bands related to boron including bonds (Cont.)

									(asymmetric stretching of 4-coordinated boron		
B-OH			1195 cm-$^{-1}$					819 cm^{-1}	1228 and 1227 cm^{-1}		
B-O-Si			870, 698 cm^{-1}	625 cm^{-1}	625 cm $^{-1}$						

Raman spectroscopy can be used to support the FTIR results as giving information concerning the molecular structure of the materials. This characterization technique is based on inelastic scattering of monochromatic light. Vibrational, rotational and other low frequency transitions in molecules can be identified by using Raman spectroscopy [37, 38]. According to Raman spectrum of borax, the sharpest peak is positioned at 580 cm-^{1} [39]. In the study performed by Almou and friends associated with glassy metaborates [46], the highest frequency value for borax is seen at 576 cm^{-1} in Raman spectrum which is close to 580 cm^{-1}. This peak is formed due to presence of hydroxyl tetraborate ions $[B_4O_5(OH)_4]^{-2}$ [46]. In a study related to Raman spectra of borax, kernite and colemanite, Krishnamurti report that borax sample includes 7 bands in Raman spectrum which are positioned at 578, 853, 891, 942, 3340 3455 and 3374 cm^{-1} [47]. The frequency at 942 cm^{-1} is caused by the valence oscillation of boron and oxygen elements. The frequencies at 3345 cm^{-1} and 3574 cm^{-1} show the presence of hydroxyl group in borax [47].

Scanning Electron Microscope (SEM) is used to obtain information about the external morphology, chemical composition and also crystalline structure of the borax raw material and also synthesized geopolymers which have varying boron contents. The knowledge of borax microstructure may help to define unreacted particles after geopolymerization reaction. SEM micrograph of the borax illustrates spherical particles with varying sizes [44]. In the study performed by Yüksel on natural and additive included boron, the anhydrous borax particles exhibit microspheres with the sizes around 200 μm with monoclinic structure according to SEM images [26]. The study on thermal decompositon of borax also uses SEM images to detect the effect of tempearature on borax structure. According to this study, the raw borax material has monoclinic structure with a combination of prisms and dihedrons [59]. SEM images of dehydrated borax samples without thermal treatment show non-uniform distribution compared to the sample treated with heat. Both anhydrous and thermally treated samples have crystalline structures [26].

TGA is applied to analyze the behavior of the sample at different temperatures. According to a study in which the thermal stability of borax is determined by TGA analysis, there are two phases in the TGA diagram of borax.

No weight loss is observed until 100 ºC. The first stage of weight loss lies at the temperature range of 120 and 150 ºC. The second decomposition continues up to 490 ºC and the system becomes stable [44].

1.3. Proposed Work

The main focus of this study is to investigate the effect of addition of borax on structural properties of geopolymers. In this regard, boroaluminosilicate based geopolymers with different B/Si ratios in the range between 0 and 1 are synthesized and characterized in detail. Metakaolin and fly ash are chosen as aluminosilicate source. Therefore, various structural characterization techniques are performed to analyze this set of borax- aluminosilicate based geopolymers.

Metakaolin is chosen as the aluminosilicate source in the first part of the thesis (Chaper 2) to be employed in the synthesis of geopolymers since it is an active material for geopolymerization and has high purity compared to other raw materials such as fly ash and red mud. Purity might be advantageous during the evaluation process of characterization results that would lead better observation of the effect of inclusion borax. In the second part of the study (Chapter 3); metakaolin and fly ash are used as aluminosilicate source to be able to perform a comparative study. The synthesis procedures are also different in these sections.

In the literature, there are only few studies regarding boron including geopolymers that involves complete structural characterization combining diffraction, spectroscopy and microscopy together to present structural changes. with inclusion of boron to geopolymer matrix. Moreover, to the best of our knowledge, there is no reported research studying the utilization of boron synergistically with metakaolin and C type fly ash in geopolymer systems.

The characterization studies of synthesized geopolymers and raw materials in this thesis are performed using X-Ray Diffraction (XRD), Fourier transform infrared spectroscopy (FT-IR), Raman Spectroscopy and Scanning Electron Microscopy (SEM). XRD measurements are performed to investigate the amorphous or crystalline phase of the synthesized geopolymers. FTIR and Raman spectroscopy are utilized to understand the vibrational fingerprints of geopolymers, SEM analysis are performed on synthesized geopolymers to resolve their surface microstructures. Compressive strength measurements are also carried out to obtain the effect of boron inclusion on mechanical strength values. By performing both mechanical and characterization tests on the specimens, it is possible to relate the mechanical performance of the geopolymers with the structural properties.

2. STRUCTURAL CHARACTERISTICS OF BORAX-METAKAOLIN BASED GEOPOLYMERS

2.1. Introduction

The prominent and rapid deteriorations observed in environment are stimulated society to take precautions concerning environmental issues. The climate change is one of the crucial threats that the world is struggling in the recent years. Greenhouse gases like carbon dioxide (CO_2) caused by human activities are the most significant driver of climate change. The usage of fossil fuels result in emission of more than six billion tons of CO) into the atmosphere each year [49]. Production of cement has a negative environmental affect as it is responsible of release of considerable amount of toxic gases. As being the world's most important construction material, concrete is also the second commercialized good coming after water due to economic and technological reasons compared to other construction materials such as steel or glass [50]. The Portland cement industry causes significant amount of CO_2 emissions. To illustrate, annual formation of 3.5 billion tons of CO_2 will be expected in the next ten years based on cement industry [25]. International Energy Authority World Energy Outlook 1995 claims that seven percent of the total CO_2 emitted around the world is caused by worldwide cement production [51]. Therefore, the studies aim to reduce the negative effect of Portland cement and alternative solutions in this regard gain importance. This situation resulted in significant improvements in this area.

Alternative solutions that the researchers proposed as an alternative to Portland cement usage can be lined up as below.

- The substitution of new materials as partially replacing the Portland Cement, [52, 53].

- The usage of alternative cements which produced by low energy as calcium sulfoaluminates, [54, 55].
- The production of alkali activated materials as aluminosilicate materials which includes geopolymers [50, 56].

The usage of geopolymer is claimed to reduce the CO_2 emission up to 64 % compared to cement [57]. This scenario brings necessity to study the geopolymer production. Geopolymer concrete researches have gained popularity due to their potential to remove the global dependency to cement.

Traditional geopolymer production includes the reaction between aluminosilicate materials such as metakaolin, fly ash, slag and alkaline liquids like Sodium Hydroxide (NaOH), Potassium Hydroxide (KOH), and Sodium Silicate (Na_2O_3Si) [57, 58]. The materials used as aluminosilicate source are generally industrial by-products such as fly ash and red mud [4, 8, 9, 11], which gives opportunity to utilization of these waste materials. In addition to the potential usage of geopolymers as an alternative to Portland cement for construction, other applications areas for geopolymers such as nuclear waste immobilization have been proposed.

Despite the fact that there is a noticeable increase of researches globally about the production, characterization, mechanical performance and the durability of metakaolin based geopolymer materials [25, 56], several concerns are on debate related with the large-scale use of metakaolin as aluminosilicate sources. The first reason is the high water demand of the metakaolin-based geopolymers. The second reason is related with the cost of the metakaolin since it is not a by-product like fly ash [56].

In this part, borax is employed in the production of borax-metakaolin-based geopolymers. This could motivate utilization of borax materials which exist in huge amounts due to great boron reserves of Turkey in different sector as construction.

In the literature, to the best of our knowledge, there are only a few studies involving the use of boron in geopolymerization. There is no reported research as far as we know studying the utilization of boron synergistically with metakaolin in geopolymer systems. Nazari reported the utilization of borax with fly ash for boroaluminosilicate geopolymer synthesis. In his studies, the effect of NaOH concentration and curing temperature are also investigated [23, 24]. The synthesized geopolymers are characterized with FTIR and SEM techniques. B-O bond formation is observed from FTIR results of boroaluminosilicate geopolymers. The FTIR band regarding B-O vibrations is seen to increase in intensity with increasing boron content. Microstructure of geopolymers changes with boron addition exhibiting star like crystalline structural units. According to these studies, compressive strength of geopolymers reach up to 64 MPa with addition of optimum amount of borax to geopolymer mixture (borax to NaOH ratio of 0.912). Williams and Riesen synthesized borosilicate geopolymers using silica fume and borax and performed XRD and SEM measurements to see the effect of boron [22]. It is seen that geopolymer specimens display amorphous microstructure with minor amounts of boron according to XRD results. The microstructure shows glassy matrix with pores similar to traditional geopolymers. The compressive strength of this borosilicate geopolymer is seen to be a promising value (56 MPa).

This study aims to synthesize and characterize borax-metakaolin based geopolymers with different B/Si ratios in the range between 0 and 1. This range of compositions is achieved by varying the relative amounts of metakaolin and borax in the system. The main focus of this study is to investigate the effect of inclusion of boron on structural properties of geopolymers. Therefore, various structural characterization techniques are performed to analyze this set of borax-metakaolin based geopolymers with molar B/Si ratios of 0, 0.5, 0.6, 0.8 and 1.0. The main structural characterization techniques employed are Fourier Transform Infrared Spectroscopy (FT-IR), X-Ray Diffraction (XRD), Scanning Electron Microscope(SEM) and Termogravimetric Analysis (TGA).

2.2. Experimental

In this study, geopolymers with varying boron contents are synthesized using a similar technique compared to the literature [23, 24]. A previous study on a borax- and fly ash-based boroaluminosilicate geopolymers reported a synthesis procedure involving synthesis of a NaOH and borax solution initially, followed by mixing of this activating solution with fly ash. In this study, the activating solution is obtained using sodium silicate solution and borax which is then mixed with metakaolin. Afterwards, the synthesized geopolymers are analyzed with several characterization techniques, namely XRD, FT-IR, SEM and TGA.

2.2.1. Synthesis Procedure

The first step for geopolymer synthesis involves calcination of kaolinite at 700 ^{o}C at atmospheric pressure for 1 hour in order to transform kaolinite into metakaolin. Metakaolin exhibits a disordered structure compared to kaolinite. In this study, metakaolin is selected as aluminosilicate source due to two main reasons: i) metakaolin is known to be active for geopolymerization [25] and ii) it is a relatively pure compound compared to industrial wastes. Purity is an advantage in the interpretation of characterization results. After heat treatment, metakaolin is allowed to rest for 1 day before being used in geopolymerization. The chemical composition of metakaolin used in this study is given at Table 2.1.

Table 2.1. Chemical Composition of Metakaolin (wt %)

Chemical Composition	Percentage (wt%)
SiO_2	56.21
Al_2O_3	41.04
TiO_2	1.15
K_2O	0.46
Fe_2O_3	0.36
CaO	0.09
MgO	0.09

As boron source, borax decahydrate obtained from ETİBOR is used. In order to obtain anhydrous borax, borax is dehydrated by heating borax decahydrate ($Na_2B_4O_7.10H_2O$) at 150 ^oC for 30 minutes. Then, it is subsequently heated at 300 ^oC for 15 hours to remove intermolecular water. Sodium silicate (9% of Na_2O, 28% of SiO_2, 63 % of H_2O with 1.401g/ml of density at 20 ^oC) solution and distilled water are mixed to be used as the activating solution. The geopolymer synthesis is illustrated in Figure 2.1. The procedure involves the following steps:

(i) Calcination of kaolinite at 700 ^oC for 1 hour to obtain metakaolin,

(ii) Calcination of borax decahydrate to obtain anhydrous borax at 150 ^oC for 30 minutes, then, 300 ^oC for 15 hours,

(iii) Preparation of the activating solution by mixing anhydrous borax and sodium silicate solution,

(iv) Mixing metakaolin with the activating solution,

(v) Heat treatment of geopolymers (70 ^oC for 1 day and subsequently resting at room temperature for 3 weeks).

Table 2.2 presents all of the geopolymer compositions that are studied in this part. The geopolymer samples are named based on their B/Si and Liquid/Solid (L/S) ratios, respectively. For instance, GP 0.5-2.5 represents the geopolymer which has B/Si ratio as 0.5 mole percent and L/S ratio as 2.5 weight percent.

The ratio of liquid to solid content of geopolymers are varied by changing the water content. The L/S that are used are 2.5 and 3 weight percent. These values seem high compared to what is reported in the literature for aluminosilicate geopolymers with L/S ratios changing between 1.05 and 1.12 [25]. However, a mixing problem is observed during addition of metakaolin. Therefore the water content is therefore increased to provide adequate mixing.

Amount of sodium silicate is calculated according to the decided Si/Al molar ratio which is fixed at 1.8 for all specimens. The molar Si/Al ratio is 1.16 for the metakaolin. With the aim of increasing this ratio to 1.8, the required amount of sodium silicate solution is used during synthesis. The amount of boron is varied in geopolymers; the specimens are designed to have B/Si ratios between 0 and 1 (Table 2.2).

Anhydrous borax and sodium silicate is mixed at different concentrations during the synthesis of alkali activator (activating solution). The mixing of borax and sodium silicate is continued for a few minutes until obtaining a homogenous solution. Next, metakaolin is added to alkali activator solution and mixed by a mechanical stirrer for 10 minutes. Before transferring the geopolymer paste to furnace, the mixture is poured into molds with dimensions of 4 cmx 4 cmx 3 cm and are allowed to rest for 1 day. Thermal treatment procedure for geopolymer synthesis includes curing at 70 ^{o}C for 1 day and subsequently resting at room temperature for 3 weeks (Figure 2.1).

The molar Si/Al is 1.16 for all the synthesized geopolymer whereas Na/Al ratios change between 1.27 and 2.35. B/Si molar ratio varies between 0 and 1 (Table 2.2). In order to see the effect of boron inclusion, the reference geopolymer is synthesized without adding borax content. The molar ratios regarding the synthesized geopolymers are illustrated in Table 2.2.

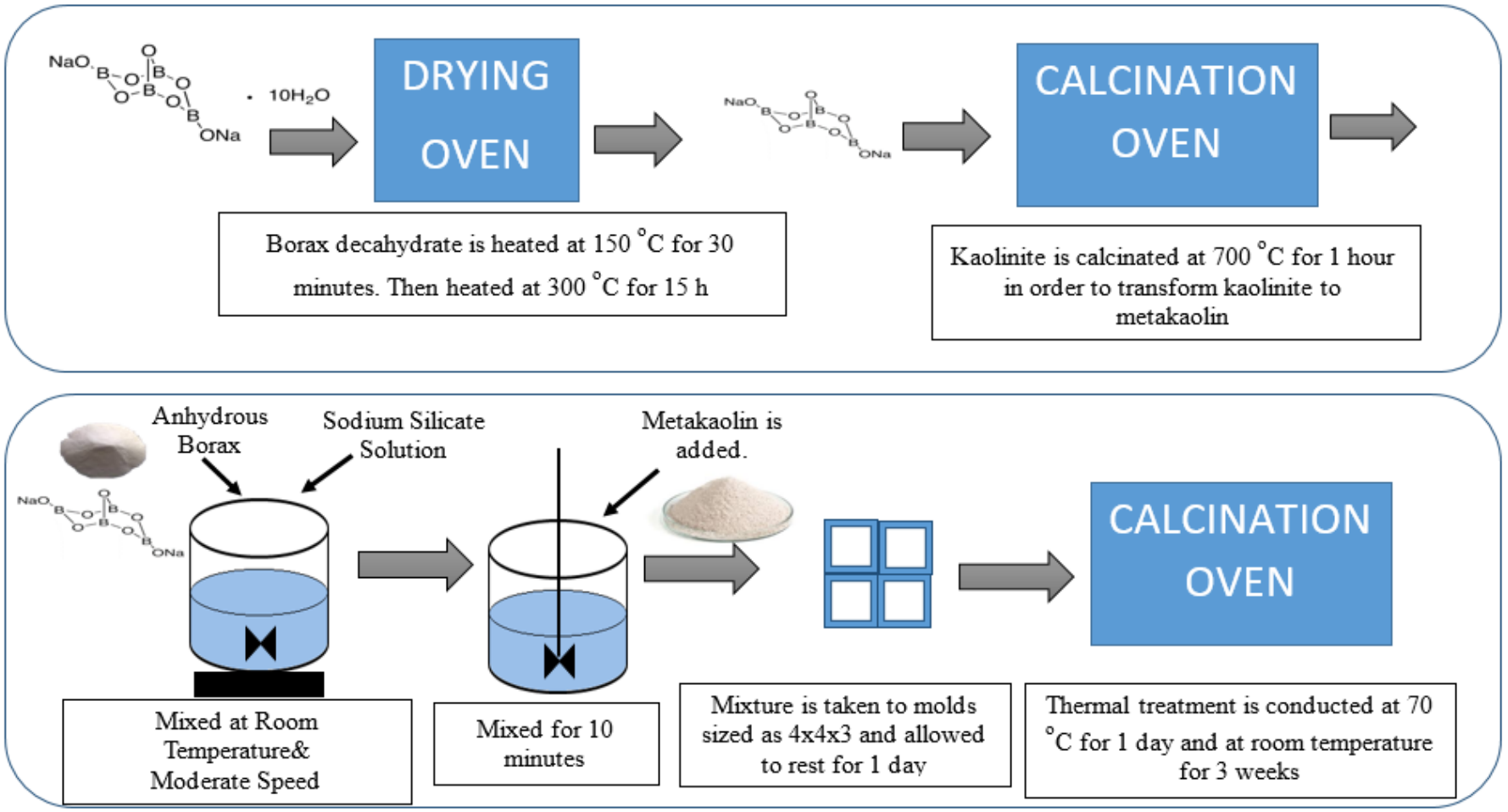

Figure 2.1. Synthesis procedure of boron-metakaolin based geopolymers

Table 2.2. Molar ratios used in Metakaolin based geopolymer synthesis.

Geopolymer	**Si/Al**	**B/Si**	**Na/Al**	**Na/Si**	**Liquid to Solid (L/S) Ratio (g/g)**
GP 0-2.5	1.8	0	1.27	0.87	2.5
GP 0.5-2.5	1.8	0.5	1.72	0.96	2.5
GP 0.6-2.5	1.8	0.6	1.81	1	2.5
GP 0.8-2.5	1.8	0.8	1.99	1.11	2.5
GP 1-2.5	1.8	1	2.08	1.16	2.5
GP 0-3	1.8	0	1.27	0.87	3
GP 0.5-3	1.8	0.5	1.72	0.96	3
GP 0.6-3	1.8	0.6	1.81	1	3
GP 0.8-3	1.8	0.8	1.99	1.11	3
GP 1-3	1.8	1	2.17	1.20	3
GP 1.2-3	1.8	1.2	2.35	1.31	3

2.2.2. Characterization Techniques

2.2.2.1. X-Ray Diffraction (XRD). X-Ray Diffraction is the elastic scattering of X-Rays by atoms in periodic lattice. It is a non-destructive method and used to have information about chemical compositions, particle size distributions and crystallographic structure of materials. A Bruker D8 Discover diffractometer with a CuK radiation source employing a wavelength of 1.5418 Å in 2θ range of 10-90° with step size of 0.01263° is used to characterize the synthesized geopolymers.

XRD plays crucial role for characterization of geopolymers as providing information on the crystalline phases and amorphous character of the samples. In addition, effect of boron on crystalline structure can be studied with XRD technique.

2.2.2.2. Attenuated total reflectance - Fourier transform infrared spectroscopy (ATR-FTIR). FTIR spectroscopy is an analytical technique used for both qualitative and quantitative measurements of mainly organic and inorganic materials. FTIR is used to identify the different chemical bonds in a molecule from the absorption of infrared radiation at various wavelengths. The ATR technique provides some conveniences such as investigation of samples directly without further preparation like mixing with Potassium Bromide (KBr) [29].

In this study, the vibrational spectra of geopolymer samples are collected using Bruker Vertex 80 V ATR-FTIR spectrometer. Spectra analysis is performed over the wavelength range of 4000 to 400 cm^{-1} at a resolution of 4 cm^{-1}. The geopolymer samples are grinded into powder, spread on the testing plate (ATR crystal) and pressed to obtain good contact before measurements. The effect of boron inclusion is investigated by analysis of the FTIR spectra of geopolymers.

2.2.2.3. Scanning Electron Microscope (SEM) Measurements. SEM is used to characterize the microstructure of geopolymers. The microstructure of the geopolymers are investigated using FEI-Philips XL30 ESEM-FEG SEM at an accelerating voltage of 5 and 10 kV. The external surfaces of the geopolymer samples are not used for measurements due to exposure to air during curing step which may lead to the formation of different microstructure that may not be seen in the entire geopolymer sample. All examined samples are coated before the SEM examination. The effect of the boron content on the geopolymer structure can be observed from SEM images.

2.2.2.4 Thermogravimetric Analysis (TGA). The weight loss versus temperature changes is measured by TGA. Information about the thermal stability of the samples is obtained. TGA is performed using TA Instruments TGA Q500 model instrument. The analysis is done by using Nitrogen at a flow rate of 40 cc/min and raising temperature of samples from room temperature to 800°C by 10°C/min. Approximately 20 mg of sample in powder form is loaded into a platinum pan for each measurement.

2.3. Results

The synthesized geopolymers with various molar B/Si ratios and with L/S ratios of 2.5 and 3 are characterized with a combination of different techniques. X-Ray Diffraction, FTIR spectroscopy, SEM and TGA tests are performed in order to investigate the variation of structural characteristics in this system.

2.3.1. X-Ray Diffraction (XRD)

X-ray diffraction is used to investigate the presence of crystalline components and amorphous character in the raw materials (borax and metakaolin) and the geopolymer samples. XRD pattern of metakaolin is shown in Figure 2.2.

Due to dehydroxylation process, achieved by heating kaolinite at 700 ^{o}C, characteristic crystal structure of kaolinite changes into the amorphous form given in Figure 2.2. The main feature in the XRD pattern of metakaolin appears at 20-28^{o} indicating the loss of crystallinity [25]. Quartz is present as a crystal component in XRD pattern of metakaolin.

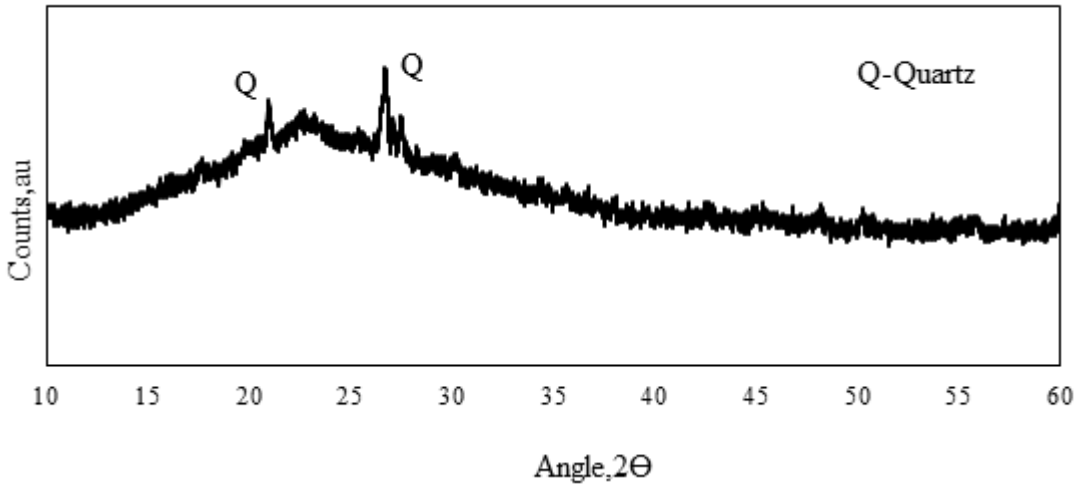

Figure 2.2. XRD Pattern of Metakaolin

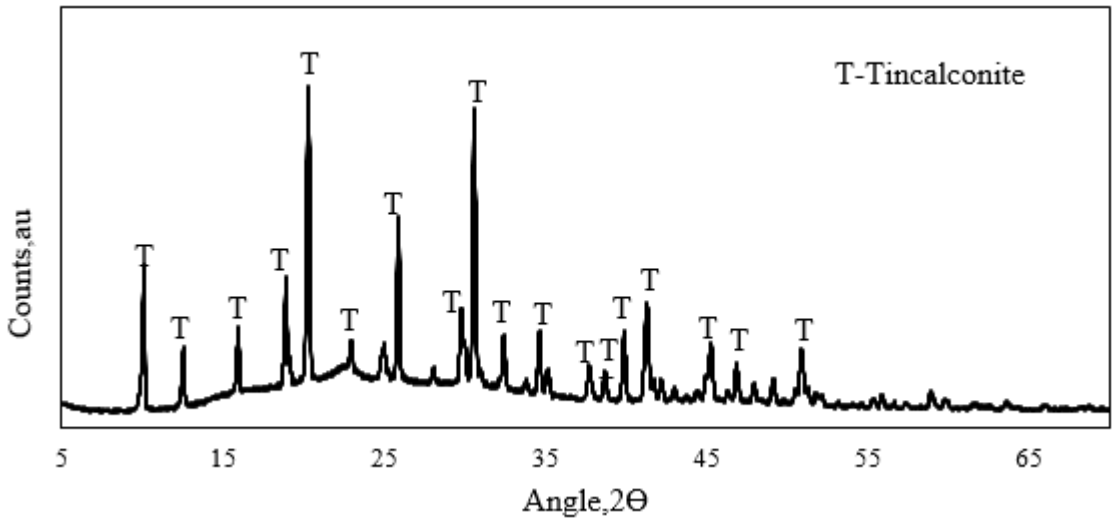

Figure 2.3. XRD Pattern of Anhydrous Borax

In Figure 2.2, XRD pattern of anhydrous borax is given. As it is pointed out earlier, anhydrous borax is obtained by heating borax decahydrate ($Na_2B_4O_7.10H_2O$) at 150 ^oC for 30 minutes followed by a subsequent heating process at 300 ^oC for 15 hours to get rid of intermolecular water.

As it is evident from Figure 2.3, boron source used in synthesis of geopolymer displays crystalline structure. Borax taken from EtiBOR consists of tincalconite mineral known as Sodium Borate Hydrate ($Na_2B_4O_7 \cdot 5H_2O$) according to Search &Match method applied on Eva (XRD software). The main peaks observed at 10.06^o, 20.28 ^{o}, 30.60^o, 41.33^o and 50.98^o are similar to the values reported in the literature [87, 88, 89].

The XRD pattern of borax-metakaolin based geopolymers with $0 \leq B/Si \leq 1.0$ (all with L/S ratio of 2.5) are presented in Figure 2.4. It is aimed to see the changes at the XRD patterns of geopolymers as a function of B/Si ratio. The XRD measurements are performed only for the specimens with L/S ratio as 2.5. XRD patterns for geopolymers with L/S ratio of 3 are not studied since their FTIR spectra are quite similar to the specimens with L/S=2.5. Geopolymer sample synthesized based on only metakaolin (GP 0-2.5) exhibits a broad feature located in the region between 20-28^o which is the indicator of formation of an amorphous matrix [25]. Quartz is also seen to be present in the structure of all the synthesized geopolymers. Addition of boron to the geopolymer system gives rise to systematic changes in geopolymer structure. To illustrate, tincalconite peaks are not observed at sample with B/Si Ratio of 0.5 (GP 0.5-2.5). Since there is no change in XRD pattern of the sample, the boron content can be considered as participated to the geopolymer structure. The main peaks of tincalconite positioned at 20.30 ^{o} and 30.56 ^{o} begin to appear at the geopolymer composition with molar B/Si ratio of 0.6 (GP 0.6-2.5). The intensity of tincalconite peaks increase with increasing B/Si ratio. The increase in the intensity of tincalconite peaks reveals the existence of boron content which does not contribute to amorphous geopolymer structure (presence of unreacted boron). The presence of tincalconite becomes more apparent in high boron containing geopolymers with molar B/Si ratio of 0.8 and 1. XRD patterns of these geopolymers also display silicon boron oxide- RUB-13 ($Si_{30.72}\ B_{1.28}\ O_{64}$).

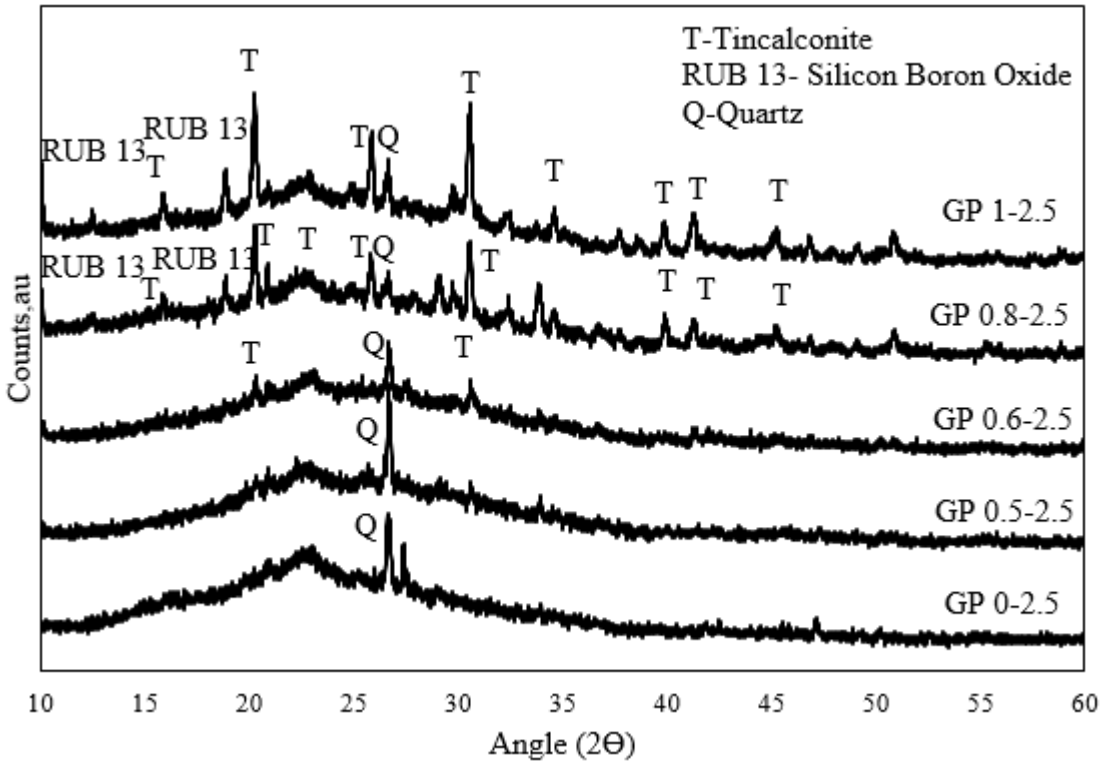

Figure 2.4. XRD patterns of borax-metakaolin based geopolymers with L/S= 2.5

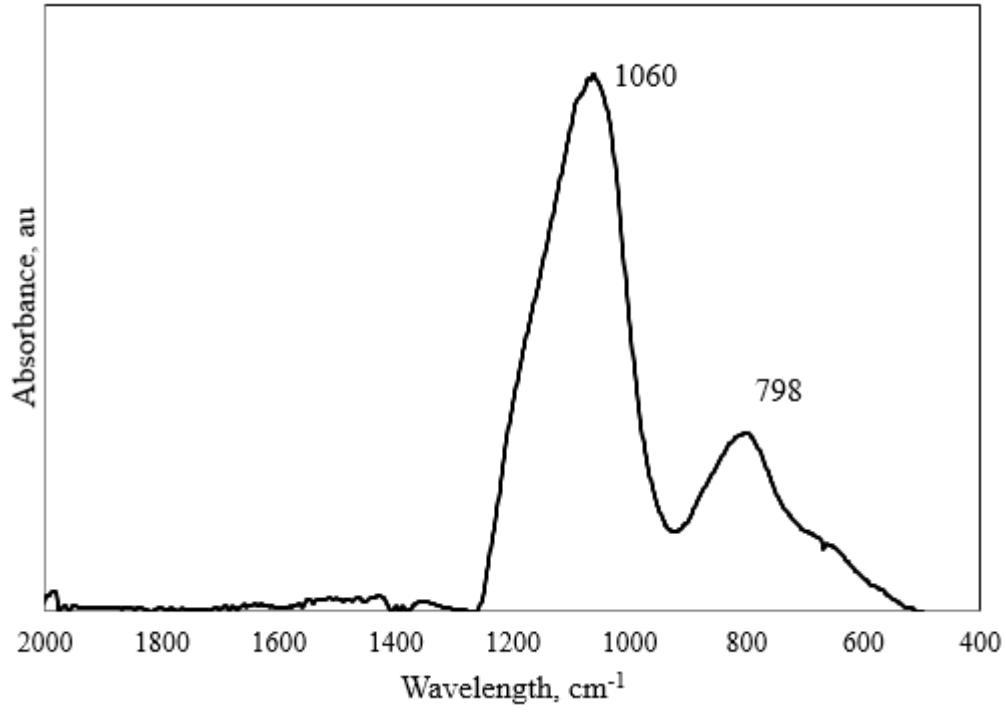

Figure 2.5. FTIR spectrum of metakaolin.

This formation is not encountered in geopolymers GP 0.5-2.5 and GP 0.6-2.5 which have relatively lower B/Si ratios, namely 0.5 and 0.6. A previous study on amorphous SiBCO ceramics claims that typical amorphous borosilicate peak centered at 22^{o} in XRD pattern corresponds to B-O-Si bond formation [60]. To sum up, according to XRD results, amorphous geopolymer structure is formed in borax-metakaolin based geopolymers. The amorphous character is preserved with boron addition in geopolymer system together with quartz and boron-including crystalline components. The intensity of peaks belonging to Tincalconite and RUB-13 crystalline phases increase in intensity with increasing amount of borax in the system.

2.3.2. Fourier Transform Infra-Red Spectroscopy (FTIR)

Figure 2.5 shows the FTIR spectrum of metakaolin. The sharp features in the FTIR spectrum of kaolinite mineral [25] is transformed into a form where the bands become much broader supporting the XRD results. FTIR spectrum of metakaolin is dominated by two broad peaks positioned at 1060 cm^{-1} and 798 cm^{-1}. The band with the highest intensity positioned at 1060 cm^{-1} is due to stretching Si-O bonds indicating amorphous SiO_2. The broad band appeared at 798 cm^{-1} shows the presence of vibrations of the AlO_4 tetrahedron in metakaolin.

Figure 2.6 presents the infrared spectrum of anhydrous borax. According to the FTIR analysis, the absorption bands are positioned at 705, 935, 983, 1336, 1662, 2352, 2904, 2989 and 3300 cm^{-1}. These peaks are compatible with characteristics peaks of tincalconite mineral which are positioned at 705, 941, 992, 1337 and 1658 cm^{-1} according to a study on utilization of tincalconite on hydrothermal synthesis of copper borates. The peaks between 1170–980 cm^{-1} shows the presence of asymmetric stretching of tri-coordinated boron (B_4O) [88]. The bands between 1400 and 1300 cm^{-1} might belong to asymmetric stretching of tri-coordinated boron B_3O [89]. The symmetric stretching of B_3O is observed between 980–870 cm^{-1}.

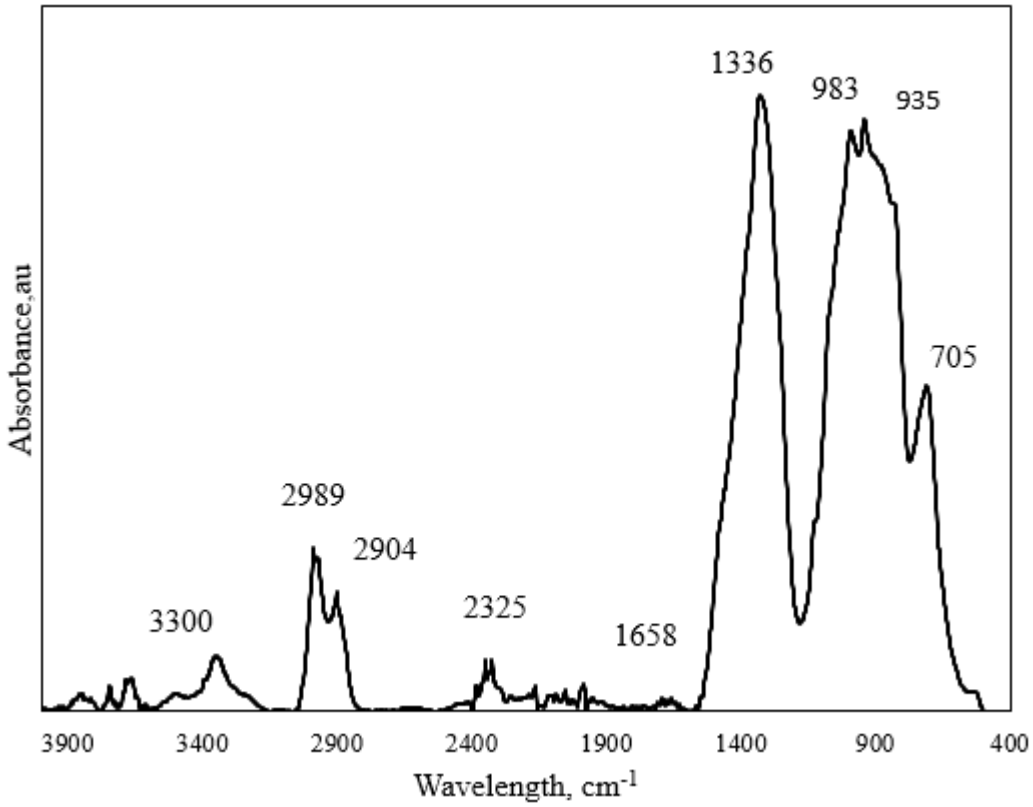

Figure 2.6. FTIR Spectrum of Anhydrous Borax

The peaks which are positioned lower than 750 cm^{-1} in the FTIR spectrum of tincalconite stands for the bending of B_3O [88]. The FTIR spectrum of boron source used in this study has also similar bands with sodium borates from different regions in Turkey [87, 89]. Due to the presence of water in the structure of borax, a broad band is observed in the hydroxyl region (3300 cm^{-1}) due to O-H stretching vibration.

The FTIR spectrum of borax-metakaolin based geopolymers with $0 \leq B/Si \leq 1.0$ for different liquid to solid (L/S) ratios of 2.5 and 3 are presented in Figure 2.7 and Figure 2.8, respectively. The Al–O and Si–O in plane and bending modes at 430 cm^{-1} are observed in all of the synthesized geopolymers irrespective of boron content in the system [31]. FTIR spectrum of metakaolin, one of the main raw materials in this system, displayed two broad features at 1060 and 798 cm^{-1} as mentioned above in Figure 2.6.

Upon geopolymerization, the main FTIR band of metakaolin shifts to 1050 cm^{-1} in Figure 2.7 indicating that a structural change took place. However, the feature at 810 cm^{-1} does not appear in fully reacted metakaolin based geopolymers [24]. As it is evident in Figure 2.7, the broad feature at 810 cm^{-1} is still predominant indicating that metakaolin has not fully reacted to form an amorphous geopolymer network. One reason of this could be the high L/S ratio maintained in this system.

High L/S ratio is selected in this study to be able to provide appropriate mixing of borax including activating solution. The peak in the 1050-1100 cm^{-1} region is related to the asymmetric Si-O-Al stretching and is denoted as main peak of geopolymerization [25, 30, 31]. This peak is seen in all of the geopolymer samples. In addition, it should be noted that the positon of this band does not change with varying B/Si ratios [32]. The intensity of the FTIR peaks of metakaolin- borax based geopolymers with L/S ratio of 2.5 generally increases systematically depending on B/Si ratio. As the B/Si ratio increases, Si-O stretching band at around 1050 cm^{-1} becomes sharper as demonstrated in Figure 2.7. The geopolymers with highest B/Si ratio (B/Si=1) have the sharpest and most intense peaks. The change in intensity of peaks is associated with the structural reorganization of the bonds. Furthermore, the peaks become narrower as it is evident from the existence of more crystalline phases in the XRD pattern of geopolymers (Section 2.3.1).

The presence of crystalline peaks are supported by XRD pattern of geopolymers with high B/Si ratio (B/Si is 0.8 and 1). As it is mentioned before, the intensity of crystalline phases related with the boron amount in geopolymer matrix. This situation is also consistent with observation of needle and star like structures in the SEM measurements as it is pointed out later which show the relatively high level of crystallinity in the samples B/Si ratio as 0.8 and 1.

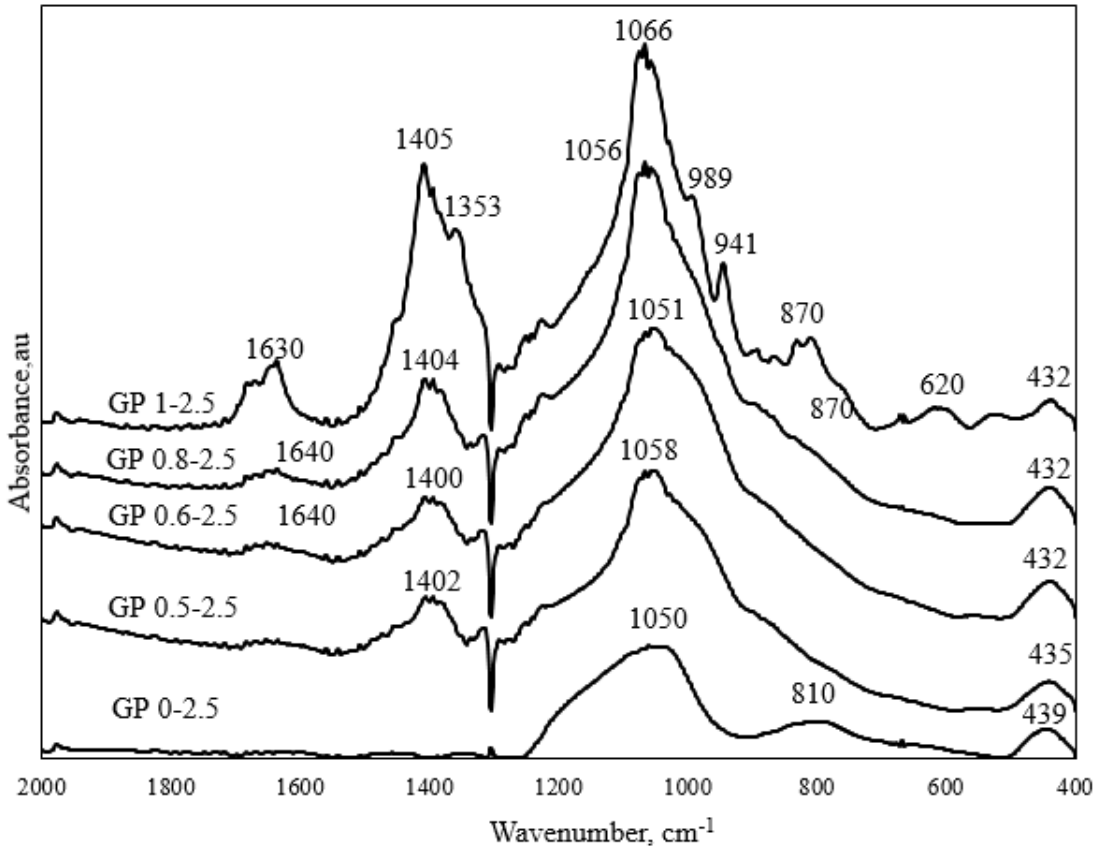

Figure 2.7. FTIR spectrum of geopolymers with Liquid/Solid Ratio of 2.5

The effect of boron addition leads to the formation of main B-O stretching bonds at 1400 cm^{-1} in all of the borax-metakaolin based geopolymer samples with $0<B/Si\leq1.0$ (Figure 2.7). The broad band at 1400 cm^{-1} is related with B-O asymmetric stretching of trigonal B. This band is considered as one of the most useful diagnostic bands for the presence of boron compounds [33]. The peaks at 1350 cm^{-1} is also belongs to the asymmetric stretching of tricoordinated boron [89]. The geopolymer with the highest boron content (L/S = 2.5 and B/Si = 1) displays a peak at 620 cm^{-1}. This peak is accepted as the fingerprint of the polyborosiloxane bridges, -B–O–Si– [34, 35]. Presence of this peak and the band positioned between 720- 900 cm^{-1} are evidences for the incorporation of boron atoms into the silica network [34]. The increase of amount of boron content gives rise to increases in the intensity of polyborosiloxane peaks.

The peaks at 941 and 989 cm^{-1} in Figure 2.7 indicates the presence of tincalconite mineral and are also observed in sample with L/S of 2.5 and B/Si of 1.

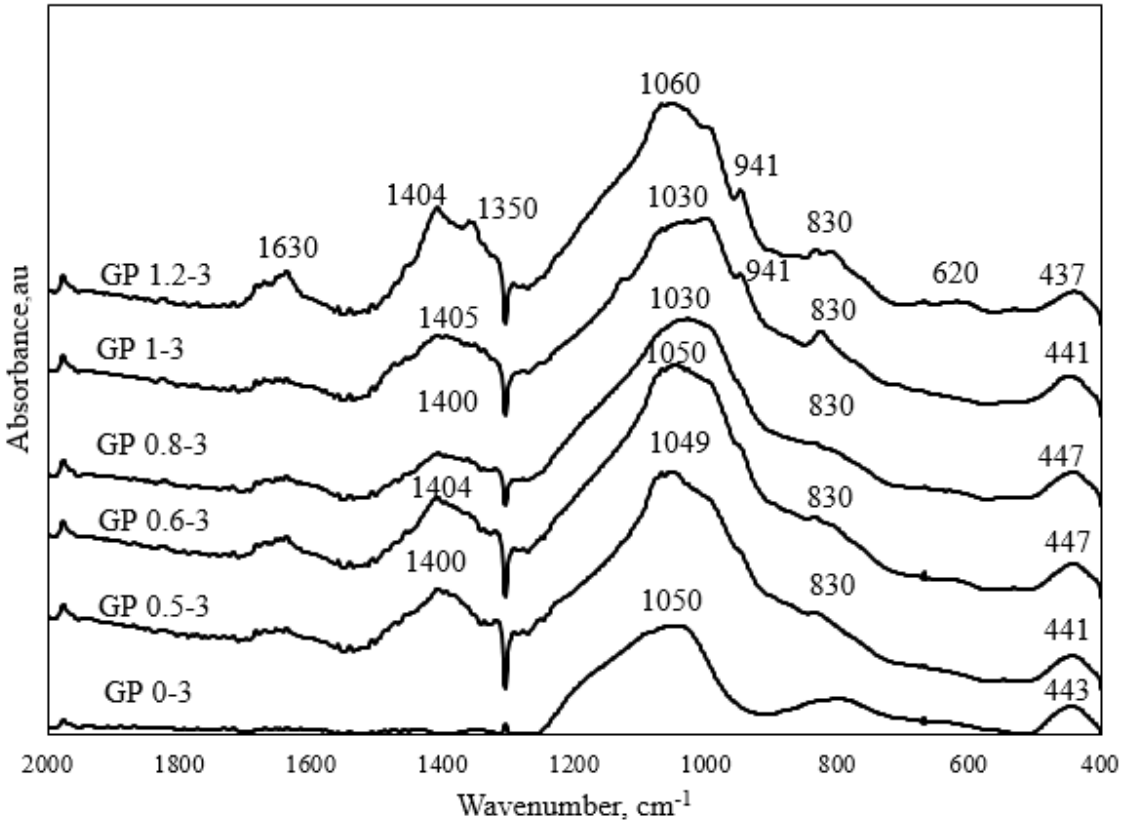

Figure 2.8. FTIR spectrum of geopolymers with Liquid/Solid Ratio of 3

The appearance of these peaks are the evidences of the presence of unreacted boron content which is also supported by XRD pattern of geopolymer with relatively high boron content (B/Si=0.8 and 1). The absorption bands around 1640 cm^{-1} is related to H-OH vibrations, corresponding to the presence of water in the geopolymer [31, 32]. Geopolymer samples with L/S ratio of 2.5 (Figure 2.7) have much narrower FTIR band widths compared to geopolymer with L/S ratio of 3 (Figure 2.8). Therefore, the samples with L/S ratio of 2.5, have more crystallinity than geopolymers with L/S ratio of 3 according to FTIR spectra. The water content may have effect on the crystallinity of the samples.

The geopolymers with L/S ratio of 3 have similar Si-O-Al and boron formations as illustrated in Figure 2.7 when compared with the geopolymers with L/S ratio of 2.5. The only difference can be stated as that the geopolymers with L/S ratio of 3 have more amorphous character compared to geopolymers with L/S ratio of 2.5.

2.3.3. Scanning Electron Microscopy (SEM)

SEM images of anhydrous borax at different magnifications are illustrated in Figure 2.9 a and b. Micromorphologies of the raw materials provides insights for understanding the effect of boron in metakaolin based geopolymers. In addition, unreacted phases present in the geopolymer structure can be identified from analysis of SEM images. Borax samples are spherical particles with varying sizes according to SEM images as in the study of borax included polymer composites [44]. In one of the previous studies which utilize the borax samples taken from different areas of Turkey to determine their neutron transmission properties, the borax samples are also presented as spherical shapes but they have also particles with sharp edges [87]. This difference might be resulting from the heating of borax to obtain anhydrous borax.

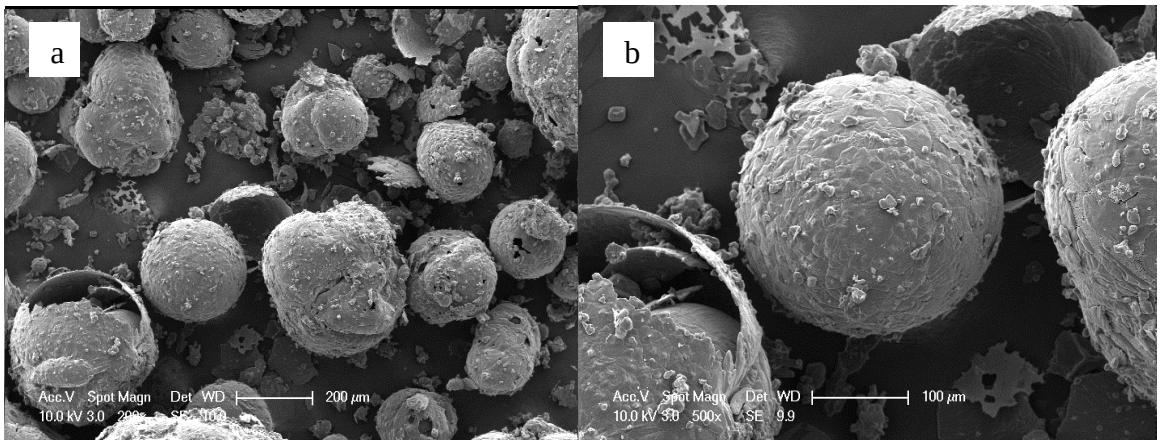

Figure 2.9 (a). SEM micrograph of the anhydrous borax at 100X (b) at 500X thermally treated

The Figure 2.10 shows SEM images of metakolin based geopolymer with B/Si ratio of 0 at different magnifications. The microstructure of this geopolymer is composed of 2 different regions as pointed with red circles. The discrete, flake shaped particles are observed in the region highlighted by the right circle whereas the area shown by the left circle consists of dense, continuous surfaces without layer formation or particle boundaries. Due to almost pure structure of metakolin, the impurities are not seen in the geopolymer structure. The presence of layers in the synthesized geopolymer surface is possibly associated with unreacted metakaolin particles due to high L/S ratios. High L/S ratio is chosen to dissolve borax component homogenously in geopolymer mixture. L/S ratio is determined to be constant in all samples. High L/S ratio might have a negative effect on geopolymerization reaction and also may lead to presence of unreacted metakaolin as in Figure 2.10. The effect of water on the compressive strength of geopolymers is investigated in the previous studies in literature. In the study which effect of water to geopolymer binder ratio was analyzed for the fly ash based geopolymers, it is observed that the compressive strength of fly ash based geopolymers decreases with increase of water-to-geopolymer binder ratio [48]. The presence of excess water leads to low compressive strength as a result of slower geopolymerization.

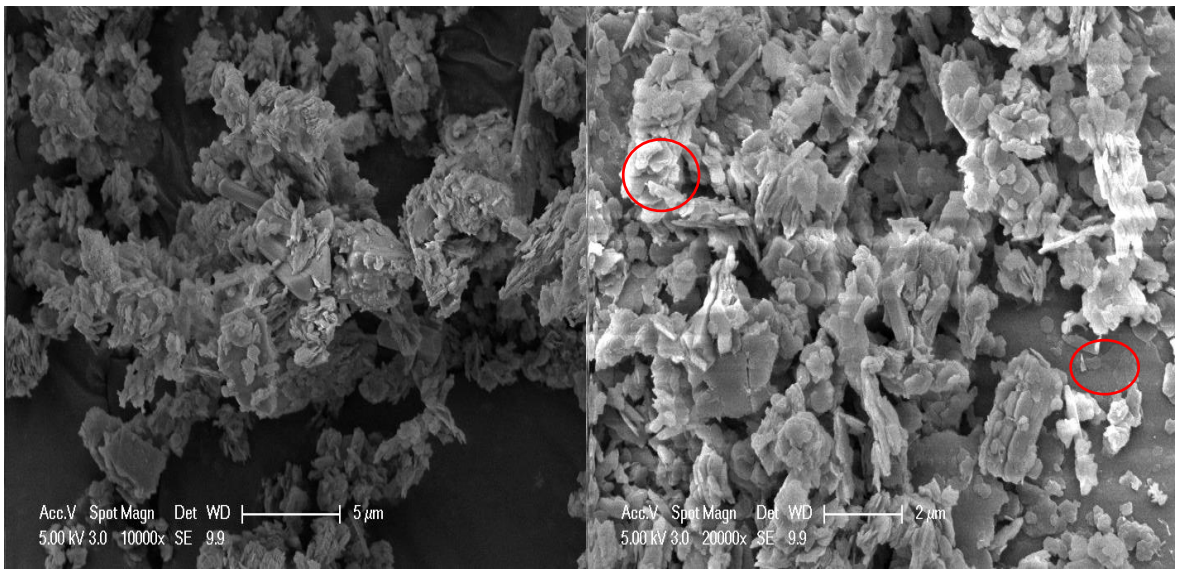

Figure 2.10. SEM micrograph of the geopolymer without borax content

The SEM morphologies of borax-metakaolin based geopolymers with different B/ Si molar ratios ($0 < B/S \leq 1$) are given at Figure 2.11. The microstructures of the geopolymers with varying B/Si ratios are different than each other. To illustrate, geopolymers with B/Si ratios of 0.5 and 0.6 have smooth surfaces. The star-like needles and micro scale long needles appear in geopolymers with B/Si ratios of 0.8 and 1 due to increase of the amount of borax in geopolymer matrix. These samples also have rougher surfaces compared to geopolymers with low B/Si ratios of 0.5 and 0.6. Geopolymers with boron content ($0 < B/Si \leq 1$) have more continuous and relatively dense phase while geopolymer without boron content (GP 0-2.5) is more bulky. The unreacted particles displayed as layers are less visible in boron containing samples compared to the samples without boron as in Figure 2.10. However, the unreacted metakolin flakes still preserve their presence with increasing B/Si ratio. As mentioned before broad feature at 810 cm^{-1} in the FTIR spectrum of geopolymers are seen in all of the geopolymers indicating that metakaolin has not fully reacted to form an amorphous geopolymer network without depending on B/Si ratio. The SEM and FTIR results are consistent as they reveal the unreacted metakaolin in geopolymer system. The star and needle-like crystal formations are pointed with red cycle in the left whereas the unreacted metakolin flakes are shown with the cycle in the right.

Needle and star like crystals structures are not observed in traditional aluminosilicate geopolymers. These structures can be taken as proof of formation of boron containing crystalline phases. This claim is supported by XRD patterns of geopolymers with borax inclusion due to presence tincalconite and RUB-13 compounds. Needle like structures appear as similar to tubular rectangular crystals with sharp edges which belong to tincalconite mineral [87].

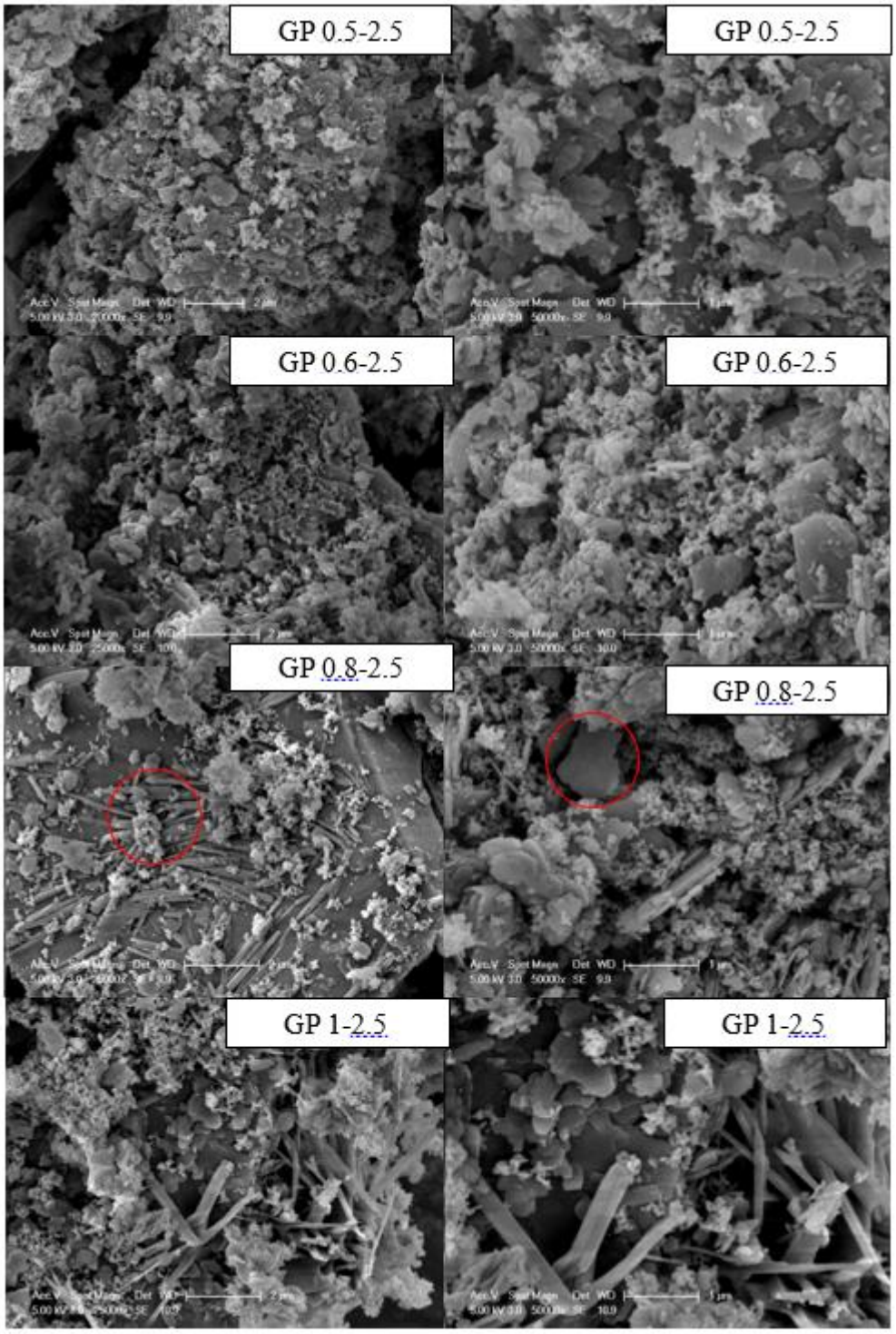

Figure 2.11. SEM micrograph of the borax- metakaolin based geopolymers

2.3.4. Thermogravimetric Analysis (TGA)

In order to understand the effect of boron inclusion on thermal behavior of geopolymers, TGA of geopolymers are utilized. TGA graph of metakaolin is given in Figure 2.12. Weight loss of metakaolin consists of two stages. The first stage lies within the temperature up to 492 °C and the second stage comprise the region between 492-650 °C. From the TGA curve of metakaolin, it is possible to say that there is a linear loss observed up to 492 ºC. The weight loss in this region (first phase) is about 0.6 %. At the end of the heating up to 650 °C, metakaolin loses 1.1 % of its total mass.

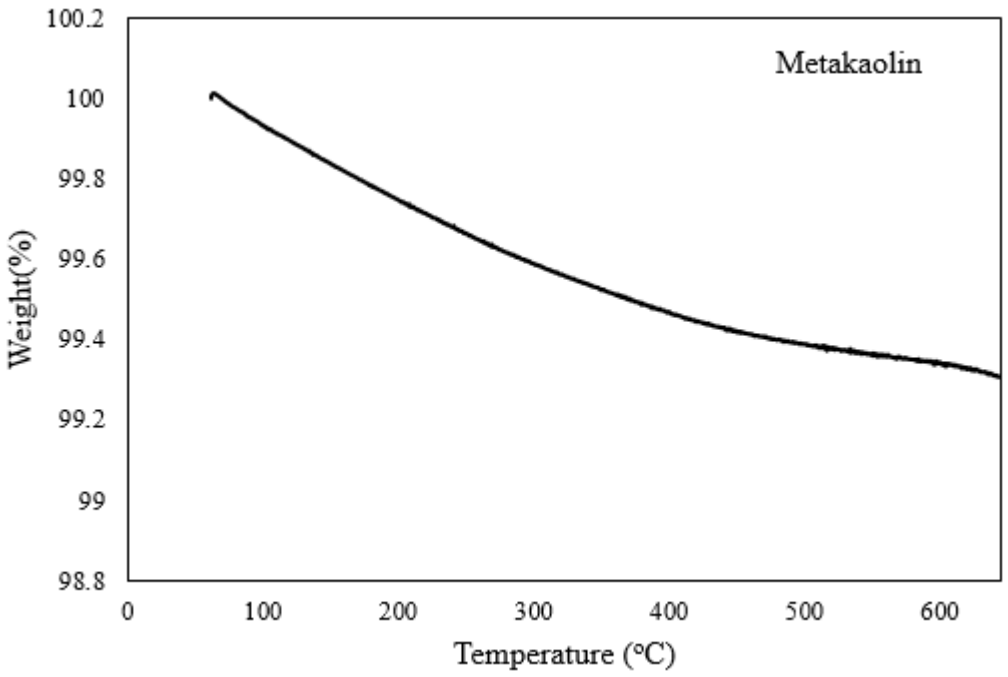

Figure 2.12. TGA curve of metakaolin

The reason of the low total weight loss of metakaolin could be related with loss of water content while it is transformed from kaolinite by heating. Thermal behavior of metakaolin is compatible with the TGA curve in the previous study associated with investigation of the thermal response of metakaolin-phosphoric acid based geopolymers [61]. Weight loss at the first stage can be considered as evaporation of free water.

On the other hand, weight loss in the second stage results from also physio-chemically bonded water molecules in the structure.

Figure 2.13 shows the thermogravimetric analysis of borax-metakaolin based geopolymers with different B/ Si molar ratios ($0 \leq B/Si \leq 1$). Based on TGA results, it is easily seen that geopolymers present different thermal behaviors compared to metakaolin. This can be explained by presence of higher amount of water in the structure of geopolymers. In the study including waste catalyst-metakaolin based geopolymers, the thermogravimetric steps for the performance of thermogravimetric analysis of geopolymers are classified as i) dissipation of free water molecules, ii) decomposition of geopolymer components, iii) dehydroxylation of zeolitics, iv) stabilization of the weight [86]. The thermal curve of only metakaolin based geopolymer includes three thermal stages according to Figure 2.12. At first, the weight loss displays as linearly up to approximately 104 °C as 3.14%.due to removal of free and interstitial water. After this point, different thermal behavior occurs in a slower rate up to 450 °C which stands for the elimination of structural water. The weight loss of metakaolin based geopolymer stabilizes after 450 °C. After this point, weight loss of geopolymer is ended. The total weight loss of the geopolymer is about 6.52 %.

Thermal behavior of borax- metakolin based geopolymers includes also three sequential thermal stages. Most of the weight loss is observed at the first stage up to 145 ^{o}C. The weight loss observed in this region is related to the evaporation of free water from the geopolymer surface [85]. Moreover, loss of Si-OH groups also occurs at this stage. In the second stage which lies between the temperatures 150-450 °C, the weight loss is considered as a result of dehydration of chemically bonded water.

The weight loss increases and becomes more visible with the increasing B/Si molar ratio. To illustrate, the weight loses are 9.41%, 10.26 %, 11.73% and 14.61% for borax-metakaolin based geopolymers with B/Si ratios of 0.5, 0.6 0.8 and 1; respectively. This result can be explained with increased water molecules trapped in the geopolymer structure due to increased boron.

TGA results are compatible with the FTIR findings as exhibiting an increase in the intensity of the FTIR bands at 1600 cm^{-1} which is correlated with the existence of water in the geopolymeric system.

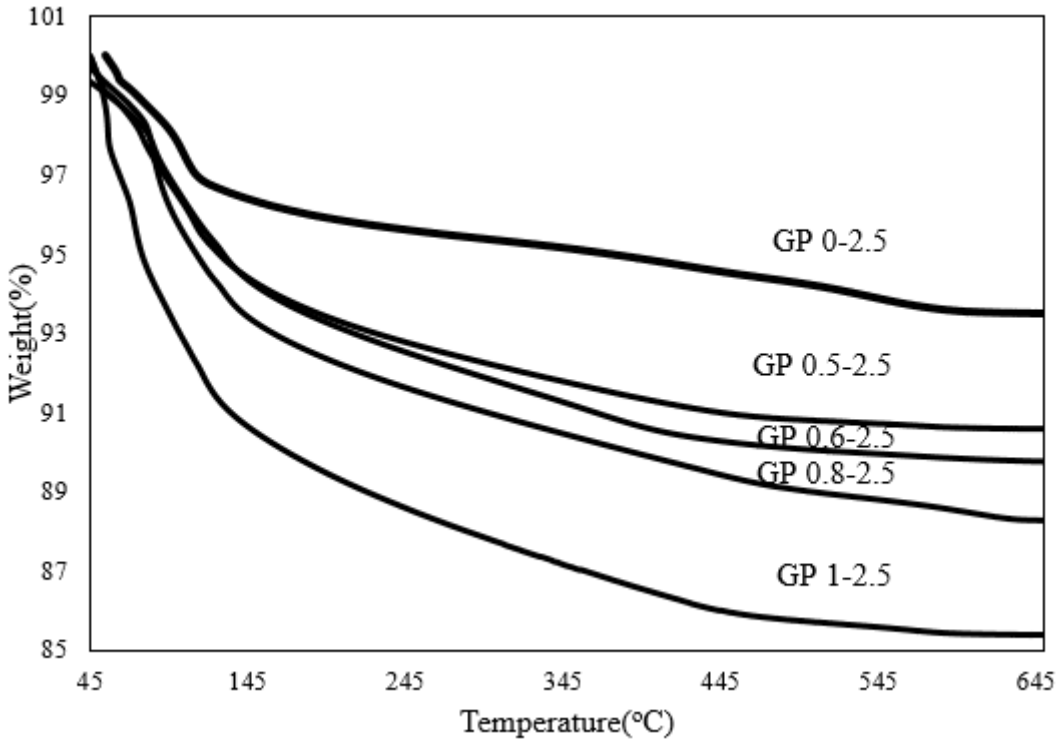

Figure 2.13. TGA curve of geopolymers with differerent B/Si content

In one of the previously studied research on boron nitride coated pyrolytic carbon particles, weight loss of carbon particles with and without boron nitride coatings are very close to each other before 650 °C [62]. The reason of this results is explained with the removal of water content absorbed by amorphous boron nitride up to this point. After 650 °C, the effect of boron nitride on thermal behavior is clearly seen due to higher weight loss of carbon particles without boron reaching up to 100 % at 920 °C. On the other hand, the weight loss of particles with boron nitride remains 60% at 1200 °C. Therefore, in order to see the effect of boron addition in this part, the TGA curves might be studied at higher temperatures.

2.4. Conclusions

In this part of the thesis, borax-metakaolin based geopolymers are synthesized with different B/ Si molar ratios (0 <B/S≤ 1) and analyzed with different characterization techniques including XRD, FT-IR spectroscopy, SEM and TGA. In order to observe of the effect of water content, L/S ratio is changed as 2.5 and 3.

According to XRD results, amorphous structure of geopolymers is preserved with borax addition. The crystalline phases stand for unreacted boron, exhibiting an increasing fashion with the amount of borax in the geopolymer mixture. The main geopolymerization peak which shows the presence of asymmetric Si-O-Al stretching is observed in all of the geopolymer samples. The FTIR spectrum of geopolymers support the XRD results since FTIR peaks become narrower showing the presence of more crystalline phases. The intensity of main geopolymerization peak increases as the B/Si ratio is increased. SEM results also show evidences of the crystalline structures in the form of needle and star like structures. The B-O peak appears at geopolymer which has B/Si ratio of 0.6 which shows the presence of unreacted boron. The characteristic band of metakaolin standing for the Al-O stretching disappears as the amount of boron increases. Therefore, addition of boron to geopolymer matrix has a positive effect on geopolymerization reactions. The geopolymers with highest B/Si ratios as 1 show the peaks considered as fingerprint of the polyborosiloxane bridges (-B–O–Si–). Presence of this bond is the evidence the incorporation of boron atoms into the geopolymer network. The crystallinity of samples could be associated with increase of L/S ratio according to FTIR results.

According to TGA results, the weight loss of geopolymers is higher for the geopolymers with boron content in spite of the high thermal stability of boron. This is the consequence of removal of moisture absorbed by amorphous boron content in the geopolymers. The effect of boron addition should be studied at higher temperatures.

3. COMPARISON OF THE STRUCTURAL CHARACTERISTICS OF BORAX-METAKAOLIN AND BORAX-FLY ASH BASED GEOPOLYMERS

3.1. INTRODUCTION

Global warming is one of the crucial treats to world by affecting the environment and leading to climate change. Carbon dioxide (CO_2) is known as a major reason of global warming. Therefore, the researches related to the reduction of CO_2 concentration in atmosphere gain importance [95]. Cement production causes 6-7 % of total CO_2 emissions in world. Nearly two billion tons of CO_2 is emitted annually for two billion cement produced. 3.5 billion tones CO_2 is expected to be released by 2025 if the cement production continues with that pace. This amount is almost equal to total CO_2 emission of Europe now from all of the industrial groups [97]. Beside the studies aiming to lower CO_2 emission, the researchers started to focus on environmentally friendly, alternative building materials to Portland cement.

The search for alternative materials to Portland cement leads to utilization of studies with alkali-activated materials. The pioneering work associated with alkali cement belongs to Purdon in 1940 and Glukhovsky in 1957 [74]. The term “geopolymer” is given by Joseph Davidovits in 1972 to a group of alkali activated binders [74, 98]. Natural aluminosilicate sources such as metakaolin or industrial byproducts such as fly ash and rice husk reacts with alkaline liquid to produce geopolymers. The geopolymerization reaction results in formation of a three-dimensional polymeric chain and ring structure consisting of Si-O-Al-O bonds [3].

Geopolymers display superior characteristics such as high compressive strength, low shrinkage, acid resistance, fire resistance and low thermal conductivity [17, 18, 19, 20].

Therefore, geopolymers are utilized at wide variety of application areas such as construction and immobilization of toxic and radioactive waste [72].

In this study, the employment of two different aluminosilicate source, metakaolin and fly ash, are utilized in geopolymerization reaction with the addition of varying amounts of boron to geopolymer matrix. Metakaolin is chosen as aluminosilicate source since it is known to be active for geopolymerization [25] and being a relatively pure compound compared to industrial wastes such as fly ash and red mud. The utilization of pure aluminosilicate source could provide advantages to analyze the effect of boron addition to geopolymer structure. Fly ash is an industrial waste obtained from thermal power plants. Globally, 750 milliom tones of fly ash is produced ever year [74]. The fly ash produced in Turkey is about 15 million tons annually; however, only 1% of the total amount is used in cement and brick production process [93]. Fly ash is classified according to its calcium content. To illustrate, the class F fly ash have calcium content smaller than 20 %. On the other hand, the calcium content in class C fly ash is higher than 20 % [9]. Most of the studies including fly ash based geopolymers, utilize class F type fly ash [72, 74, 69]. Although class C fly ash includes also silica and alumina, the amount is comparable lower than class F fly ash. Therefore, potential utilization of class C fly ash in geopolymerization reactions is a new research area since there are only a few studies in the literature as far as our knowledge [82]. Borax is added to geopolymer matrix during production of geopolymers. Similar to fly ash, borax ores are produced in huge amounts due to great boron reserves of Turkey. Therefore, new industrial areas might be created both for the fly ash and borax such as construction. Moreover, to the best of our knowledge, there are quite rare studies associated with the use of boron in geopolymerization. The utilization of boron synergistically with metakaolin in geopolymer sytnthesis in this thesis will be the first research as far as we know. Borax and fly ash are used in order to produce boroaluminosilicate geopolymers by Nazari [23, 24]. FTIR and SEM techniques are used to investigate the effect of borax on geopolymer structure. However, the synthesis procedure is different in this thesis. Nazari employed class F type fly ash whereas class C type fly ash is utilized in this thesis during geopolymer synthesis.

Williams and Riesen studied on borosilicate geopolymers with the utilization of silica fume and borax. XRD and SEM measurements are performed for characterization in their work [22].

This study aims to synthesize and characterize borax- metakaolin and borax-fly ash based geopolymers in order to evaluate their structural characterstics comparatively. The specimens with different B/Si ratios in the range between 0 and 1 are prapared. In order to obtain various molar B/Si ratios, the amount of aluminosilicate source and borax in the geopolymer matrix are changed. The main focus of this study are to investigate the effect of boron on structural properties of metakaolin and fly ash based geopolymers. The structural characterization techniques utilized for this purpose are X-Ray Diffraction (XRD), Fourier Transform Infrared Spectroscopy (FT-IR), Raman Spectroscopy, Scanning Electron Microscopy (SEM) and Termogravimetric Analysis (TGA). The effect of boron inclusion on mechanical strength of geopolymers are also analyzed with the help of compressive strength measurements.

3.2. Experimental

In this study, geopolymers are synthesized with different aluminosilicate sources which are metakaolin and fly ash. Boron content in the geopolymers are also varied to investigate the effect of boron inclusion on geopolymer structure. Geopolymer synthesis route is different compared to the first part of the thesis and also the studies related to boron inclusion to geopolymer matrix in literature [23, 24]. The previous studies associated with synthesis of boroaluminosilicate geopolymer included borax and fly ash as raw material. The synthesis route involves mixing of NaOH solution and borax at first. This solution is called as activating solution and mixed with fly ash. In this study, aluminosilicate source is mixed with borax initially and then sodium silicate solution is added to geopolymer matrix. The synthesized geopolymers are analyzed by utilization of X-Ray Diffraction (XRD), FT-IR spectroscopy, Raman spectroscopy, Scanning Electron Microscopy (SEM) and Thermogravimetric analyses (TGA).

In order to investigate the effect of varying B/Si ratio on mechanical characteristics of geopolymers, compressive strength measurements are also performed.

3.2.1. Synthesis Procedure

The borax- metakaolin and borax- fly ash based geopolymers with varying boron content ($0 \leq B/Si \leq 1$) are produced in this part of the research. As in the first part of the thesis (Chapter 2), the first step includes the calcination of kaolin at 700 ^{o}C at atmospheric pressure for 1 hour in order to transform kaolinite to metakaolin. According to a previous study concerning the effect of calcination temperature of kaolinite on geopolymers, 700 ^{o}C is selected as the optimum calcination temperature since the setting time of geopolymers with metakaolin reduces as temperature is increased up to 700°C [63]. After heat treatment, metakaolin is allowed to rest for 1 day before being used in geopolymerization. The chemical composition of metakaolin used in this study is given at Table 3.1.

The fly ash is obtained from Yatağan Thermal Power Plant. A thermal pretreatment is not applied to fly ash before geopolymer synthesis. The chemical compositions of metakaolin and fly ash are presented in Table 3.1. It is possible to say that metakaolin is a relatively pure aluminosilicate source compared fly ash since it includes high amounts of calcium oxide (about 24%) and sulfur trioxide (about 10%) together with Al_2O_3, SiO_2,Fe_2O_3, and other oxides.

Table 3.1. Chemical Composition (wt %) of metakaolin and fly ash

Compound	Metakaolin	Fly Ash
SiO_2	56.21	23.92
Al_2O_3	41.04	11.4
CaO	0.09	24
SO_3	-	9.523
Fe_2O_3	0.36	6.064
K2O	0.46	1.88
MgO	0.09	1.49
TiO_2	1.15	0.628
Na_2O	-	0.22
P_2O_5	0.06	0.078

The borax decahydrate obtained from ETİBOR is used as boron source. In order to obtain anhydrous borax, borax is hydrated as heating borax decahydrate ($Na_2B_4O_7.10H_2O$) at 150 ^oC for 30 minutes. Then, it is subsequently heated at 300 ^oC for 15 h to remove intermolecular water.

Sodium silicate (9% of Na_2O, 28% of SiO_2, 63 % of H_2O with 1.401g/ml of density at 20 ^oC) is used as the activating solution. Sodium silicate solution is mixed with distilled water to prepare the activating solution.

In the first experiment set in Part 3, metakaolin is used as the aluminosilicate source. The geopolymer synthesis is illustrated in Figure 3.1. The procedure involves the following steps:

(i) Calcination of kaolinite to obtain metakaolin (1 hour at 700 ^oC),

(ii) Calcination of borax decahydrate to obtain anhydrous borax (150 ^oC for 30 minutes, then, 300 ^oC for 15 hours),

(iii) Mixing of metakaolin and anhydrous borax (solid mixture),

(iv) Addition of sodium silicate solution to solid mixture,

(v) Heat treatment of geopolymers (70 ^oC for 1 day and subsequently resting at room temperature for 3 weeks).

In the second experiment set in Part 3, fly ash is used as the aluminosilicate source. The geopolymer synthesis is illustrated in Figure 3.2. The procedure involves the following steps:

(i) Calcination of borax decahydrate to obtain anhydrous borax (150 ^oC for 30 minutes, then, 300 ^oC for 15 hours),

(ii) Mixing of untreated fly ash and anhydrous borax (solid mixture),

(iii) Addition of sodium silicate solution to solid mixture,

(iv) Heat treatment of geopolymers (70 ^{o}C for 1 day and subsequently resting at room temperature for 3 weeks).

Table 3.2 presents all of the geopolymer compositions that are studied in this part. The geopolymer samples are named based on their B/Si and aluminosilicate source respectively. For instance, GP- M 0.5 represent the geopolymer which has B/Si ratio as 0.5 molar percent and metakaolin is used as aluminosilicate source during geopolymerization. GP- F 0.5 is stands for the geopolymer with B/Si ratio of 0.5 and produced with fly ash. The liquid to solid ratios (L/S) that are used are 2.5 for borax-metakaolin based geopolymers and 3 for borax-fly ash based geopolymers. Previous studies indicate that in order to obtain geopolymers with high compressive strength values molar Si/Al and Na/Al ratios should be selected as in the regions between 1.8–2.2 and 0.9–1.2, respectively [22, 64, 65]. Hence, amount of sodium silicate is calculated according to the decided Si/Al molar ratio which is fixed at 1.8 for metakaolin based geopolymers. The Si/Al ratio is 1.16 for the raw metakaolin.

With the aim of increasing this ratio to 1.8 for borax-metakaolin based geopolymers, the required amount of sodium silicate solution is added during synthesis. Sodium Silicate solution is used as activator to obtain geopolymers with Si/Al ratio as 2.40. The Si/Al ratio of raw Fly Ash is 1.77. Sodium Silicate solution is used as activator to obtain borax-fly ash based geopolymers with Si/Al ratio as 2.40. The amount of boron is varied in geopolymers; the all of the geopolymers display B/Si ratios between 0 and 1 (Table 3.2). Na/Al is obtained as 1.2 for the metakolin based geopolymers without boron addition. However, increase of the boron addition leads to increase of Na content due to presence of Na in anhydrous borax. Therefore, Na/Al ratio is changing in the 1.2-2 range according to boron content of the borax-metakaolin based geopolymer (Table 3.2). Na/Al ratio is 1.29 for the fly ash based geopolymer with no boron content. This ratio increases up to 2.48 with changing B/Si ratio.

In the second part of the thesis, anhydrous borax and sodium silicate is mixed at different concentrations during the synthesis of alkali activator (activating solution) before addition of metakaolin. However, the mixture of activating solution and aluminosilicate source become too viscous to mix. Therefore, it could be possible to encounter unreacted aluminosilicate source after geopolymerization. In the first experimental set in this part of the thesis, metakaolin and boron source are blended initially (solid mixture). Afterwards, the activating solution is added to solid mixture and mixed by mechanical stirrer. The mixing of components is continued for 10 minutes until obtaining a homogenous solution. The geopolymer paste is allowed to rest at room temperature for 1 day after transferring into molds with dimensions 4cm x 4 cm x 3 cm. Thermal treatment procedure for geopolymer synthesis includes curing at 70 ^{o}C for 1 day and waiting subsequently at room temperature for 3 weeks. The molar Si/Al is 1.16 for all the synthesized geopolymer whereas Na/Al ratios change between 1.27 and 2.17. B/Si molar ratio varies between 0 and 1. With the aim of the see the effect of boron compounds, the reference geopolymer is synthesized without adding borax content. The molar ratios of the synthesized geopolymers are illustrated in Table 3.2.

In the second experiment set in this part of the thesis, fly ash is used as aluminosilica source for the geopolymer production. First of all, borax decahydrate is thermally treated to transform into anhydrous borax as mentioned before. Fly ash and anhydrous borax is mixed subsequently. (Solid mixture). This solid blend which includes boron and fly ash is mixed with Sodium Silicate solution. After mixing solid blend with activator solution for 10 minutes, geopolymers are poured into molds with 4cm x 4 cm x 3 cm dimensions. They are allowed to rest for one day before heating in the furnace. The synthesized borax-fly ash based geopolymers are cured at 70 ^{o}C for one day followed by further treatment at room temperature for 3 weeks. Characterization and performance tests are utilized after curing period.

The chemical compositions of metakaolin and fly ash based geopolymers are illustrated at Table 3.2.

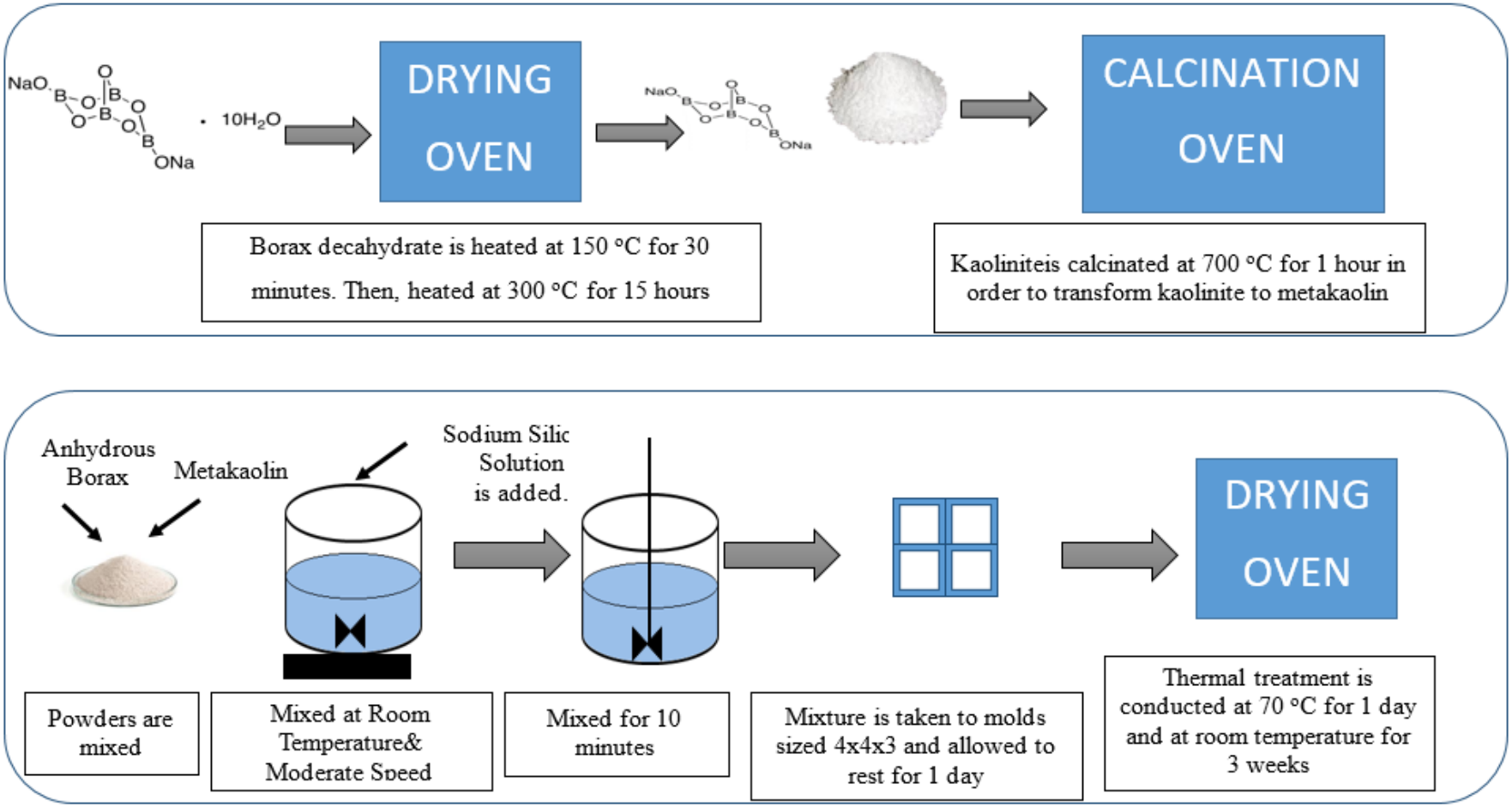

Figure 3.1. Synthesis procedure of borax-metakaolin based geopolymers

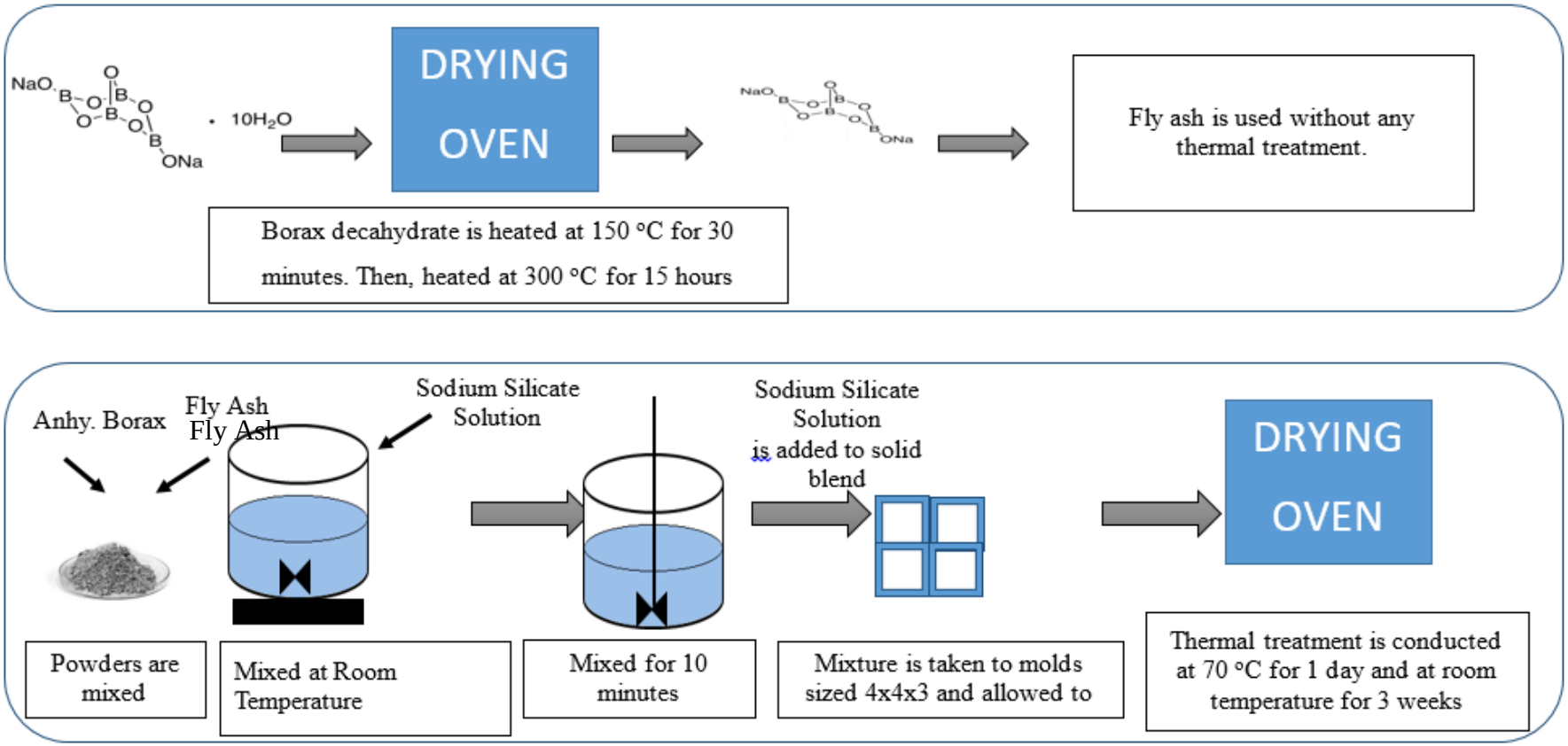

Figure 3.2. Synthesis procedure of borax- fly ash based geopolymers

Table 3.2. The chemical compositions of metakaolin and fly ash based geopolymers

Geopolymer	**B/Si**	**Aluminosilicate Source**	**Si/Al**	**Na/Al**	**Na/Si**	**Ca/Si**	**Cal/Al**	**L/S**
GP M-0	0	Metakaolin	1.80	1.27	0.70	-	-	2.5
GP M-0.5	0.5	Metakaolin	1.80	1.72	0.96	-	-	2.5
GP M-0.6	0.6	Metakaolin	1.80	1.81	1	-	-	2.5
GP M-0.8	0.8	Metakaolin	1.80	1.99	1.11	-	-	2.5
GP M-1	1	Metakaolin	1.80	2.17	1.20	-	-	2.5
GP F-0	0	Fly Ash	2.40	1.29	0.54	1.07	1.91	2
GP F-0.5	0.5	Fly Ash	2.40	1.88	0.79	1.07	1.91	2
GP F-0.6	0.6	Fly Ash	2.40	2.0	0.84	1.07	1.91	2
GP F-0.8	0.8	Fly Ash	2.40	2.24	0.94	1.07	1.91	2
GP F-1	1	Fly Ash	2.40	2.48	1.04	1.07	1.91	2

3.2.2. Characterization Techniques

3.2.2.1. X-Ray Diffraction (XRD). X-Ray diffraction is used in order to analyze the crystalline nature of the specimens. The diffraction pattern obtained from XRD measurements is used to qualitatively identify the crystalline phases present in geopolymers. The elements in the sample can be identified since each pattern belongs to specific element or crystalline structure.

The produced geopolymers are analyzed by Bruker D8 Discover diffractometer The instrument has a CuK radiation source employing a wavelength of 1.5418 Å. The measurements are performed in 2θ range of 10-90o with step size of 0.01263°.

3.2.2.2. Attenuated total reflectance - Fourier transform infrared spectroscopy (ATR-FTIR). Fourier Transform Infrared Spectroscopy is a vibrational spectroscopy technique which is widely used in industry to characterize the materials. This characterization technique can be used to obtain information concerning chemical structures and physical properties of samples as providing FTIR spectra just like fingerprint of the chemical structures. FTIR analyses present the vibrational modes in a structure such as bending and stretching vibrations. These characteristics taken from FTIR measurements give information on the functional groups in geopolymers including configuration of atoms and molecules.

Since the geopolymers are classified as amorphous to semi-crystalline aluminosilicate materials, they generate broad halo peak when they characterize with diffraction techniques instead of sharp diffraction. Therefore, evaluation of spectrum techniques with diffraction techniques provides more comprehensive understanding of molecular structure.

FTIR spectroscopy (Vertex 80v spectrometer, resolution: 4 cm^{-1}, Bruker) is performed in 400–2000 cm^{-1} spectral region to obtain the vibrational spectra of the synthesized geopolymers.

3.2.2.3. Raman Spectroscopy. Raman spectroscopy is a vibrational spectroscopic technique like Fourier Infrared Spectroscopy. However, Raman spectroscopy can provide certain information which Fourier Infrared Spectroscopy technique cannot give as a result of its different working principle. Infrared spectroscopy is based on the change of dipole moment of a molecule arising from the interaction of the molecule with light whereas Raman spectroscopy is based on the change in the polarizability of molecule [66].

Geopolymers are produced from the reactions of aluminosilicate source and activating solutions. The structural formation regarding the degree of polymerization is easily detected by Raman spectroscopy based on the vibrational fingerprint of the specimens [67]. Furthermore, in order to detect the boron configuration in geopolymer matrix, Raman spectroscopy is selected as one of the characterization methods. Borosilicate systems can also be studied by Raman spectroscopy to obtain information about their structure [78].

Raman spectroscopy is carried on by Renishaw in Via Raman Microscope. Raman spectroscopy system works in single monochromator mode. Microscope objective is with 5 times magnification. The 514 nm Argon Ion laser is used with 20 mW power. The exposure time is 10 seconds whereas number of accumulations are 5. The Raman spectra are recorded in the region of 200–1800 cm^{-1}.

3.2.2.4. Scanning Electron Microscopy (SEM). Scanning electron microscopy is used to analyze the surface morphologies of the samples. The conjunctive evaluation of microscopic measurements with spectroscopic and diffraction methods are crucial to detect the effect of boron addition on geopolymer structure.

The SEM images of synthesized geopolymers are taken by using Zeiss Ultra Plus (FEG-SEM) scanning electron microscope with a secondary electron (SE) detector to obtain the micromorphology and microstructure of the samples.

3.2.2.5. Thermogravimetric Analyses (TGA). Thermogravimetric analysis (TGA) is used to measure the physical changes of specimen under the influence of heat. With this technique, the thermal stability of synthesized geopolymers can be detected by monitoring the change of weight during heating of samples. Geopolymers are grinded before subjecting to thermogravimetric analysis (TGA) and temperature is raised up to 800 ^{o}C with a heating rate of 10 C/min. TGA is performed using TA Instruments TGA Q500 model instrument. The analysis is done by using Nitrogen at a flow rate of 40 cc/min and raising temperature of samples from room temperature to 800°C by 10°C/min. Approximately 20 mg of sample in powder form are loaded into platinum pans for each measurement.

3.2.3. Performance

Compressive strength measurements are performed according to ASTM D5731 standard test method which is the standard test method for determination of the point load strength index of rock and application to rock strength classifications. This method is done by applying an increasingly concentrated load to an object until failure occurs by splitting the specimen. The concentrated load is subjected through coaxial or truncated conical platens. It is a common method to estimate the uniaxial compressive strength.

3.3. RESULTS

In this study, metakaolin and fly ash are activated to form new products called as a boroaluminosilicate geopolymer. Various amounts of boron is added to geopolymers to obtain different chemical compositions.

The synthesized geopolymers with different aluminosilicate source (metakaolin and fly ash) and B/Si ratio are characterized with various characterization techniques. These techniques are X-Ray Diffraction, FTIR and Raman spectroscopy, and TGA. Mechanical strength of geopolymers are studied with point load strength measurement.

3.3.1. X-Ray Diffraction (XRD)

X-Ray Diffraction of geopolymers are studied to analyze the effect of borax addition on structure and crystallinity of geopolymers. The Figure 3.3 shows the X-Ray Diffraction pattern of borax-metakaolin based geopolymers. There is broad feature in the range of 20-28 ^{o} which shows the formation of geopolymeric amorphous phase in all of the borax-metakaolin based geopolymers [25, 81, 82]. All of these specimens consist of quartz (SiO2) and nepheline (NaAlSiO4) structural units.

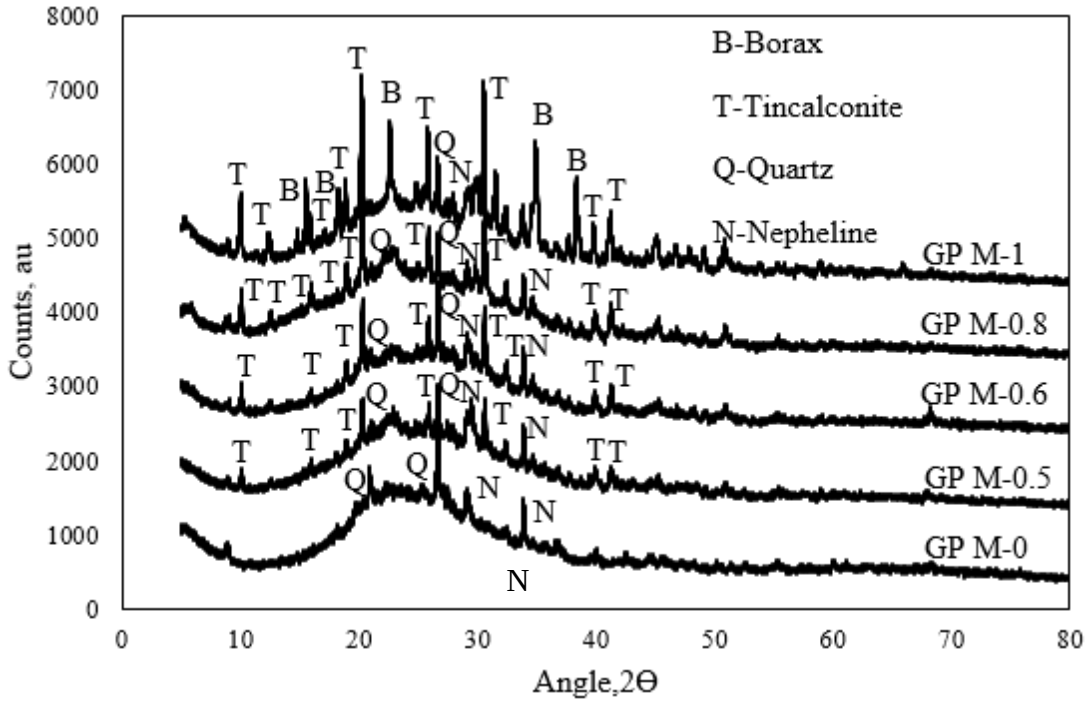

Figure 3.3. XRD pattern of geopolymers with metakaolin

These formations preserve their presence with increasing B/Si ratio. Tincalconite ($Na_2B_4O_7 \cdot 5H_2O$, Sodium Borate Hydrate) which is the main component of borax material utilized in geopolymer matrix appears with boron addition in XRD pattern of geopolymers ($0.5 \leq B/Si \leq 1$). The main peaks of tincalconite mineral are seen at 10.06º, 20.28º, 30.60º, 41.33º and 50.98º similar to the values reported in the literature [87, 88, 89]. The borax mineral peak turns into a distinct form in the geopolymer with the highest B/Si ratio which is 1. It is clear that with the increasing B/Si ratio, the XRD pattern of geopolymers become more crystalline. Borosilicate formation is seen as a broad peak between 21 and 24º which proves the participation of boron to silica network by featuring new product [60]. The intensity of this peak increases and becomes sharper with boron addition into the system.

The Figure 3.4 shows the X-Ray Diffraction pattern of fly Ash and borax-fly ash based geopolymers. The crystalline mineral phases are present in the fly ash namely quartz (SiO_2), albite (Na Al Si_3 O_8), anhydrite ($CaSO_4$) and calcite ($CaCO_3$). Quartz and anhydrite minerals observed in XRD pattern of fly ash, also appear in XRD pattern of borax-fly ash based geopolymers without affected from geopolymerization reaction or boron addition. The peaks belong to albite mineral reduce their intensity with increasing B/Si ratio. Calcite mineral preserves its presence only in the geopolymer with B/Si=0.5. As the boron content increases, calcite mineral disappears. The peaks at 9.53 º in the XRD pattern of fly ash indicates the presence of unburnt coal. Since fly ash is by product obtained from burning of coal, it is expected to observe this formation. Unburnt coal peak vanishes with geopolymerization reaction. Diffraction peaks for tincalconite at 10.06º, 20.28 º, 30.60 º and 41.33 º are seen in XRD pattern of geopolymers with B/Si ratios of 0.6, 0.8 and 1 [87, 88, 89]. With the addition of boron, the sodium borosilicate (Na (SiO4)B) peaks appear in the geopolymers with B/Si ratios of 0.6, 0.8 and 1.

The traditional amorphous structure of geopolymers is not affected from increasing B/Si ratio. Since there is no appearance of any peak associated with boron structure in the geopolymer with B/Si ratio of 0.5, it can be claimed that boron units participate the geopolymer structure.

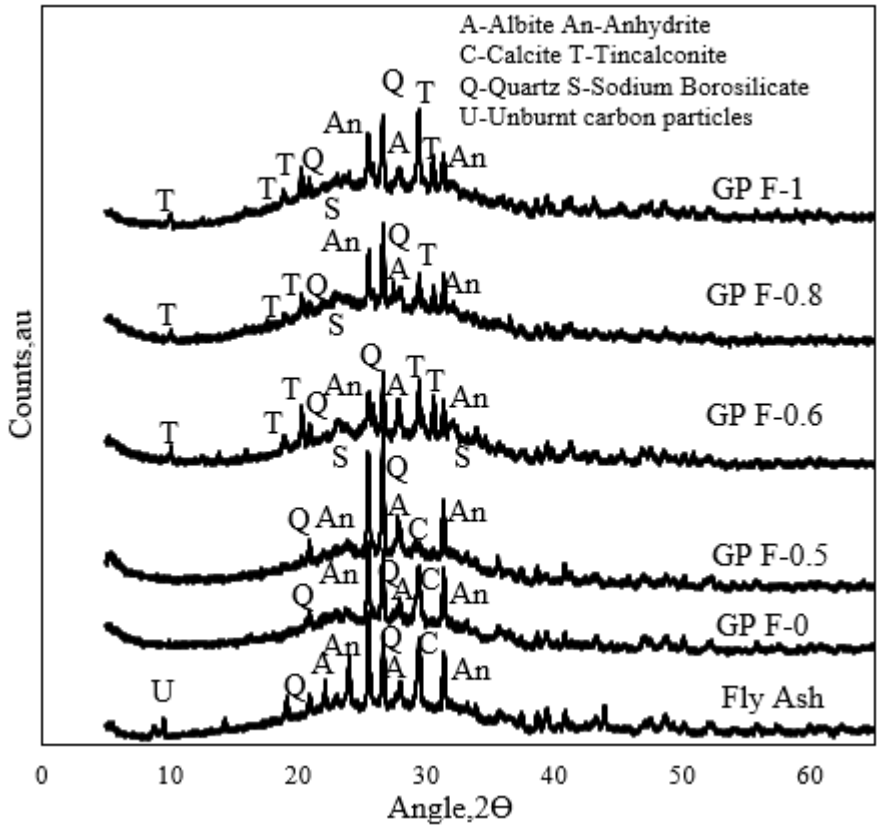

Figure 3.4. XRD pattern of fly Ash and borax-fly ash Based Geopolymers

3.3.2. Fourier Transform Infra-Red Spectroscopy (FTIR)

FTIR spectroscopy measurement is performed to obtain information concerning chemical bonds of the materials and also to investigate the geopolymerization process with the addition of boron. The FTIR spectra of borax-metakaolin based geopolymers with $0 \leq B/Si \leq 1.0$ are given in Figure 3.5. The characteristic geopolymerization band is observed in the region between 900-1200 cm^{-1} region [50, 68, 69, 70, 71, 72]. This main geopolymerization band is present in all of the synthesized samples This broad band is assigned to asymmetric stretching of T-O-Si bonds where T is Si or Al. Formation of this structural feature is related to the rearrangement TO_4 units during geopolymerization reactions [25, 68, 73]. The geopolymerization band position is located at 1031 cm^{-1} for the geopolymer solely based metakaolin whereas the position of this feature is positioned at 997 cm^{-1} for the geopolymer with B/Si ratio of 1 as being the highest ratio in this study.

There is no systematical shift to lower frequencies. Geopolymer sample with B/Si ratio of 0, displays a feature at 810 cm-1 which is assigned to tetrahedral Al-O stretching mode. As the molar B/Si ratio increases in the system, the presence of this characteristic band shows that metakaolin (Al(IV)-O stretching vibration) is not completely consumed in the system. However, the intensity of this band reduces. Therefore, addition of boron to geopolymer matrix somewhat contributes geopolymerization reaction [32].

The intensity of the FTIR peaks increase systematically depending on B/Si ratio. As the B/Si ratio increases, geopolymerization band becomes more distinct. The geopolymer with highest B/Si ratio which is 1 have the most intense peaks. The new structural reorganization of the bonds attributes the change at the intensity of spectrum. It is also evident from the existence of more crystalline phases. The existence of crystalline peaks in FTIR spectrum is consistent with XRD pattern of geopolymers with high B/Si ratio (B/Si is 0.8 and 1). Moreover, the presence of needle and star like structures in the SEM images are seen in the samples B/Si ratio as 0.8 and 1 which have relatively high level of crystallinity according to both XRD and FTIR results. The broad absorption bands observed in all of the geopolymers in Figure 3.4 at about 1660 cm^{-1} shows the presence of H–O–H bending vibrations of water molecules in the geopolymer structures.

As a result of synthesis of boroaluminosilicate geopolymers based on metakaolin and borax, the presence of B-O bond is expected. The main B-O broad band is observed at 1340 cm^{-1} in the geopolymers with borax addition [23, 24]. The B-O bands become sharper and more intense with increasing B/Si ratio.

The presence of boron in geopolymer matrix enhances the presence of B-O-B bond at 1400 cm^{-1} [34]. In addition to these bands, δB-O-Si bonds belong to borosiloxane bridge is observed as a small peak at 685 cm^{-1} and shoulder at 875 cm^{-1}. Therefore, it is evident that boron atoms are incorporated into the geopolymer network in borax-metakaolin based geopolymers.

The peak positioned at around 950 cm^{-1} for the sample with B/S ratio of 1 is related to the tincalconite mineral [88]. The appearance of this formation shows presence of unreacted boron content which is also supported by XRD pattern of geopolymer with relatively high boron content.

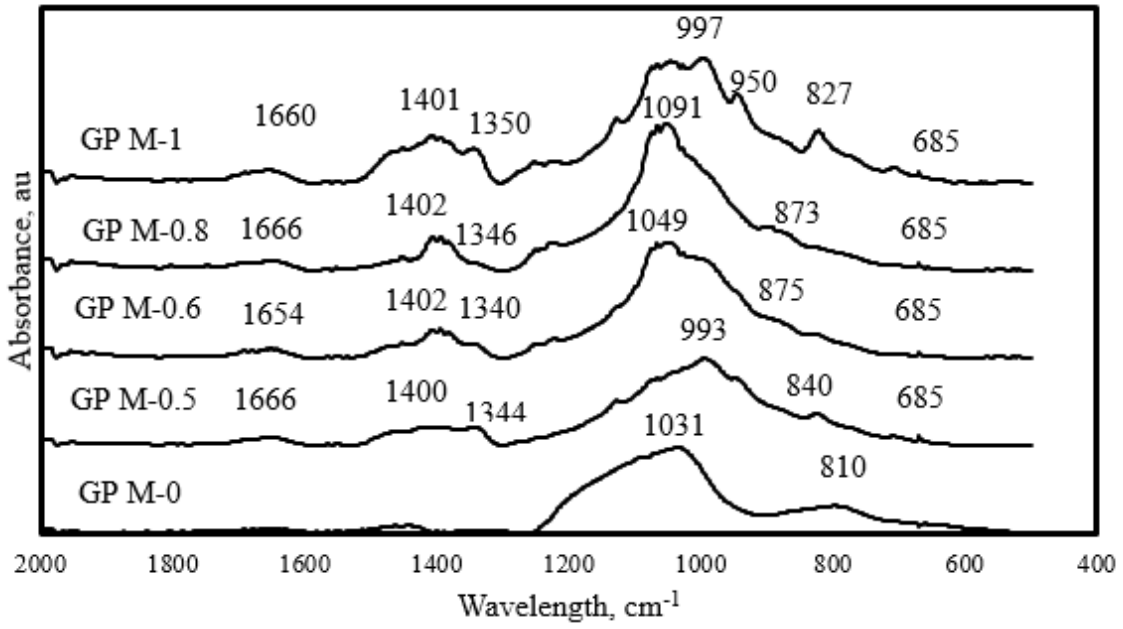

Figure 3.5. FTIR Spectrum of Geopolymers with metakaolin

Figure 3.6 shows the FTIR spectrum of fly ash. The FTIR spectrum of fly ash is dominated by an intense feature at about 1066 cm^{-1} corresponding to asymmetric stretching vibrations of Si-O-T bonds where T is tetrahedral Al or Si [70, 71, 72]. The presence of C-O vibrations are seen at 890 cm^{-1} with appearance of a broad band [94]. The bands at about 584, 609 and 671 cm^{-1} are the evidences of anhydrite presence [95].

This fact is also associated with XRD results. The peak around 1410 cm^{-1} is attributed to C–O stretching. Asymmetric Al–O and Si–O stretching bands is positioned in the region between 900– 1030 cm^{-1} [81].

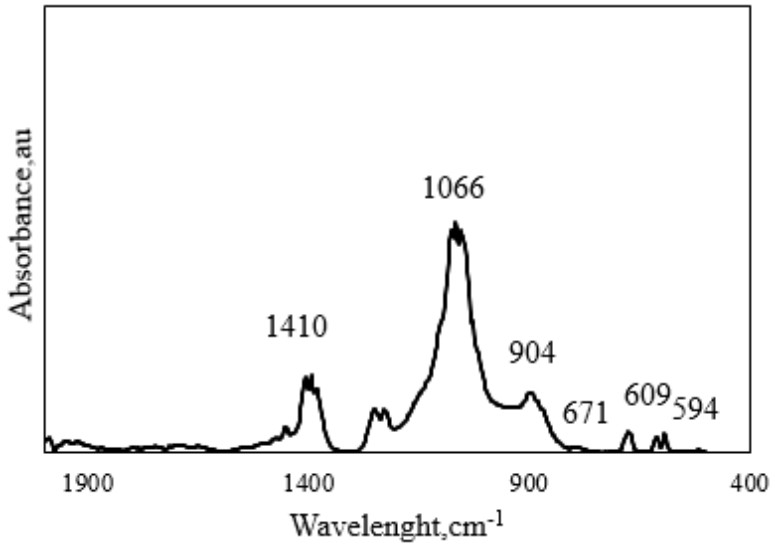

Figure 3.6. FTIR Spectrum of Fly Ash

The FTIR results of borax-fly ash based geopolymers ($0 \leq B/Si \leq 1$) are illustrated in Figure 3.7. First of all, the broad geopolymerization band is observed at about 1020 cm^{-1} for the geopolymer with B/Si ratio of 0. This peak indicates the presence of Si-O-T bond and becomes broader compared to raw fly ash with geopolymerization reaction. The decrease in the intensity of this band means an increase of Al incorporation into geopolymer matrix [75]. The decrease of the intensity of main peak could be associated with increased geopolymerization and disorder in the structure of the materials. This band signifying geopolymerization (for specimen with B/Si=0) shifts to lower frequency region between 970-985 cm^{-1} due to boron addition. The geopolymerization reaction is associated with the dissolution of the fly ash in the strong alkaline activating solution [69]. The movement of main band is related with the formation of new products by indicating the changes in the angle and length of the Si-O-Si bonds [70]. The highest amount of movement is obtained for the geopolymer specimen with B/Si ratio of 0.8. In addition, the peak centered at 904 cm^{-1} in the spectrum of fly ash disappears in the FTIR spectrum of geopolymers. The disappearance of this band which stands for the asymmetric Al–O and Si–O stretching is the evidence of formation of new product due to geopolymerization reaction.

The specimen with no boron addition (B/Si=0) displays a broad band at about 1460 cm^{-1} assigned to vibrations of O-C-O bond showing atmospheric carbonation. The amount of excess sodium in geopolymer blend may have interacted with CO_2 and leading to formation of sodium bicarbonate [25, 74]. Atmospheric carbonation seems to be lessened with the addition of boron. The characteristics peaks showsthat the presence of anhydrite is not affected from geopolymerization and boron addition since they are positioned in FTIR spectrum of all of the geopolymers.

The FTIR spectrum of boron containing geopolymers ($0<B/Si\leq1$) is dominated by two broad features located at around 970 cm^{-1} and 1100 cm^{-1} (Figure 3.7). It should be noted that high Ca containing C type fly ash is used in this study. In this context, it is reasonable to assign the band positioned at about 970 cm^{-1} to the asymmetrical stretching vibrations of Si-O bonds in high calcium environments based on a previous study associated with compatibility between sodium aluminosilicate hydrate (N-A-S-H) and calcium silicate hydrate (C-A-S-H) gel. On the other hand, in the low calcium environment, the positions of the bands related to asymmetrical stretching vibrations (T–O T is Si or Al) shift to higher wavenumbers such as 1020 cm^{-1} [76]. These peaks merge for the geopolymer specimen with no boron and no calcium content. In this thesis, the design of geopolymerization synthesis is utilized taking L/S ratio as constant. As the addition of boron is increased, the solid amount in the geopolymer matrix is also increased. In order to synthesize the geopolymer with constant L/S ratio, the amount sodium amount (liquid sodium silicate) is used at higher amounts in the geopolymers with higher boron ratio. For example, the Na/Si ratio is 0.54 for geopolymer with B/Si ratio of 0 whereas the Na/Si ratio is 1.04 for geopolymer with B/Si ratio of 1. According to FTIR analysis in a research studying the effect of alkalis on fresh C–S–H gels, it is reported that different concentrations of sodium contributes to modifications at C–S–H gel [94]. The band at around 970 cm^{-1} would be related with asymmetric stretching vibrations in calcium based gel. On the other hand, the band positioned at 1020 at cm^{-1} would be associated with a silica- rich gel. Therefore, it is possible to say that change of sodium content in geopolymer matrix leads to formation of two distinct gel structures and also phase separation.

The main B-O broad band is observed around 1340 cm^{-1} in all of the borax-fly ash based geopolymers. The peak around 1430 cm^{-1} associated with B-O-B band [34]. This formation is considered as one of the most prevalent diagnostic peaks and seen in also all geopolymers with boron [33]. In addition, the presence of Si-O-B bond is verified with the shoulder around 870 cm^{-1} which is peculiar to polyborosiloxane bridges [34]. Occurrence of Si-O-B bond shows the incorporation of boron content with silica network.

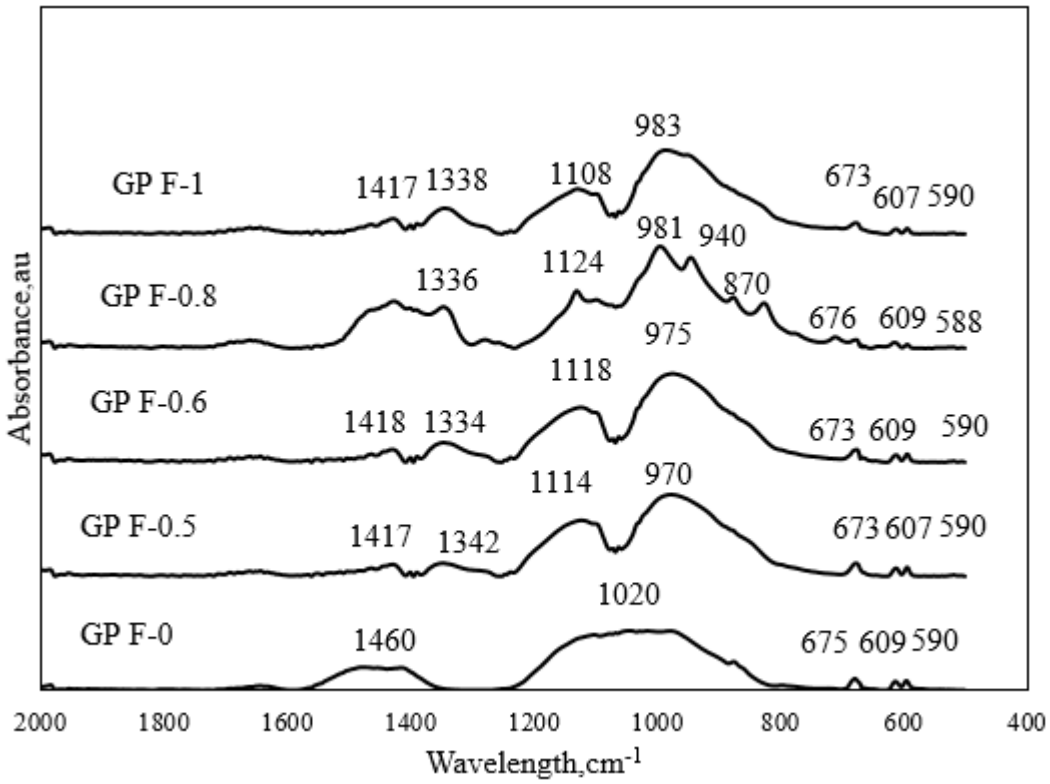

Figure 3.7. FTIR Spectrum of geopolymers with fly ash

A band positioned at around 940 cm^{-1} is observed in the geopolymer with B/Si ratio of 0.8. This peak is also seen in tincalconite mineral [88]. This formation is the evidence of unreacted boron content which is also supported by the corresponding XRD pattern.

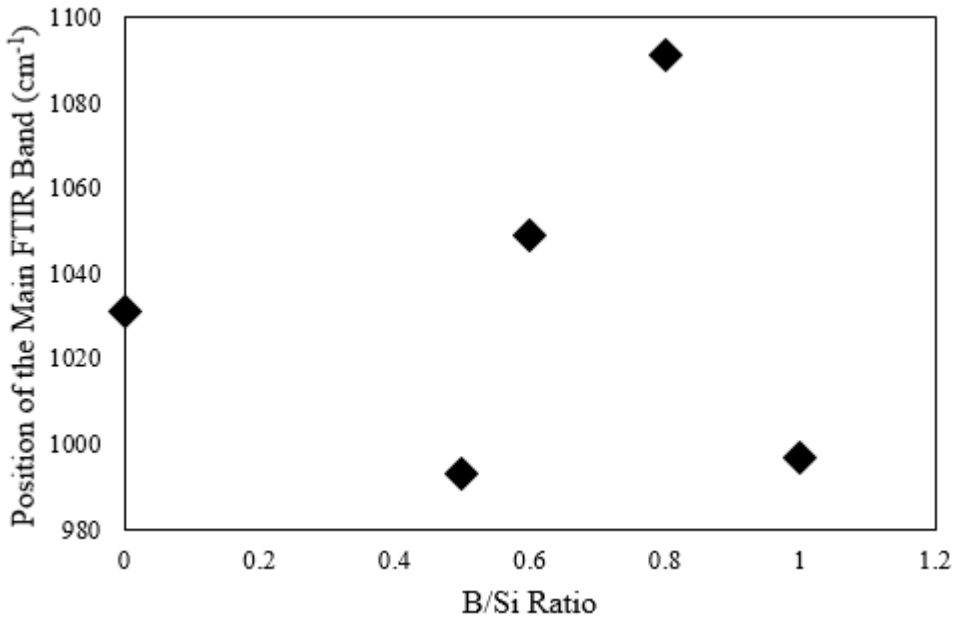

Figure 3.8. The positions of the main FTIR bands in geopolymers with metakaolin as a function of B/Si ratios

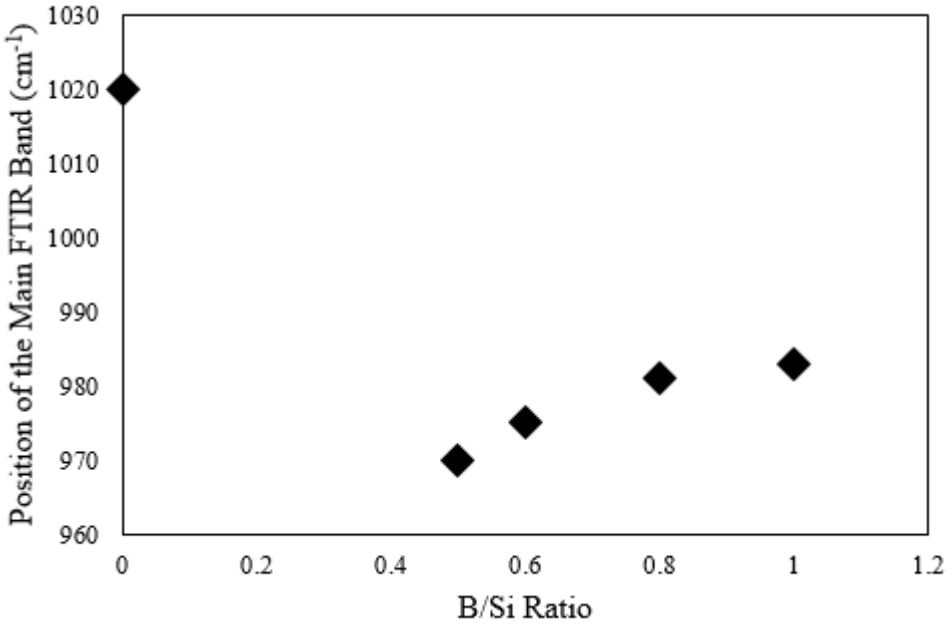

Figure 3.9. The positions of the main FTIR bands in geopolymers with fly ash as a function of B/Si ratios

The effect of B/Si ratio on position of main geopolymerization peak is investigated both for metakaolin and fly ash based geopolymers. There is no direct relation between position of main peak and boron content for the metakaolin based geopolymers as shown in Figure 3.8. On the other hand, the main band shifts to lower frequencies with boron addition in the FTIR spectrum of borax-fly ash based geopolymers as in Figure 3.9. The movement can be related with dissolution of the fly ash amorphous phase in the alkaline activating solution and increase in the degree of geopolymerization [70].

3.3.3. RAMAN Spectroscopy

Raman spectroscopy is utilized to analyze the synthesized geopolymers. This method is used to complement the FTIR results since all the bond information cannot be obtained from FTIR spectrum. In addition, information regarding SiO_4 polymerization can be determined by Raman spectroscopy.

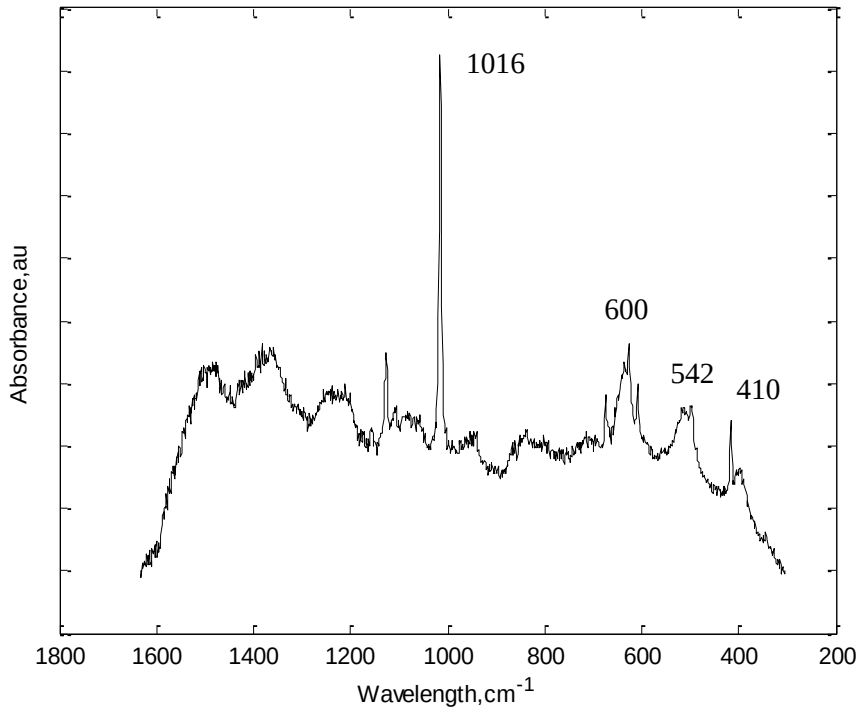

Figure 3.10. RAMAN spectrum of metakaolin

Figure 3.10 shows the Raman spectrum of metakaolin. The peaks between 400-500 cm^{-1} stands for the quartz component. Furthermore, the origin of the peak near 600 cm^{-1} is associated with Si-O-Si bonds. The sharp peak at 1016 cm^{-1} comes from the Si-O stretching motion of quartz [67].

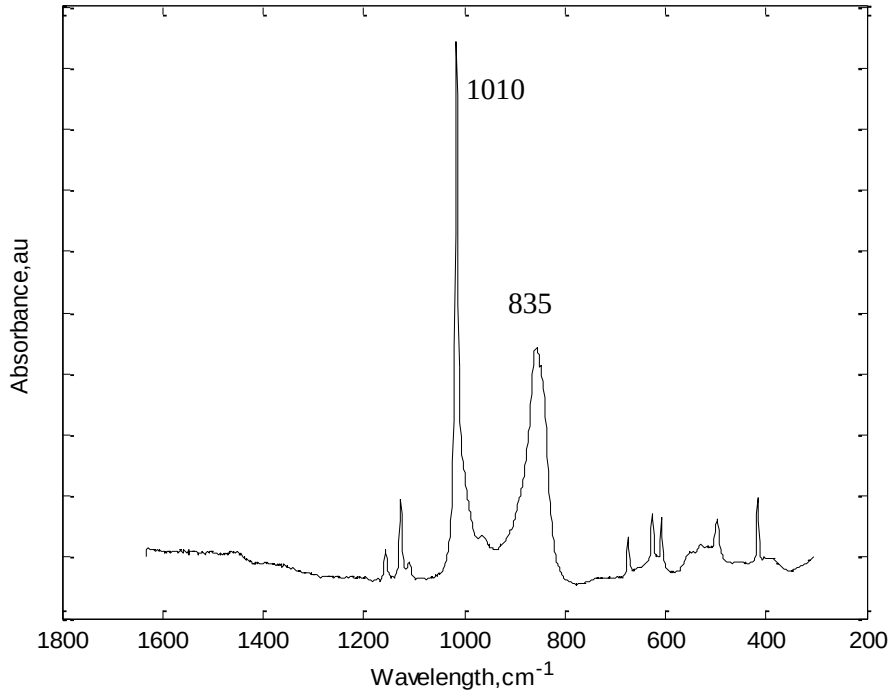

Figure 3.11. RAMAN spectrum of fly ash

The Figure 3.11 belongs to Raman spectrum of Fly Ash. The peak at about 835cm^{-1} is attributed to SiO_4 oligomers [100]. This peak vanishes with geopolymerization reaction. The sharp peak in the region at about 1000 cm^{-1} is assigned to vibration in silicate structural units, most probably resulting from quartz [79].

The Raman spectrum of anhydrous borax is illustrated at Figure 3.12. The main tincalconite peak, which is the main component of borax source utilized in geopolymerization reaction shows its presence at 578 cm^{-1}. The peak at 344 cm^{-1} belongs to B_2O_3. The peaks positioned at 944 and 766 cm^{-1} belongs to (υB(3)–O) and (υ(B(4)–O) formations; respectively [87].

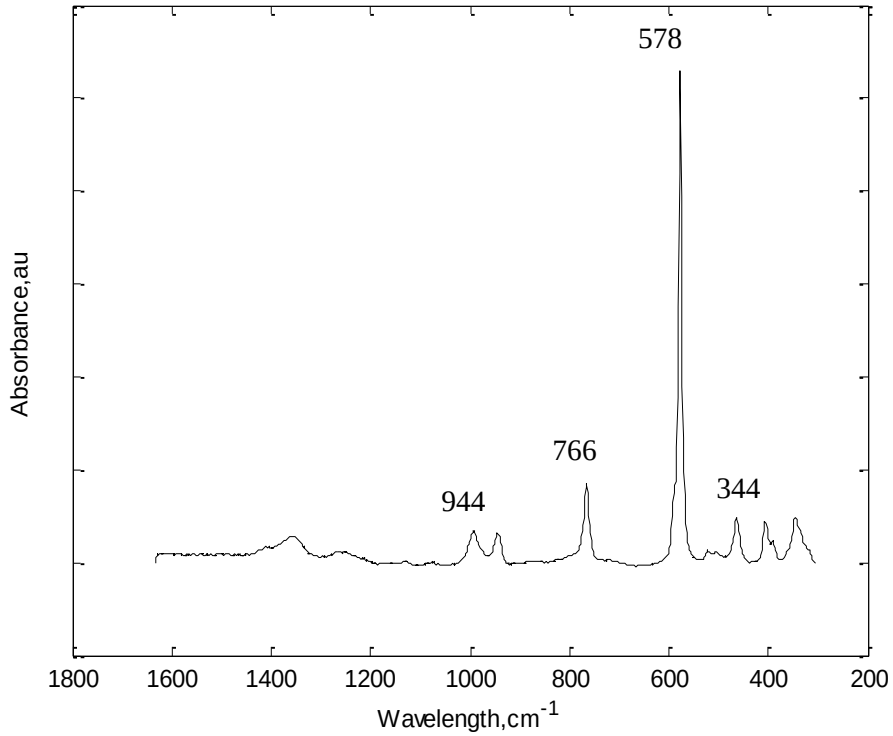

Figure 3.12. RAMAN spectrum of anhydrous borax

Figure 3.13 displays the Raman spectrum of borax-metakaolin based geopolymers with varying B/Si ratio ($0 \leq B/Si \leq 1$). According to Raman Spectrum, all of the geopolymers have bands positioned at around 401, 464, 514 and 1070 cm^{-1}. The narrow peak around 464 cm^{-1} in the low frequency region is attributed to alpha quartz spectra [77]. The peak at 514 cm^{-1} is related with the structures of four membered SiO_4 rings (O-Si-O bending) [67]. The bands lying in the region 850-1250 cm^{-1} are associated with Si-O stretching motion Therefore, the peak positioned at 1060 cm^{-1} is enhanced by Si–O stretching vibration in structural unit with one non-bridging oxygen per silicon [79]. Raman method is applied by focusing on a certain part of the sample. Therefore, the peak intensities might vary. For example, the metakaolin- borax based geopolymer with B/Si is 0.8 has the highest intensity of the peak which shows the presence of Si-O stretching vibration of tetrahedral units. Tetrahedral vibrations of TO_4 tetrahedrons (T is Si or Al) are visible in spectrum for all specimens as positioned at 401 cm^{-1} [67]. Region of silicates in Raman spectrum is positioned in two different areas which are high and medium wavenumber region.

The characteristic silicate Raman band for high wave number is centered at 1000 cm^{-1} whereas the medium wave number region is located at 500 cm^{-1} [77]. Vibrations of bridging oxygen or Si-O-Si bending motion against its tetrahedral cage show its presence in the region from 200 to 850 cm^{-1} [79].

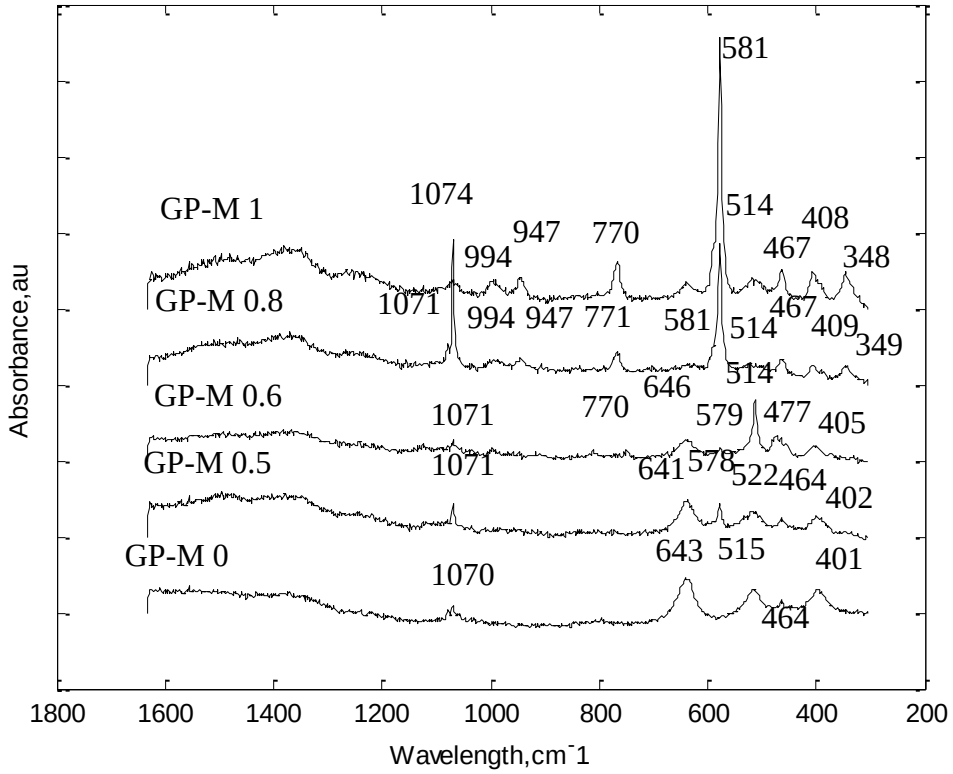

Figure 3.13. RAMAN spectrum of borax-metakaolin based geopolymers

Borax-metakaolin based geopolymers have Raman peaks displayed around 579-581, 770, 947 and 994 cm^{-1}. The bands positioned in the region at around 578-581 cm^{-1} are seen all of the borax-metakolin based geopolymers. The peaks in the regions at around 770, 947 and 994 cm^{-1} appear with increasing B/Si ratio. The band at 581 cm^{-1} is the main Raman band of tincalconite mineral which is the major component of boron source in geopolymer matrix. This band stands for the bending of three-coordinated and four coordinated boron existence (δ(B(3)–O)/ δ (B(4)–O).

According to Raman spectrum of tincalconite, the peak at 994 cm^{-1} is also an evident of presence of tincalconite mineral which becomes more distinct with increasing B/Si ratio. The peaks at around 947 and 770 cm^{-1} belongs to (υB(3)–O) and (υ(B(4)–O); respectively [87]. The bands showing the three and four coordinated boron existence is consistent with FTIR results.

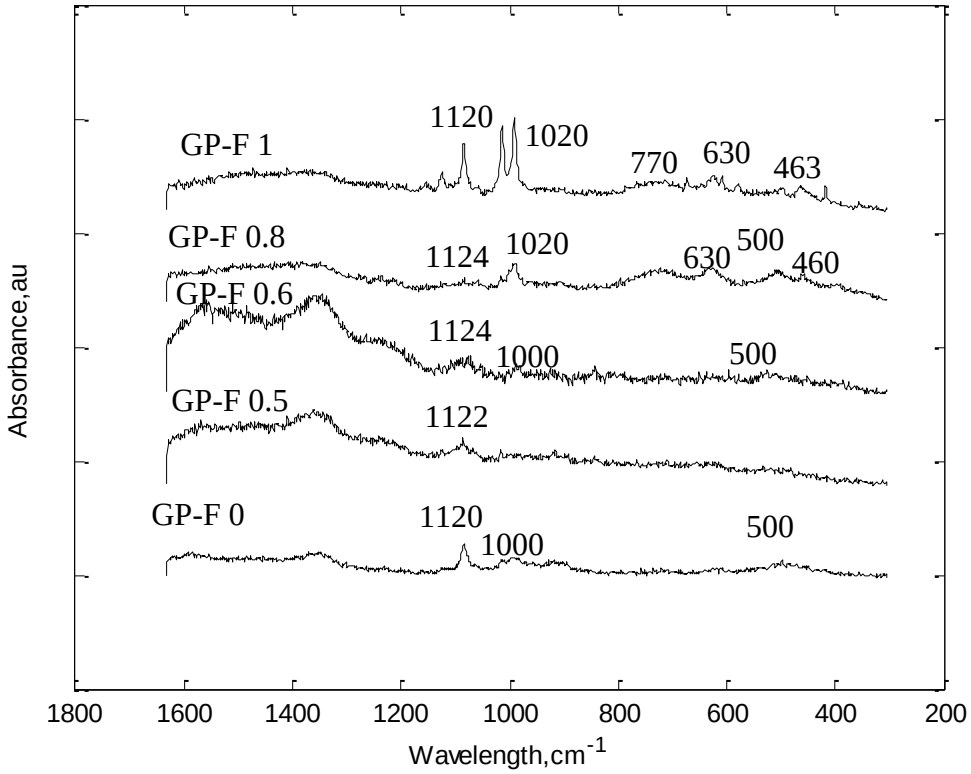

Figure 3.14. RAMAN Spectrum of borax-fly ash based Geopolymers

The Figure 3.14 displays the Raman spectrum borax-fly ash based geopolymer samples. The peaks observed lying in the region between 850 and 1250 cm^{-1} are attributed to Si-O stretching vibrations [79]. The band at around 1120 cm^{-1} is assigned to the presence of fully polymerized silicate units and seen at Raman spectrum of all of the metakaolin based geopolymers [80]. In addition, the formation of large band in the region between 1000 and 1050 cm^{-1} is assigned to the vibration of silicate structural units due to the alkaline cation and observed in all of the samples without depend on boron inclusion.

The peak at around 500 cm^{-1} stands for Si-O-Si bending [80]. The addition of boron leads to several changes in Raman spectrum of geopolymers. To illustrate, the presence of quartz formation around 460 cm^{-1} originates in geopolymers with B/Si ratio are 0.8 and 1.Borosilicate structural units are observed at 630 cm^{-1} in the Raman spectrum of geopolymers with B/Si ratios of 0.8 and 1 [80]. The addition of boron to the geopolymer matrix contributes to the formation of borosilicates. This result is supported by FTIR spectrum of the borax-fly ash based geopolymers. The band around 770 cm^{-1} observed in geopolymers with B/Si ratios of 0.8 and 1 corresponds to four coordinated boron species [80].

3.3.4. Scanning Electron Microscopy (SEM)

In order to analyze the effect of boron content on microstructure of geopolymers SEM measurements are performed. Figure 3.15 displays the SEM images of borax-metakolin based geopolymers. The geopolymer without boron includes flake shaped particles. The presence of flakes in structure results from unreacted metakaolin druing geopolymerization [28].

The glassy geopolymer matrices with more crystalline structures are observed in the samples with higher boron content ($0.5 \leq B/Si \leq 1$). In addition to crystalline structures, geopolymer surfaces become more porous attributed to porous structure of borax [83]. The increase of crystalline structures supports X-Ray results due to presence of sharper peaks at XRD diagram of geopolymers with boron. In the XRD diagrams, the presence of new structural units related to boron addition (tincalconite and borax) are observed same as the SEM images. As the amount of boron changes in geopolymer blend, the SEM results also show several differences. To illustrate, it is possible to say that the distribution of structural units is more homogenous in geopolymers with B/Si ratios of 0.5, 0.6 and 0.8 than geopolymer with B/Si ratio of 1. The reason of non-uniform distribution might be the unreacted tincalconite presence. The star and needle like structures are seen in geopolymers with boron and become more distinct in geopolymer with the highest B/Si ratio which is 1.

SEM images of borax-fly ash based geopolymers are shown in Figure 3.16. The geopolymer synthesized with only fly ash (without boron) displays dense and continuous surface without flake formation. However, the spherical cenospheres are observed. Spherical cenospheres are smooth aluminosilicate particles which are typically seen in the microstructure of fly ash [81]. The presence of these features in the geopolymer microstructures can be explained by unreacted fly ash compounds. The agglomerated particles and partially broken cenospheres are also seen in microstructure of geopolymer without boron. The effect of boron content is seen in microstructural images of the borax-fly ash based geopolymers easily. To illustrate, spherical cenospheres vanish which can be explained by improved geopolymerization process and formation of new structures with boron addition. Star like irregular features are displayed in borax-fly ash based geopolymers indicating crystalline phases. The main feature is the fibrous products on the surfaces of the geopolymers with boron inclusion. The morphological changes occured in geopolymers result from the dissolution of SiO_2 and Al_2O_3 contents in the cenospheres by addition of alkaline solution [84]. This reaction attributes to aluminosilicate gel formation for geopolymer.

The boron content in the geopolymers, therefore the solid content is increased in this study to obtain higher B/Si ratios while Si/Al ratio is kept constant values. In order to synthesize the geopolymers with the same L/S ratio, liquid amount (sodium silicate and water) is increased. As a result of higher amount of sodium in the geopolymer matrix, the microstructure of geopolymers change with boron inclusion. As mentioned before in FTIR results of borax-fly ash based geopolymers, phase separation is observed. Moreover, silica and calcium rich phases are formed. The gel phases are seen SEM mages of borax-fly ash based geopolymers ($0.5 \leq B/Si \leq 1$).

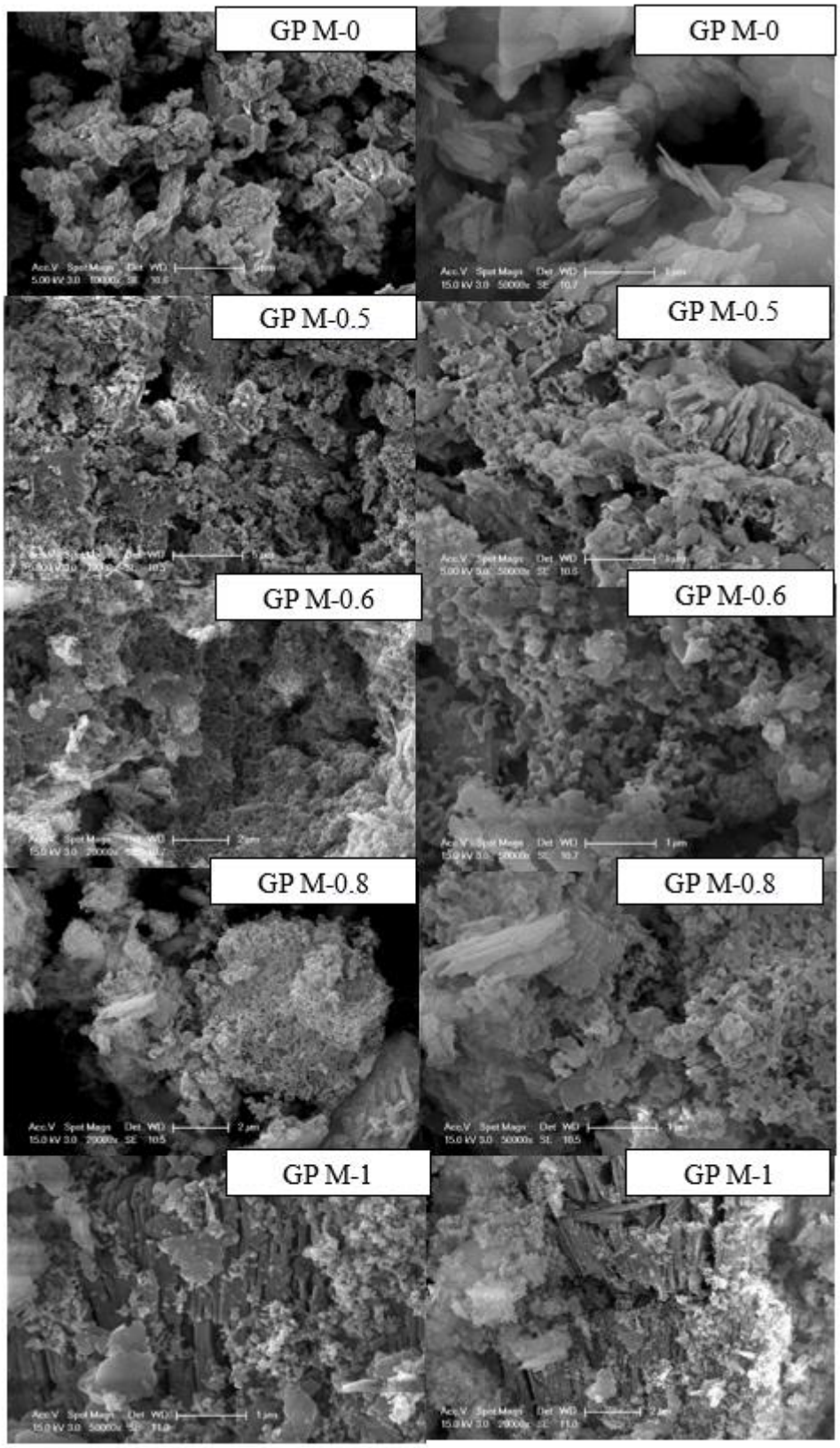

Figure 3.15. SEM images displaying morphology of borax-metakaolin based geopolymers

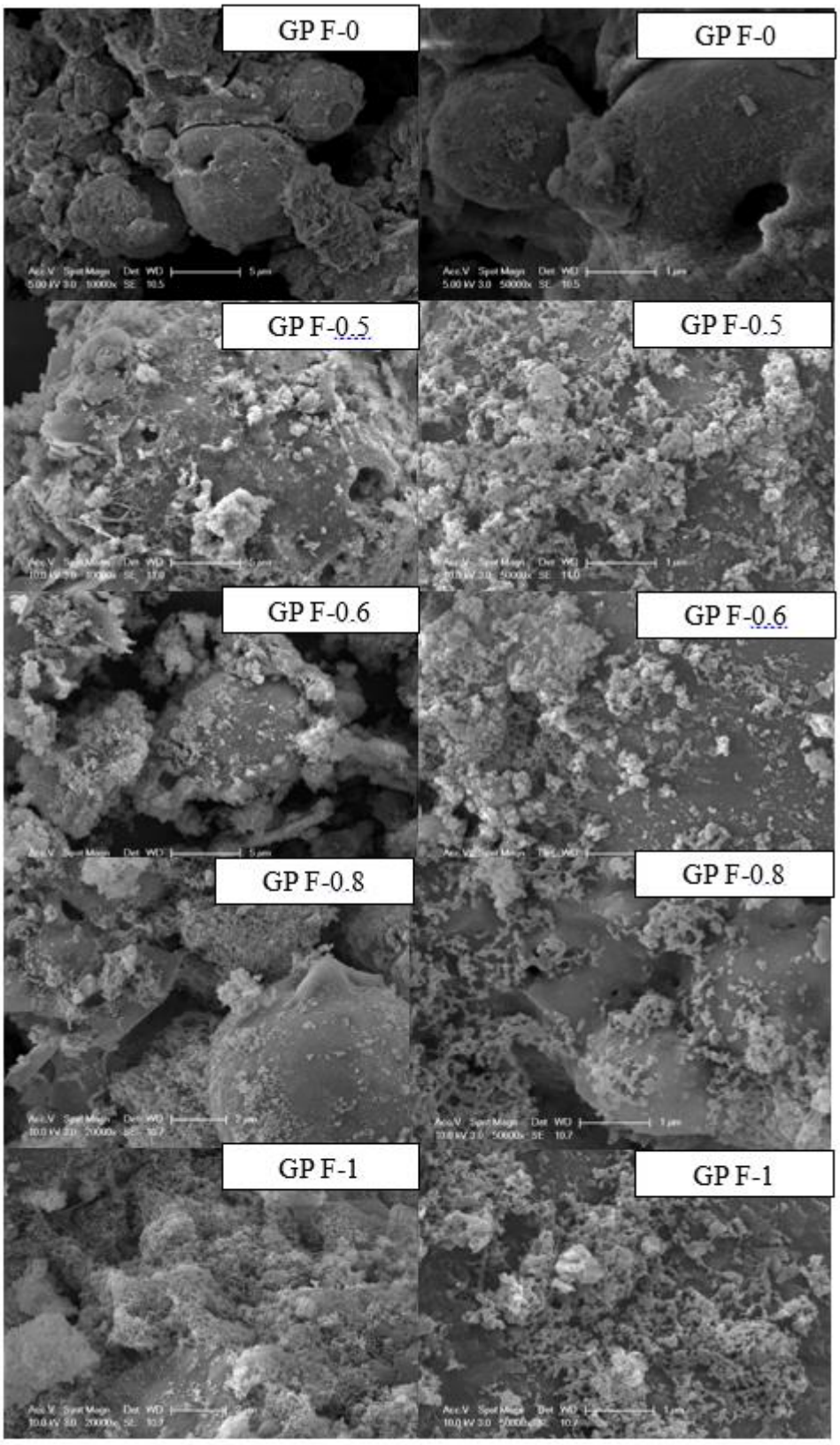

Figure 3.16. SEM images displaying morphology of borax-fly ash based geopolymers

3.3.5. Thermogravimetric Analysis (TGA)

Thermogravimetric measurements are performed to analyze the effect of boron addition on thermal behaviour of metakolin and fly ash-based geopolymers. Figure 3.17 displays the thermogravimetric diagram of borax-metakaolin based geopolymers. The temperature values are varied between room temperature and 800 °C. It is seen from this graphs that borax-metakaolin based geopolymers have different thermal characteristics compared to pure metakaolin (Figure 2.12) mainly due to the presence of water in the structure of geopolymers. Therefore, the weight loss of geopolymers are quite higher compared to pure metakaolin, especially in the boron containing geopolymers. Total weight loss of metakaolin is about 1.1% at the end of heating procedure. On the other hand, the weight losses of borax-metakaolin based geopolymers are 8.35, 15.23, 15.11, 17.52, 22.84 % for varying B/Si ratios of geopolymers namely 0, 0.5, 0.6, 0.8 and 1; respectively.

In a study including waste-catalyst-metakolin based geopolymers, the characteristic subsequent phases observed in the thermogravimetric analysis of geopolymers are as i) dissipation of free water molecules, ii) decomposition of geopolymer components, iii) dehydroxylation of zeolitics, iv) stabilization of the weight [86].

However, thermogravimetric analysis diagram of borax-metakaolin based geopolymers in this thesis seem to exhibit three main sequential stages. The first stage includes the temperature starting from room temperature to 120, 144, 156 and 163 °C for the geopolymers with B/Si ratios of 0, 0.5,0.8 and 1; respectively. The weight loss becomes more distinct with the increasing B/Si molar ratio and also most of the weight loss occurs in this phase. The weight loss observed in this region is associated with evaporation of free water from the geopolymer surface and also from large pores including weakly absorbed water molecules. Second stage is the region up to approximately 630 °C. Weight loss at the second stage might be related with dehydration of chemically bonded water to geopolymer structure units and also dehydroxylation of zeolitics present in the binder [85, 86]. The weight loss of geopolymers is stabilized at approximately 630 °C.

The weight loss increases as a function of increasing boron content in geopolymers. As a result of thermal stability of boron, the weight loss is expected to reduce with boron addition in contrast to the obtained results. However, this situation can be expressed that moisture imprisoned in amorphous boron is removed by heating.

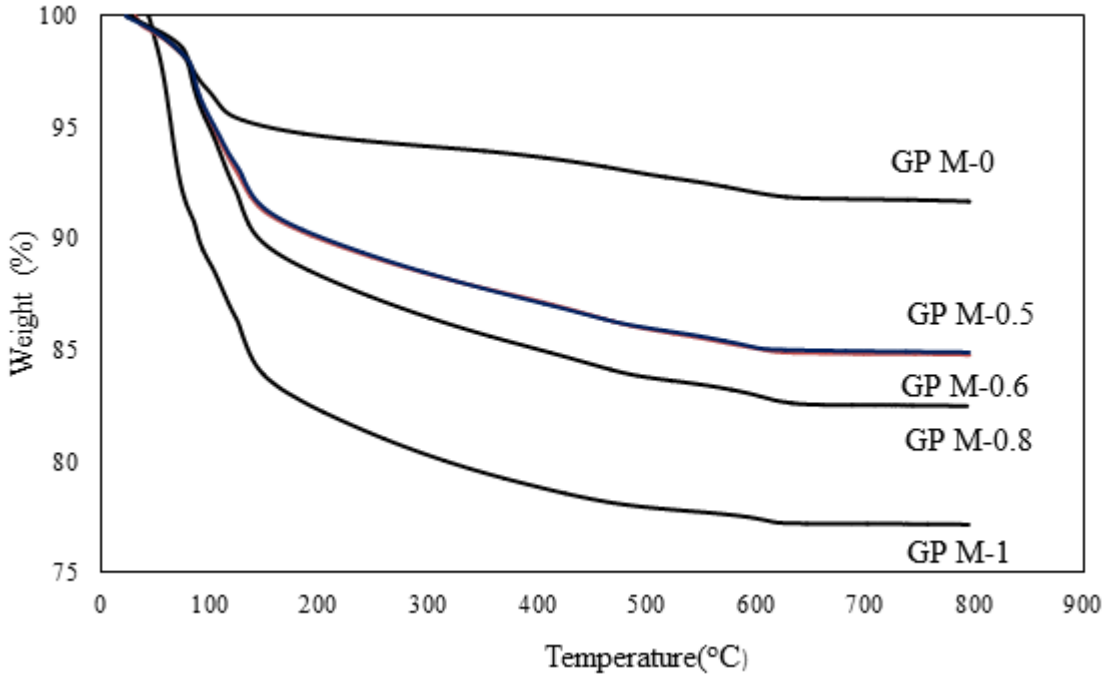

Figure 3.17. TGA curve of borax-metakaolin based geopolymers

Thermogravimetric results of fly ash is illustrated at Figure 3.18. The weight loss of fly ash consist of five stages. The first stage includes the region between room temperature and 412 °C. The weight loss occurs linearly up to 412 °C with the same slope. The second stage is between 412-436 °C. The slope of weight loss curve increases in this region. The third stage is in the temperature values between 436-550°C. The weight loss curve becomes stable in this region. After a fast weight loss up to until 643 °C which is the fourth stage, the curvature becomes stable again in the fifth region. Total weight loss of the fly ash is 1.42 % of its total mass. Weight loss at the first three stage is associated with the evaporation of physio-chemically bonded water molecules in the fly ash structure [85]. Weight losses in the last two stage is related with oxidation and combustion of unburned coal particles present in the fly ash [85, 86].

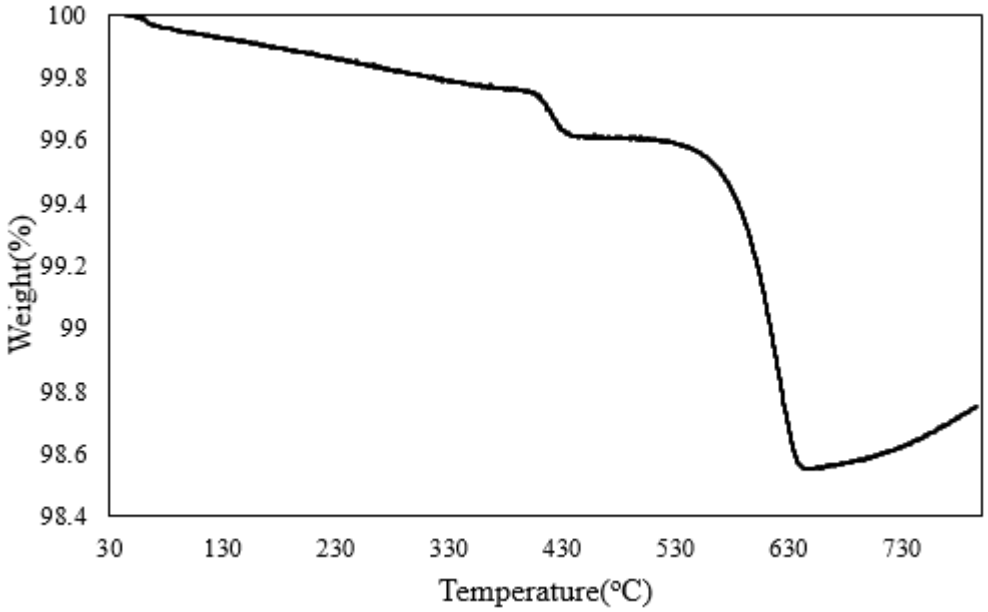

Figure 3.18. TGA curve of fly ash

Thermal diagram of borax-fly ash based geopolymers is given in Figure 3.19. The thermal behavior of geopolymer without boron is noticeably different than the geopolymers with boron content. The weight loss of geopolymers consist of three sequential phases. The first stage lies within the temperature range between room temperature and 226 °C for the geopolymer with B/Si is 0 whereas for the geopolymers with B/Si ratio 0.5 to 1, the region is up to around 150 °C. As mentioned before, the weight loss in the first region is associated with dissipation of free water from surface of geopolymers. Second stage is between the temperatures 226 and 670 °C for the geopolymer with B/Si ratio of 0. On the other hand, the region between 150 and 645 °C constitutes the second region of geopolymers with B/Si ratio between 0.5 and 1. The reason of weight loss at the second stage is evaporation of chemically bonded water to geopolymer structure as in the case of borax-metakaolin based geopolymers. Moreover, burning of the organic content and combustion of unburned coal in the geopolymer systems occur in this region [85, 86]. The geopolymer with no boron content reaches thermal stability at 670 °C, on the contrary; the geopolymers with boron are at 645 °C at their third stage.

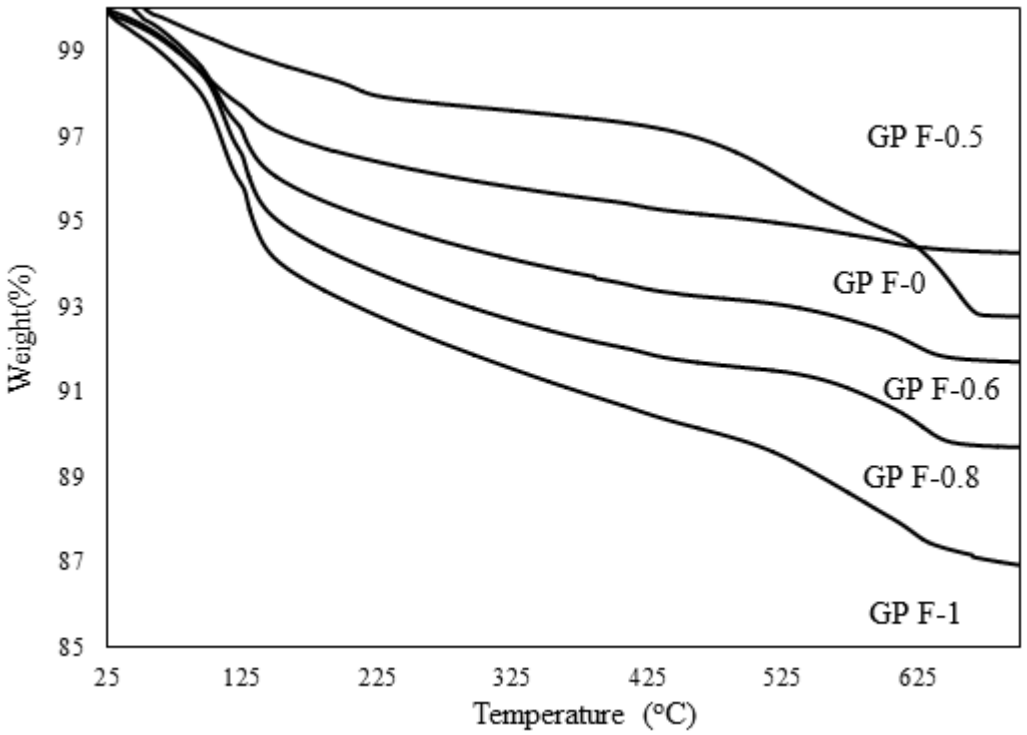

Figure 3.19. TGA curve of borax-fly ash based geopolymers

The weight loss increases systematically with the increasing B/Si ratio except the geopolymer with B/Si ratio of 0.5. The weight losses of borax-metakaolin based geopolymers are 7.24, 5.74, 8.31, 10.32, 13.09 % for geopolymers with varying B/Si ratios of 0, 0.5, 0.6, 0.8 and 1; respectively. The weight loss of borax-fly ash based geopolymers are quite less compared to weight loss of borax-metakaolin based geopolymers. As a result of absorbed moisture in amorphous boron, weight loss is higher at lower temperatures (first and second phases) for the geopolymers with boron. To evaluate the effect of boron on thermal behavior, thermal measurements should be studied at higher temperatures as 1200 °C according to a study related to boron nitride coated pyrolytic carbon particles [62].

3.3.6. Compressive Strength Results

Figure 3.20 displays compressive strength values measured for the borax-metakolin based geopolymers investigated in this study as a function of molar B/Si ratios.

These values seem to be rather low for engineering applications. However, it should be noted that the compressive strength is measured with the point load strength method which gives lower results compared to servo-hydraulic test machine. It is seen that geopolymer with B/Si ratio of 0 displays the highest compressive strength as 0.56 MPa expected their rough and amorphous nature. The lowest compressive strength as 0.21 is obtained from the geopolymer with B/Si ratio of 0.5. Compressive strength values seem to systematically increase with increasing boron content (B/Si ratio) in the system. According to previous studies related with boroaluminosilicate geopolymer synthesis, the compressive strength of geopolymers increases as being related with increasing boron content of geopolymer matrix instead of their crystalline structure. The reason of this result is explained as the B-O bond observed in FTIR spectrum of geopolymers. This is stated as the most crucial parameter to determine compressive strength since geopolymers with no B–O bond display the lowest compressive strengths.[23, 24]. The boron containing geopolymers synthesized in this thesis also display this B-O bond as displayed in their FTIR spectrum.

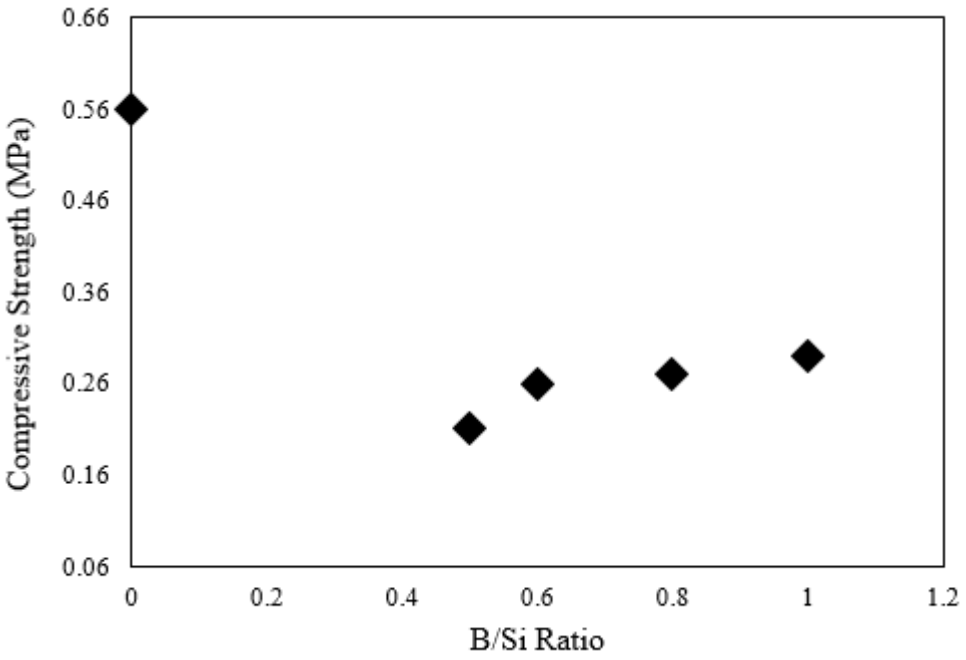

Figure 3.20. Compressive Strength of the borax-metakaolin based geopolymers

Compressive strength values for borax-fly ash based samples as a function of molar B/Si ratio are given in Figure 3.21. As mentioned before, low compressive strength results are obtained because of the point load strength method. The compressive strength of geopolymers increase systematically depending on molar B/Si ratio. It is observed that the geopolymer with no boron have the lowest compressive strength value of about 0.04 MPa. The possible reason for this lowest compressive strength value arise from presence of unreacted fly ash in the geopolymer structure. Unreacted fly ash is also seen as spherical cenospheres in the corresponding SEM images. The highest compressive strength value belongs to geopolymer with highest B/Si ratio. Although the geopolymers with higher B/Si ratio as 0.8 and 1 have crystalline phases, the compressive strength values are not affected negatively from presence of crystalline structures. XRD patterns of these specimens display crystalline tincalconite and borax compounds which could be responsible for low compressive strength results. Moreover, the crystalline structure is also observed in SEM images. However, formation of B-O or B-O-Si bonds might have a positive effect on compressive strength of geopolymers.

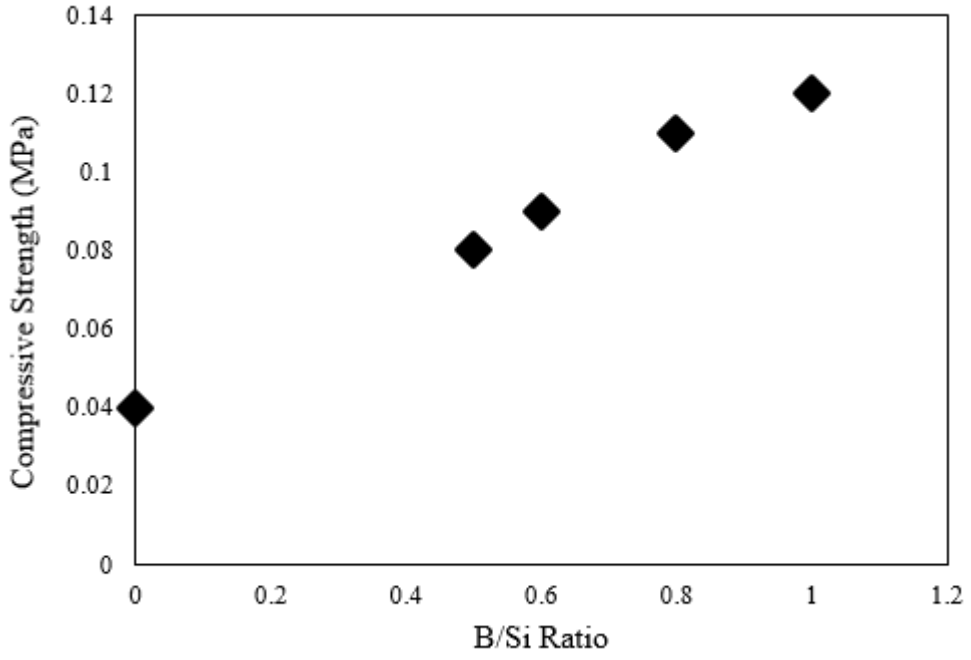

Figure 3.21. Compressive Strength of the borax-fly ash based geopolymers

3.4. Conclusion

A comparative study related with structural properties of borax-metakaolin and borax-fly ash geopolymers are utilized in this part of the study. Metakaolin and C type fly ash are used as aluminosilicate source during geopolymerization. In order to see the effect of boron inclusion to geopolymer system, B/Si ratio is changed between 0 and 1. The synthesized geopolymers are characterized by XRD, FTIR and Raman spectroscopy, SEM and TGA. Compressive strength of geopolymers are also measured with point-load determination method. The borax-metakaolin based geopolymers shows amorphous structure with quartz and nepheline crystal units. The traditional amorphous structure of metakaolin and fly ash based geopolymers are not affected from increasing B/Si ratio. The main component of borax material, tincalconite, utilized in geopolymer matrix appears with boron addition in XRD pattern of both metakaolin and fly ash geopolymers.

B-O-Si bonds belonging to borosiloxane bridge is observed as a small peak at 685 cm^{-1} and shoulder at 875 cm^{-1} in the FTIR spectrum of borax-metakolin based geopolymers whereas only the presence of Si-O-B bond is seen with the shoulder around 870 cm^{-1} in the FTIR spectrum of borax-fly ash based geopolymers. The presence of Si-O-B bond in the structure of borax-fly ash geopolymers is proved by Raman spectroscopy with the peak positioned at 630 cm^{-1}. Two different phases are identified by FTIR spectroscopy in fly ash based geopolymers at around 970 cm^{-1} and 1100 cm^{-1}. The band at around 970 cm^{-1} is related with asymmetric stretching vibrations in calcium based gel. On the other hand, the Si-O vibration positioned at 1020 at cm^{-1} would be associated with silica- rich gel. There is a single major band for the geopolymer specimen with no boron content. SEM results of geopolymers supports the diffraction and spectroscopic characterization methods. The crystalline structures are observed in SEM images of borax-metakolin based geopolymers. The spherical cenospheres related with fly ash vanish with boron addition according to SEM imaged of fly ash based geopolymers as exhibiting the improved geopolymerization process Star like irregular features are displayed in borax-fly ash based geopolymers indicating the increase of crystalline phases.

4. CONCLUSIONS AND RECOMMENDATIONS

4.1. Conclusions

The aim of this study is to identify the effect of borax utilization on structural properties of geopolymers. Therefore, metakaolin and fly ash based geopolymers are synthesized with different molar B/Si ratios of 0, 0.5, 0.6, 0.8 and 1. Different structural characterization techniques are performed to investigate the changes in the geopolymer structure. The characterization techniques utilized are X-Ray Diffraction (XRD), Fourier Transform Infrared Spectroscopy (FT-IR), Raman Spectroscopy, Scanning Electron Microscope(SEM) and Thermogravimetric Analysis (TGA). The effect of boron inclusion on mechanical strength of geopolymers are also analyzed to correlate the structural properties with mechanical performance.

The first part of the study includes the synthesis and characterization of borax-metakaolin based geopolymers. The geopolymers have amorphous structure with quartz components according to XRD results. The amorphous character of geopolymers is not affected boron addition. The characteristic geopolymerization band is observed for all the geopolymers in the region between 900 and 1200 cm^{-1} region. The intensity of the FTIR peaks increase systematically as a function of B/Si ratio. The existence of crystalline peaks in FTIR spectrum is consistent with XRD pattern of geopolymers. The presence of needle and star like structures in the SEM images are seen in the samples with B/Si ratios of 0.8 and 1. These specimens have relatively high level of crystallinity according to both XRD and FTIR results. These structures can be taken as proof of formation of boron crystalline phases within geopolymer framework.

In the second part of the thesis, a comparative study is performed by utilizing borax in both metakaolin and C type fly ash based geopolymers. The synthesis route is different than the first part of the study.

The amorphous phase is observed both in metakaolin and fly ash based geopolymers. Addition of borax leads to formation of borosilicate compounds. The presence of borosilicate formation, B-O-Si bond, proves the participation of boron to silica network by featuring a new product. The B-O-Si crystalline phase is seen in XRD pattern of borax-metakaolin based geopolymers. The FTIR results also support the XRD patterns. The unreacted boron particles are also identified by both XRD and Raman measurements of borax- metakaolin based geopolymers. The presence of needle and star like structures in SEM images stands for the new crystalline formations in boron involving geopolymer systems. On the other hand, phase separation is observed in fly ash based geopolymer systems. The band at around 970 cm^{-1} is related with asymmetric stretching vibrations in calcium based gel whereas the Si-O formation positioned at 1020 cm^{-1} would be associated with silica- rich gel. The phase separation is also seen in SEM images of fly ash based geopolymers due to presence of gel formation. As borax-metakaolin based geopolymers, borax-fly ash geoplymer system have B-O-Si bond formation. The presence of the bond is observed in FTIR and Raman results. The highest compressive strength of 0.56 MPa belongs to metakaolin based geopolymer with no boron content. However, compressive strength values seem to systematically increase with increasing boron content (B/Si) ratio for both borax-metakaolin and borax-fly ash geopolymers. The formation of B-O or B-O-Si bonds might have a positive effect on compressive strength of geopolymers.

4.2.Recommendations

Metakaolin has high water demand due to its high fineness. In order to reduce to water need of metakaolin, flash calcination method can be applied to increase its workability. Flash calcination methods includes combustion process as passing kaolinite near a frame for 10 % of a second.

With the aim of increasing compressive strength of geopolymers, aggregates can be added to geopolymer blend. Afterward, scale up studies can be performed such as fabrication and industrialization of products.

Borax has low workability due to freezing during mixing with alkali activating solution. It is not possible to blend these materials without mechanical mixer. To increase the workability of borax, plasticizers can be used during synthesis.

To confirm the diffraction and spectroscopic results related to boron structural units, solid state nuclear magnetic resonance (NMR) method can be used. In addition, the presence of amorphous aluminosilicate or borosilicate phases in geopolymers can be identified with NMR spectroscopy.

Thermogravimetric results show that the addition of boron increase weight loss in contrast to what is expected. Therefore, to evaluate the effect of boron on thermal behavior of geopolymers, the heating temperature could be increased up to 1200 ^{o}C.

REFERENCES

1. Temuujin, J., Rickard W., Lee, M., "Preparation and thermal properties of fire resistant metakaolin-based geopolymer-type coatings. Journal of Non-Crystalline Solids", 357, pp. 1399-1404, 2011.
2. Das, A., Paul, S. K., "CO2 emissions from household consumption in India between 1993-94 and 2006-07: A decomposition analysis", *Energy Economics*, 41, pp. 94-105, 2014.
3. Rangan, B. V., "Fly ash-based geopolymer concrete". *Proceedings of the International Workshop on Geopolymer Cement and Concrete*, Allied Publishers Private Limited, Mumbai, India, December 2010, pp. 68-106, 2006.
4. Al Bakri, A. M., Kamarudin, H., Mohammed, H., "Review on fly ash-based geopolymer concrete without Portland cement", *Journal of Engineering and Technology* 3(1), pp. 1-4, 2011.
5. Davidovits, J., "Geopolymer, Chemistry and Applications", *Institute of Geopolymer, 3rd printing,* Saint-Quentin, France, 585, 2008.
6. Davidovits, J., "Chemistry of geopolymeric systems". *Terminology, Geopolymer 99 Proceedings*, Second International Conference, 1999.
7. Khale, D., Chaudhary, R., "Mechanism of geopolymerization and factors influencing its development: a review", *Journal of Materials Science* 42 (3), pp. 729-746, 2007.
8. He, J., Zhang, J., Yu, Y., Zhang, G. "The strength and microstructure of two geopolymers derived from metakaolin and red mud-fly ash admixture: A comparative study", *Construction and Building Materials*. 30 (1), pp. 80-91, 2012.
9. Zhang, M., El-Korchi, T., Zhang, G., Liang, J., Tao, M. "Synthesis factors affecting mechanical properties, microstructure, and chemical composition of red mud–fly ash based geopolymers". *Fuel*, 134, pp. 315-325, 2014.

10. Christogerou, A., Kavas, T., Pontikes, Y., Koyas, S., Tabak, Y., Angelopoulos, G.N., "Use of boron wastes in the production of heavy clay ceramics". *Ceramics International*, 35 (1), 447-452, 2009.

11. Kavas, T. "Use of boron waste as a fluxing agent in production of red mud brick", *Building and Environment*, 41 (1), 1779-1783, 2006.

12. Rajamane, N. P., Nataraja M. C., Jeyalakshmi, R. C., "Pozzolanic industrial waste based geopolymer concretes with low carbon footprint", *The Indian Concrete Journal*, 88(7), 49-68, 2014.

13. Maden Mühendisleri Odası, Güyagüler, T., "Türkiye Bor Potansiyeli", http://www.maden.gov.tr/resimler/ekler/d34d468ac887633.pdf, acsessed at March 2017.

14. Helvaci, C.,"Borates", *Encyclopedia Geol*. pp. 510–522, 2005.

15. Eti Maden İşletmeleri, Boron Sector Report, March 2011.

16. Giannopoulou, I., Panias, D., "Structure, Design and Applications of Geopolymeric Materials". *3. International Conference Deformation Processing and Structure of Materials*, Belgrad, Serbia, 2007.

17. Yunsheng, Z., Wei, S., & Zongjin, L., "Composition design and microstructural characterization of calcined kaolin-based geopolymer cement", *Applied Clay Science*, 47 (3-4), pp. 271–275, 2010.

18. Van Jaarsveld, J. G. S., Van Deventer, J. S. J., Lorenzen, L., Jaarsveld, J. G. S. Van, & Deventer, J. S. J. Van., "The Potential Use of Geopolymeric Materials to Immobilise Toxic Metals : Part 1. Theory and Applications". *Minerals Engineering*, 10(7), pp. 1–10 1997.

19. Temuujin, J., Minjigmaa, A., Rickard, W. "Thermal properties of spray-coated geopolymer-type compositions", *Journal Thermal Anaysis and Calorimetry*, 107, pp. 287–292, 2012.

20. Ozdemir, M., Ozturk, N., "Utilization of clay wastes containing boron as cement additives", *Cement and Concrete Research*, 33, pp. 1659–61, 2003.

21. Olgun, A.,Erdogan Y., Ayhan,Y., Zeybek, B., "Development of ceramictiles from coal fly ash and tincalore waste", *Ceramic International*. 31, pp. 153–158, 2005.

22. Williams, Ross P., van Riessen, Arie., "Development of alkali activated borosilicate inorganic polymers (AABSIP)", *Journal of the European Ceramic Society,* 31, pp. 1513-1516, 2011.

23. Nazari, A., Maghsoudpour, A., & Sanjayan, J. G., "Characteristics of boroaluminosilicate geopolymers", *Construction and Building Materials*, 70, pp. 262–268. 2014.

24. Nazari, A., Maghsoudpour, A., & Sanjayan, J. G., "Boroaluminosilicate geopolymers: role of NaOH concentration and curing temperature", *RSC Advances*, 5(16), pp. 11973–11979, 2015.

25. Ozer, I., Soyer-Uzun, S. "Relations between the structural characteristics and compressive strength in metakaolin based geopolymers with different molar Si/Al ratios", *Ceramics International*, 41(8), pp. 10192–10198, 2015.

26. Yüksel, M., "Doğal ve Katkılanmış Bor Minerallerinin Dozimetre Geliştirmek Amacıyla Termolüminesans (TL) Yöntemi Kullanılarak Çalışılması", Adana, Turkey: Çukurova University, 2013.

27. Duxson, P., Fernández-Jiménez, A., Provis, J.L., Lukey, G.C., Palomo, A., Van Deventer, J.S.J., "Geopolymer technology: the current state of the art", Journal of Material Science, 42, pp. 2917–2933, 2007.

28. Luukkonen, T., Sarkkinen, M., Kemppainen, K., Rämö, J., & Lassi, U. "Metakaolin geopolymer characterization and application for ammonium removal from model solutions and landfill leachate", *Applied Clay Science*, 119, pp. 266–276, 2015.

29. He, J., "Synthesis And Characterization Of Geopolymers For Infrastructural Applications", Louisiana State University, 2012.

30. Ma, Y. "Microstructure and Engineering Properties of Alkali Activated Fly Ash", University of Delft, 2013.

31. Javier, L. G., “Study of Geopolymer Adsorbents Prepared from Metakaolin and Rice Husk Silica for Targeting to Heavy Metal Capture”, Nagaoka: Nagaoka University of Technology, 2014.

32. Roviello, G., Ricciotti, L., Ferone, C., Colangelo, F., & Tarallo, O., “Fire resistant melamine based organic-geopolymer hybrid composites”, *Cement and Concrete Composites*, *59*, pp. 89–99, 2015.

33. Suarez, D. L., “Coordination of Adsorbed Boron: A FTIR Spectroscopic Study”, *Environmental Science and Technology* , *29*, pp. 302-311, 1995.

34. Li, X., Zhang, D., Xiang, K., & Huang, G., “Synthesis of polyborosiloxane and its reversible physical crosslinks”, *RSC Advances*, *4*(62), 32894. (2014).

35. Fukata, N., Jevasuwan, W., Ikemoto, Y., Moriwaki, T. “Bonding and electronic states of boron in silicon nanowires characterized by an infrared synchrotron radiation beam”, *Nanoscale*, *7*(16), pp. 7246–7251, 2015.

36. Huang, Y. F., Wu, P. F., Zhang, M. Q., Ruan, W. H., & Giannelis, E. P., “Boron cross-linked graphene oxide/polyvinyl alcohol nanocomposite gel electrolyte for flexible solid-state electric double layer capacitor with high performance”, *Electrochimica Acta*, *132*, pp. 103–111, 2014.

37. Princeton Instruments, *Raman Spectroscopy Basics*, http://web.pdx.edu./~larosaa/Applied_Optics_464-564/Project_Optics/Raman_Spectrocopy/Raman_Spectroscopy_Basics_PRINCETON-INSTRUMENTS.pdf, accessed at December 2016.

38. University of Colorado, *IR Spectroscopy Tutorial*, http://orgchem.colorado.edu./Spectroscopy/irtutor/tutorial.html, accessed at December 2016.

39. RRUFF, *Borax R070168*, http:rruff.info/Borax, accessed at December 2016.

40. McCrone Atlas, *Infrared Spectrum of Borax*, http://www.mccroneatlas.com/viewer/text.asp?IMAGE_ID=231424&PARTICLE_ID=73&TECHNIQUE_ID4&MODE=FTIR, accessed at December 2016.

41. Gautam, C., Yadav, A. K., Singh, A. K., "A Review on Infrared Spectroscopy of Borate Glasses with Effects of Different Additives", *ISRN Ceramics*. 2012.

42. Weir, C. E., "Infrared Spectra of the Hydrated Borates. Journal of Research of the National Bureau of Standarts", *Physics and Chemistry*, 1966.

43. Perchiazzi, N., Gualtieri, A. F., Merlino, S., Kampf, A. R., "The Atomic Structure of Bakerite and its Relationship to Datolite", *American Mineralogist*, 89, pp. 767-776, 2004.

44. Gumus, O. Y., Unal, H. I., Erol, O., Sari, B., "Synthesis, Characterization and Colloidal Properties of Polythiophene/Borax Conducting Composite". *Polymer Composites*, 2011.

45. Dutrow, L., Clark, C. M., Carleton College, Geochemical Instrumentation and Analysis, X-ray Powder Diffraction (XRD), http://serc.carleton.edu/research_education/geochemsheets/techniques/XRD.html, accessed at December 2016.

46. Almou, M., Rulmoni, A., Tarte, P., "Vibrational Spectrum of Trisodium Calcium Pentaborate $Na_3Ca(B_5O_{10})$ and Probable Occurrence of the Discrete Pentaborate Ion $(B_5O_{10})^{5-}$ in Some Glassy Metaborates", *Journal de la Société Ouest-Africaine de Chimie*, 012, 2001.

47. Krishnamurati, D. 1995. Raman Spectra of Borax, Kernite and Colemanite. http://repository.ias.ac.in/33290/1/33290.pdf, accessed at December 2016.

48. Patankar, S. V, Jamkar, S. S., Ghugal, Y. M., "Effect Of Water-To-Geopolymer Binder Ratio On The Production Of Fly Ash Based Geopolymer Concrete", *International Confererence on Recent Trends in Engineering and Technology*, pp. 79–83, 2013.

49. Ogbeide, S. O., "Developing an optimization model for CO2 reduction in cement production process", *Journal of Engineering Science and Technology Review*, 3(1), pp. 85–88, 2010.

50. Gomez-Zamorano, L. Y., Vega-Cordero, E., & Struble, L., "Composite geopolymers of metakaolin and geothermal nanosilica waste", *Construction and Building Materials*, *115*, pp. 269–276, 2016.

51. Malhotra, J. E., “Portland Cement Industry: Plant Information Summary”, *Portland Cement Association*, pp. 8-10, 1999.

52. van Oss Hendrick, G., “Minerals Yearbook 2010”, *Slag, Iron and Steel*, 2011.

53. Bentz, D.P. “Optimization of cement and fly ash particle sizes to produce sustainable concretes”, *Cement Concrete Components*, pp. 824–831, 2011

54. Gartner, E.,. Alternative binders for concretes with reduced CO2 emissions, 2012, http://webpages.mcgill.ca/staff/Group3/aboyd1/web/Conferences/AMW%20IX/Gartner.pdf, accessed at December 2016.

55. Popescu, C. D., Muntean, M., & Sharp, J. H., “Industrial trial production of low energy belite cement”, *Cement and Concrete Composites*, 25(7), pp. 689–693, 2003.

56. Raphaëlle, P., & Martin, C., “Formulation and performance of flash metakaolin geopolymer concretes”, *Construction and Building Materials*, *120*, pp. 150–160, 2016

57. Davidovits, J., “Geopolymers: Inorganic Polymeric New Materials Journal of Thermal Analysis”, 37(8), pp. 1633–1656, 1991.

58. Rowles, M. R., O’Connor, B. H., “Chemical and structural microanalysis of aluminosilicate geopolymers synthesized by sodium silicate activation of metakaolinite”, *Journal of the American Ceramic Society*, 92(10), pp. 2354–2361, 2009.

59. Waclawska, L., “Thermal Decomposition Of Borax”, *43*, pp. 261–269, 1995.

60. Schiavon, M. A., Armelin, N. A., & Yoshida, I. V. P. “Novel poly(borosiloxane) precursors to amorphous SiBCO ceramics”, *Materials Chemistry and Physics*, 112(3), pp. 1047–1054, 2008.

61. Douiri, H., Kaddoussi, I., Baklouti, S., Arous, M., & Fakhfakh, Z., “Water molecular dynamics of metakaolin and phosphoric acid-based geopolymers investigated by impedance spectroscopy and DSC / TGA”, *Journal of Non-Crystalline Solids*, pp. 445-446, pp. 95–101, 2016.

62. Zhou, W., Xiao, P., & Li, Y., “Preparation and study on microwave absorbing materials of boron nitride coated pyrolytic carbon particles”, *Applied Surface Science*, *258*(22), pp. 8455–8459, 2012.

63. Elimbi, A., Tchakoute, H. K., & Njopwouo, D., "Effects of calcination temperature of kaolinite clays on the properties of geopolymer cements", *Construction and Building Materials*, 25(6), pp. 2805–2812, 2011.

64. Steveson, M., Sagoe-Crentsil, K., "Relationships between composition, structure and strength of inorganic polymers. Part 2. Fly ash-derived inorganic polymers", Journal of Material Science, 40, pp. 4247–4259, 2005.

65. Duxson, P., Mallicoat, S.W., Lukey, G.C., Kriven, W.M., Van Deventer, J.S.J., "The effect of alkali and Si/Al ratio on the development of mechanical properties of metakaolin-based geopolymers", *Colloids Surface*, 292, pp. 8–20, 2007.

66. Schrader, B., *Infrared and Raman Spectroscopy*, VCH Publishers Inc.: New York, 1995.

67. Kosor, T., Naki, B., Svilovi, S., "Geopolymer depolymerization index", *Vibrational Spectroscopy, 86*, pp. 143–148, 2016.

68. Kaya, K., Soyer-Uzun, S., "Evolution of structural characteristics and compressive strength in red mud-metakaolin based geopolymer systems", *Ceramics International*, *42*(6), pp. 7406–7413, 2015.

69. Panias, D., Giannopoulou, I. P., Perraki, T., "Effect of synthesis parameters on the mechanical properties of fly ash-based geopolymers", *Colloids and Surfaces A: Physicochemical and Engineering Aspects*, *301*(1-3), pp. 246–254, 2007.

70. Siyal, A. A., Azizli, K. A., Man, Z., Ismail, L., & Khan, M. I., "Geopolymerization Kinetics of Fly Ash Based Geopolymers Using JMAK Model", *Ceramics International*, *42*(14), pp. 15575–15584, 2016.

71. Patil, A. G., & Anandhan, S., "Influence of planetary ball milling parameters on the mechano-chemical activation of fly ash", *Powder Technology*, 281, pp. 151–158, 2015.

72. Mužek, M. N., Zelić, J., & Jozić, D., "Microstructural Characteristics of Geopolymers Based on Alkali-Activated Fly Ash", *Chemical and Biochemical Engineering Quarterly*, 26(2), pp. 89–95, 2012.

73. Rees, C.A., Provis, J.L., Lukey, G.C., Van Deventer, S.J., "Attenuated total reflectance fourier transform infrared analysis of fly ash geopolymer gel aging", *Langmuir*, 23, pp. 8170–8179, 2007.

74. Ogundiran, M. B., & Kumar, S., "Synthesis of fly ash-calcined clay geopolymers: Reactivity, mechanical strength, structural and microstructural characteristics", *Construction and Building Materials*, 125, pp. 450–457, 2016.

75. Zaharaki, D., Komnitsas, K., Perdikatsiz, V., "Use of analytical techniques for identification of inorganic polymer gel composition", *Journal of Material Science*, 45 pp. 2715–2724, 2010.

76. Garcia-Lodeiro, I., Palomo, A., Fernández-Jiménez, A., MacPhee, D. E., "Compatibility studies between N-A-S-H and C-A-S-H gels", *Cement and Concrete Research*, 41(9), pp. 923–931, 2011.

77. Kosor, T., Nakić-Alfirević, B., Gajović, A., "Geopolymerization index of fly ash geopolymers", *Vibrational Spectroscopy*, 85, pp. 104–111, 2016.

78. Momose, M., Hirasaka, M., & Furukawa, Y., "Raman spectroscopic study on boron-doped silicon nanoparticles", *Vibrational Spectroscopy*, 72, pp. 62–65, 2014.

79. Lenoir, M., Grandjean, A., Poissonnet, S., & Neuville, D. R., "Quantitation of sulfate solubility in borosilicate glasses using Raman spectroscopy" *Journal of Non-Crystalline Solids*, *355*(28-30), pp. 1468–1473, 2009.

80. Manara, D., Grandjean, A., Neuville, D. R., "Advances in understanding the structure of borosilicate glasses: A raman spectroscopy study", *American Mineralogist*, *94*(5-6), pp. 777–784, 2009.

81. Kumar, S., Kumar, R., "Mechanical activation of fly ash: Effect on reaction, structure and properties of resulting geopolymer". *Ceramics International*, *37*(2), pp. 533–541, 2011.

82. Novais, R. M., Buruberri, L. H., Seabra, M. P., Bajare, D., & Labrincha, J. A., "Novel porous fly ash-containing geopolymers for pH buffering applications", *Journal of Cleaner Production*, *124*, pp. 395–404, 2016.

83. Suarez, H. G. A., Santos, A. S., Otálora, C. A. O., “Borax as flux on sintering of iron Ancor Steel 1000 under glow discharge”. *Journal of Physics: Conference Series*, *687*, 2016

84. Nyale, S. M., Babajide, O. O., Birch, G. D., Böke, N., Petrik, L. F., “Synthesis and Characterization of Coal Fly Ash-based Foamed Geopolymer”, *Procedia Environmental Sciences*, *18*, pp. 722–730, 2013.

85. ul Haq, E., Padmanabhan, S. K., Licciulli, A., “Synthesis and characteristics of fly ash and bottom ash based geopolymers-A comparative study”, *Ceramics International*, 40, pp. 2965-2971, 2014.

86. H. Cheng, K. L. Lin, R. Cui, C. L. Hwang, Y. M. Chang, T. W. Cheng, “The effects of SiO_2/Na_2O molar ratio on the characteristics of alkali-activated waste catalyst-metakaolin based geopolymers”, *Construction and Building Materials,* 95, pp. 710-720, 2015.

87. Seyhun, A., Emek, K., Derun, M., “Characterisation and determination of the neutron transmission properties of sodium – calcium and sodium borates from different regions in Turkey”, *Journal of Radioanalytical and Nuclear Chemistry*, pp. 175–188, 2014.

88. Derun, E. M., Tugrul, N., Senberber, F. T., Kipcak, A. S., Piskin, S., “The Optimization of Copper Sulfate and Tincalconite Molar Ratios on the Hydrothermal Synthesis of Copper Borates”, *Journal of Radioanalytical and Nuclear Chemistry*, *8*(10), pp. 1152–1156, 2014.

89. Yildirim, M ,. Derun, E. M., Kipcak, A. S., Piskin, S., “Characterization of the Magnesium Borates”, Akademik Platfrom, pp. 67-69, 2014.

90. *Major Producers of Kaolin in world*, 2010, http://www.mapsofworld.com/minerals/world-kaolin-producers.html, accessed at November, 2016.

91. Janotka, I., Puertas, F., Palacios, M., Kuliffayová, M., & Varga, C., “Metakaolin sand-blended-cement pastes: Rheology, hydration process and mechanical properties”, *Construction and Building Materials*, *24*(5), pp. 791–802, 2010.

92. Kovářík, T., Bělský, P., Novotný, P., Říha, J., Savková, J., Medlín, R., Holba, P., "Structural and physical changes of re-calcined metakaolin regarding its reactivity", *Construction and Building Materials*, *80*, pp. 98–104, 2015.

93. Çelik, Ö., Damci, E., Pişkin, S., "Characterization of fly ash and it effects on the compressive strength properties of Portland cement", *Indian Journal of Engineering and Materials Sciences*, 15(5), pp. 433–440, 2008.

94. García Lodeiro, I., Macphee, D. E., Palomo, A., Fernández-Jiménez, A., "Effect of alkalis on fresh C-S-H gels FTIR analysis", *Cement and Concrete Research*, *39*(3), pp. 147–153, 2009.

95. Putnis, A., "In Situ IR Spectroscopic and Thermogravimetric Study of the Dehydration of Gypsum", *Mineralogical Magazine*, *54*(374), pp. 123–128, 1990.

96. Zhao, H. Z., Zhang, Y., Chang, Y. Y., Li, Z. S., "Conversion of a substrate carbon source to formic acid for carbon dioxide emission reduction utilizing series-stacked microbial fuel cells", *Journal of Power Sources*, *217*, pp. 59–64, 2012.

97. Shi, C., Jiménez, A. F., Palomo, A., "New cements for the 21st century: The pursuit of an alternative to Portland cement", *Cement and Concrete Research*, *41*(7), pp. 750–763, 2011.

98. Davidovits, J., "Soft Mineralurgy and Geopolymers", *Proceedings of the 1st International Conference on Geopolymer '88*, 1, pp. 19–23, 1988.

99. Sun, Y., Zheng, Z., Sun, Y., Chen, L., Jin, Z., "Resistance of metakaolin-MSWI fly ash based geopolymer to acid and alkaline environments", *Journal of Non-Crystalline Solids*, *450*, pp. 116–122, 2016.

100. Asif, A., Man, Z., Azizi, K., Azizli, M., Hamidi, R. M., "Effect of Alkali and Water Content on Setting time and Strength of Fly Ash Based Geopolymer", *Applied Mechanics and Materials*, 699, pp. 93–98, 2015.